UNIVERSIDAD DE GRANADA

DOCTORAL SCHOOL IN HEALTH SCIENCES (EDCS)

DOCTORAL PROGRAMME IN BIOMEDICINE.

DOCTORAL THESIS

LIQUID BIOPSY BASED ON CIRCULATING TUMOR CELLS AND EXTRACELLULAR VESICLE MIRNAS FOR THE RELAPSE AND DEATH RISK STRATIFICATION IN NON-SMALL CELL LUNG CANCER PATIENTS

Diego de Miguel Pérez

Thesis supervisors:

José Antonio Lorente Acosta

María José Serrano Fernández

Granada, 07 February 2020

Genyo

CENTRO PFIZER-UNIVERSIDAD DE GRANADA-JUNTA DE ANDALUCÍA
DE **GENÓMICA** E **INVESTIGACIÓN ONCOLÓGICA**

Editor: Universidad de Granada. Tesis Doctorales
Autor: Diego de Miguel Pérez
ISBN: 978-84-1306-460-4
URI: http://hdl.handle.net/10481/60114

Index:

Abbreviations

Adenocarcinoma (ADC)

Axl receptor tyrosine kinase (*AXL*)

Baseline CTCs (CTC1)

Chemotherapy (ChT)

Circulating tumor cells (CTCs)

Computerized tomography (CT)

Cytotoxic T-Lymphocyte Antigen 4 (CTLA-4)

DiGeorge critical region 8 (DGCR8)

Disease-free survival (DFS)

Epidermal growth factor receptor (*EGFR*)

Epithelial cell adhesion molecule (EpCAM)

Epithelial-mesenchymal transition (EMT)

Extracellular vesicles (EVs)

Fourth CTC determination (CTC4)

Genome wide association studies (GWAS)

Glyceraldehide-3-phosphatase dehydrogenase (GAPDH)

GTP-ase Kirsten rat sarcoma virus gene (K-RAS)

Interleukin-6 receptor (IL-6R)

International Society of Extracellular Vesicles (ISEV)

Intraluminal vesicles (ILV)

Isolation by Size of tumor cells (ISET)

Large cell carcinoma (LCC)

Lymph node status (N)

Maximum standardized uptake value (SUVmax)

MET proto-oncogene receptor tyrosine kinase (*MET*)

Metastasis presence (M)

Micro-RNAs (miRNAs, miR)

Microvesicles (Mvs)

Multivesicular endosomes (MVEs)

Nanoparticle tracking analysis (NTA)

Next-generation sequencing (NGS)

Non-small cell lung cancer (NSCLC)

Overall survival (OS)

p: p-value

Phosphate-buffered saline (PBS)

Polycyclic aromatic hydrocarbons (PAH)

Positron-emission tomography (PET)

Precursor miRNA (pre-miRNA)

Primary miRNA (pri-miRNA)

Programmed cell death ligand 1 (PD-L1)

Radiotherapy (RT)

RNA-induced silencing complex (RISC)

Second CTC determination (CTC2)

Small cell lung cancer (SCLC)

Squamous cell carcinoma (SCC)

Standard Deviation (SD)

Stereotactic body radiation therapy (SBRT)

Third CTC determination (CTC3)

Toll-like Receptor (TLR)

Tumor size (T)

tyrosine kinase inhibitors (TKIs)

untranslated regions (UTR)

video-assisted thoracic surgery (VATS)

β2-Microglobulin (B2M)

1. Background

1.1 Lung cancer

According to the World Health Organization, cancer is a group of diseases, initiated in almost any tissue and characterized by an uncontrollable cell growth that can also invade adjacent or distant organs during metastasis. This excessive growth is triggered by gene mutations involved in the control of the cell cycle, cell proliferation, survival, differentiation as well as DNA repairing. In this case, lung cancer can be defined as the aberrant growth of cells located in the tissues of the lung[1].

1.2 Epidemiology

Lung cancer is the most frequent malignant neoplasia in the world, with an increasing incidence each year[2]. Worldwide, 2.093.876 new lung cancer cases were diagnosed in 2018, representing the 21.5% of all new cancer cases (**Figure 1**). This neoplasia is also the leading cause of cancer related death, with 1.761.007 deaths in 2018, 30.5% of all cancer related deaths in the world (**Figure 2**). Divided by gender, it is the most frequent in men (14.5%) while the third most common carcinoma in women (8.4%), after breast (24.2%) and colorectal carcinoma (9.5%).

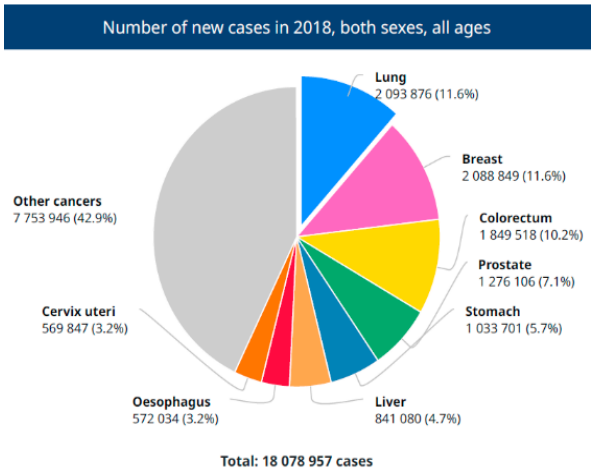

Figure 1: Incidence of all cancers in the world in 2018[1].

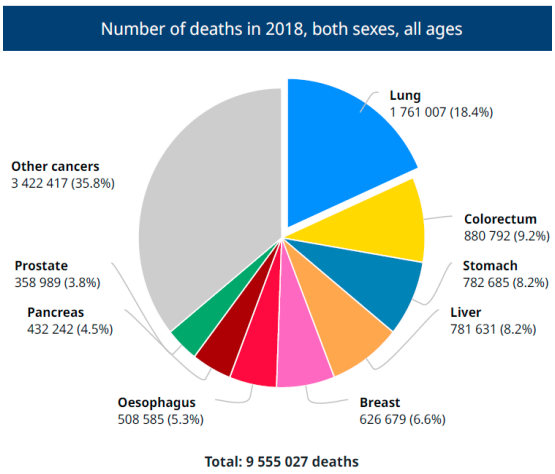

Figure 2: Mortality of all cancers in the world in 2018[1].

Lung cancer has one of the lowest survival rates among all type of cancers with a 5-year survival rate of ~18% for all stages of lung cancer. Due to the absence of validated screening procedures for large populations, most lung cancer patients are diagnosed at an advanced stage when the 5-year survival rate is only 5%.

1.3 Etiology:

Lung cancer is developed after genetic and epigenetic changes in the DNA of lung cells mainly caused by:

Smoking: Tobacco smoking is the number one risk factor for developing lung cancer and approximately 90% of all lung cancers are attributed to it. Nowadays, the association between tobacco consumption and lung cancer is evident; however, it was not until 1964 when the US Surgeon General reported that tobacco smoke was a direct cause of lung cancer[3].

Tobacco smoke contains several carcinogenic components such as polycyclic aromatic hydrocarbons (PAH), N-nitrosamines, aromatic amines, aldehydes, and other inorganic compounds such as arsenic, nickel or chromium, that are enzymatically transformed into metabolites to be excreted. Cytochrome P450 is one of the enzymes involved in this process and probably the most studied one. The resulting metabolites can react and bind to the DNA, forming intermediate compounds known as adducts[4].

DNA adducts are eliminated by the DNA repairing mechanisms but some of them may escape and lead to miscoding, causing permanent mutations during DNA replication. As a second line of protection, cells can undergo apoptosis or programmed cell death when the DNA has been altered. However, these permanent mutations can trigger the activation of oncogenes or the inactivation of tumor suppressor genes that aid the cells escape apoptosis mechanism. Finally, these cells can proliferate, accumulating sequential alterations and, ultimately, developing lung cancer[4].

Environmental exposure: The remaining 10% of lung cancer cases are attributed to the exposure to other environmental carcinogens such as radon, asbestos, air pollution or infections[2].

Genetic susceptibility: There is genetic susceptibility to lung cancer as it is estimated that only 11-12% of tobacco smokers will develop lung cancer[5]. Previous familiar history of lung cancer has been reported to an increased 1.7-fold risk. According to genome-wide association studies (GWAS), mutations in chromosome regions 5p15, 6q21, and 15q25-26, which include genes involved in acetylcholine nicotinic receptors and telomerase production, predispose to lung cancer[6]. Other genetic alterations have been associated to cancer such as alterations in oncogenes and tumor suppressor genes. The most important genetic driver mutations associated to lung cancer are the ones in the *EGFR*, the GTP-ase Kirsten rat sarcoma virus gene (*K-RAS*), *HER2*, *TP53*, *PTEN*, or *EML4-ALK*[7].

1.4 Histopathology

Lung cancer encompass a heterogeneous group of tumors with many histological subtypes[8]. Non-small cell lung cancer (NSCLC) and small cell lung cancer (SCLC) are the most predominant, covering approximately 95% of all lung cancers cases. NSCLC, normally found in peripheral areas of the lung, comprises around 80% of all lung cancer cases and is mainly divided in adenocarcinoma (ADC) (40-50%) and squamous cell carcinoma (SCC) (20-30%). Other subtype of NSCLC, called large cell carcinoma (LCC) is characterized by undifferentiated large cells and comprise around 2% of all lung cancer cases. To the contrary, SCLC (10-15%) is more common in the inner areas such as primary and secondary bronchi.

ADC is produced in glandular cells with papillary structures and mucin production while SCC are characterized by keratin pearl formation, intercellular bridging, and an associated inflammatory component. ADC and LCC usually grow in the peripheral areas while SCC tend to grow in the central part of the lungs. In the past, the therapeutic management differed only from NSCLC and SCLC. To date the accurate histological classification has been proved crucial for the management, prognosis and screening efficacy in lung cancer subtypes[9,10].

Lung cancer rates by histological subtype have changed in the last decades, reflecting the changes in the smoking habits over time. SCC used to be the most frequent subtype, particularly in men, however, in the recent years, ADC incidence has risen due to[11]:

- The increased incidence of lung cancer in non-smokers and women, where ADC is more predominant, and the decreased rates in men[12].

- The change in new cigarette composition, with lower amount of PAH (SCC inducers) but more N-nitrosamines (ADC inducers). In addition, nicotine-containing cigarettes make smokers inhale deeper what could lead to a more peripheral distribution of the smoke.

- The risk of developing ADC after smoking cessation is reduced slower than in SCC. However, other studies reported that the risk of lung cancer is not reduced over the years after smoking cessation[13].

1.4 Clinical management

1.4.1 Diagnosis

From the clinical point of view, lung cancer is usually detected at an advanced stage, when the tumor nodule may have grown for a long time or even disseminated before the patient presented any symptoms. As a consequence, most lung cancer patients are diagnosed with an unresectable stage and 20% of them with locally advanced disease. It is estimated that approximately only 20% of the patients are candidates for surgical treatment[8].

Computerized tomography (CT) scan is the gold-standard for lung cancer diagnosis and staging. The addition of positron-emission tomography (PET) improved its accuracy, due to the high sensitivity for the detection of lymph node metastasis and the differentiation of lung fibrosis. Still, some trials have reported high false-positive results due to the presence of benign pulmonary nodules[13]. Moreover, PET derived parameters such as the maximum standardized uptake value (SUVmax) have proven their prognostic value[14].

After imaging, diagnosis is confirmed by cytological or histological biopsy when possible. However, histological confirmation is only performed in ~30% of NSCLC tumors, and the rest are diagnosed from minimal biopsies or cytological specimens, what hinder the accurate staging and classification[9].

1.4.2 Staging

Lung cancer patients have been traditionally classified into groups according to the biological behavior of the tumor. Staging is performed according to the TNM system, that from its introduction in 1970 to the 8th edition published in 2017, has been extensively reviewed and improved. This system is based on three descriptors: T, corresponding to the primary tumor size (Tx, T0-T4); N, based on the presence of affected local and regional lymph nodes (Nx, N0-N3); and M, defining the presence of metastasis beyond regional lymph nodes (M0-M1c)[15].

The 8th edition is expected to help in the classification and management of lung cancer patients. However, this classification still needs to be improved as it does not include information about the SUV value nor the molecular profile of individual tumors such as the *EGFR* mutational status. Thus, this model lacks important prognostic impact that should be incorporated in future editions for a more personalized medicine.

1.4.3 Treatment

According to the tumor stage, lung cancer patients receive specific treatments that may vary from surgical resection (when possible), neoadjuvant and adjuvant treatments based on chemotherapy, radiotherapy, targeted therapies, and immunotherapy regimens.

1.4.3.1 Surgical treatment

Surgical resection is the more effective and recommended treatment in resectable early stage patients (stage I-II and some IIIa). The surgical treatment with curative intent consists in the resection of the lung parenchyma, including the primary tumor and the locoregional lymph nodes. Throughout history, lung resection has evolved by diminishing the volume of the resected tissue. Moving from the extraction of a whole lung, or pneumonectomy, to the removal of a lung lobe, or lobectomy, which is associated with better outcome and the standard resection procedure. The introduction of important advances in the diagnosis and staging of NSCLC as well as the development of new minimally invasive surgical techniques, such as the video-assisted thoracic surgery (VATS), have improved the management, treatment selection, and prognosis of NSCLC patients[16]. This way, complete resected patients have the best overall survival (OS) with a 5-year survival rate of 60%, reflecting the importance of screening programs for early detection[17].

1.4.3.2 Adjuvant chemotherapy

Despite complete resection, many of these patients relapse or die. For this reason, to eliminate any tumor remaining and improve the survival of these patients, adjuvant chemotherapy and/or radiotherapy treatments are administered. In this cases, cisplatin is one of the most recommended drugs since the publication of its benefits in the first clinical trial including stage I-III patients[18]. Nevertheless, several studies have reported controversial results, most of them reporting a benefit only in stage II NSCLC patients. Others have even reported worse prognosis in stage I patients treated with cisplatin. As a consequence, the American College of Chest Physicians recommends the administration of adjuvant platinum-based chemotherapy only in stage II patients with good performance status[19].

1.4.3.4 Adjuvant radiotherapy

In some cases, after complete resection adjuvant chemotherapy is combined with thoracic irradiation. The role of this regimen has been evaluated in some multicenter studies which reported no benefit or even a detriment in N0 or N1 patients[20] and controversial results in patients with nodal metastasis (N2). Consequently, the application of this regimen is individually evaluated in each patient[21]. Meanwhile, stereotactic body radiation therapy (SBRT) is evolving as a new viable option in early stage unresectable patients[22] or even in those after surgery[23]. To date, some clinical aspects are still uncertain but there is no doubt that SBRT is a strong candidate to lead the future treatments in early and advanced NSCLC.

1.4.3.5 Concomitant chemoradiotherapy

Platinum based chemotherapy combined with thoracic irradiation is the standard first line treatment for unresectable, locally advanced NSCLC. Several trials have evaluated the efficacy and safety of platinum drugs such as carboplatin and cisplatin. A recent meta-analysis reported no difference in the survival between the two drugs, despite a slight benefit with the cisplatin[24]. Furthermore, these platinum drugs are usually combined with other such as vinorelbine or paclitaxel, which target the microtubules of tumor cells in different phases of the cell cycle. Randomized studies have reported that cisplatin-vinorelbine and taxol-carboplatin have similar results, this way these regimens are all used to treat advanced NSCLC[25,26].

The chemotherapy treatment is combined with thoracic radiation where the drugs also act as radiation sensitizers, improving the effectivity of the radiation. Despite being the standard of care in advanced NSCLC, survival rates still low and progression is developed early[27,28]. Huge efforts have been made to identify radiation modulators, sadly with unsatisfactory results. Radiation resistance is a complex mechanism that involves significant changes of hundreds of genes[29]. This means that there must be molecules capable of regulating the expression of these genes in a broad and rapid manner. micro-RNAs (miRNAs, miR) could be those potential regulators[30].

1.4.3.6 Targeted treatments

Chemotherapy and radiotherapy have been the main stays of treatment of NSCLC patients for years. However, since the identification of oncogene biomarkers, targeted therapies have become the standard of care in *EGFR, MET, ROS*, or, *EML4-ALK* altered lung tumors. For instance, targeted therapies for *EGFR* or *ALK* mutated patients such as the tyrosine kinase inhibitor (TKI) erlotinib or crizotinib have shown improved survival vs. chemotherapy regimens. Nevertheless, resistances are still developed, patients will recur and chemotherapy will be applied[31].

1.4.3.7 Immunotherapy

The development of immune-checkpoint inhibitors has changed the paradigm of NSCLC treatment. In comparison to oncogene targeted biomarkers, immunotherapy biomarkers, such as Cytotoxic T-Lymphocyte Antigen 4 (CTLA-4) or programmed cell death ligand 1 (PD-L1), are continuous, dynamic through time, and reliant on complex interactions. The use of immunotherapy treatments such as anti PD-1 (pembrolizumab) or PD-L1 (nivolumab) antibodies have showed a benefit in the survival of both, naive and treated NSCLC patients[31]. The use of immunotherapy as a neoadjuvant, adjuvant or in combination with targeted therapy or chemotherapy is still under on-going evaluation. Nevertheless, preliminary results show a promising future in the treatment of NSCLC patients[32].

1.5 Autophagy

The process of macroautophagy, referred from now on as autophagy, is defined as a catabolic pathway of auto-proteolysis activated under stress conditions, by which eukaryotic cells recycle cellular components to maintain homeostasis. During autophagy, certain damaged organelles or proteins, pathogens, and other components are engulfed into double-membrane autophagosomes that will later fuse with lysosomes to degrade their content[33].

Autophagy can promote both, cellular adaptation to stress conditions and cell survival or apoptosis when the cellular damage is too harsh[34]. In normal conditions, autophagy has a tumor suppressive function, leading to the apoptosis of altered and potentially malignant cells. Conversely, autophagy can promote cancer cell survival under stress conditions or cell damage such as the one caused by chemotherapy and radiotherapy treatments[35].

There are controversial findings about how autophagy mediates tumor cell survival and lung cancer pathogenesis. Recent evidence has linked the upregulation of autophagy to an increased resistance to chemotherapy drugs as cisplatin[36], vinorelbine[37], or radiation[38] by the removal of damaged organelles.

1.5.1 Mechanism of autophagy

The mechanism of autophagy is divided in initiation, vesicle nucleation, elongation, fusion, and cargo degradation (**Figure 3**). Autophagy starts after a starvation or stress signal that provoke the dissociation of the ULK1 complex from the mTOR1, what initiates the formation of the phagophore. During nucleation, the ULK1 complex phosphorylate and activate Beclin-1, which is included in the PI3K complex and facilitates the engulfment of the cargo during phagophore nucleation. Beclin-1 is inhibited by the union of anti-apoptotic Bcl-2 family members such as Bcl-2 and Bcl-xL to its BH3 domain, preventing its association to the autophagosome inducing complex. To the contrary, it is activated by the association of Ambra1/UVRAG/Atg14 to its central coiled-coil domain, stabilizing the PI3K complex[39].

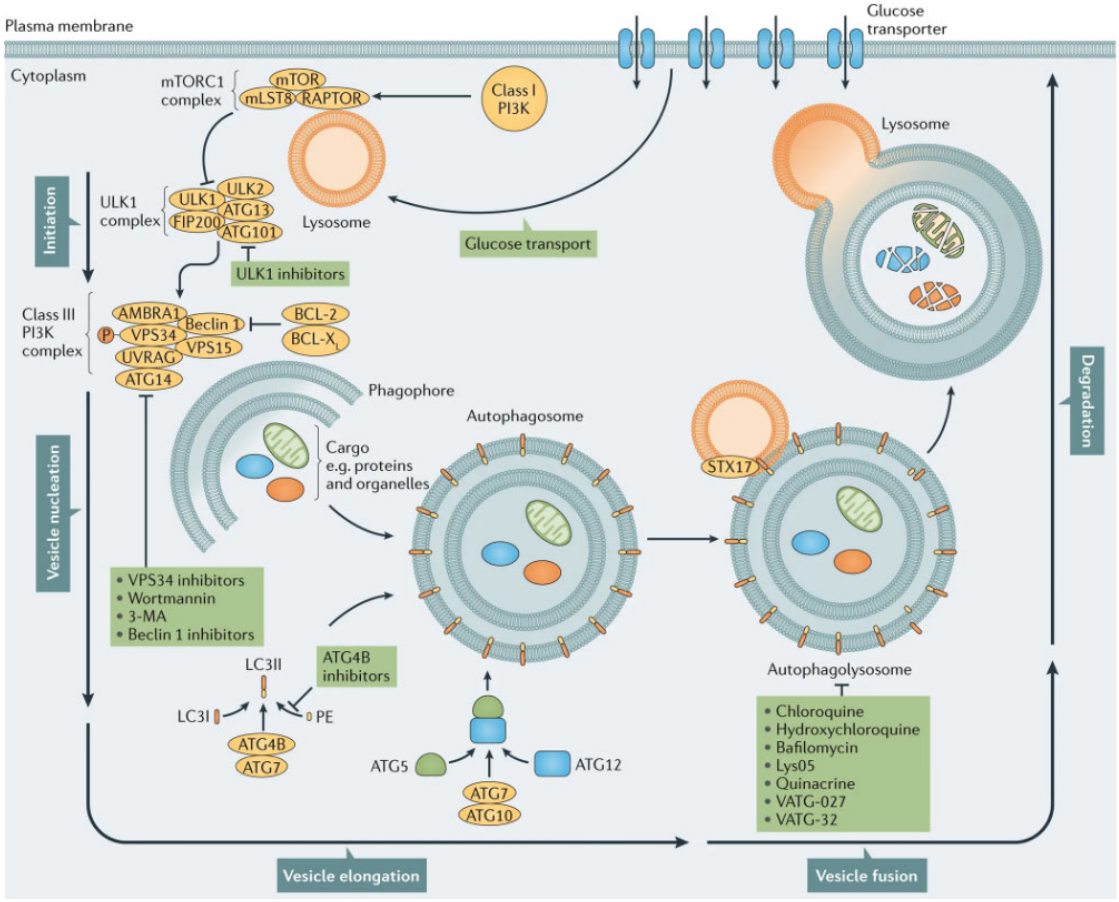

Figure 3: **Mechanism of autophagy**[40]**.**

During vesicle elongation, LC3A is conjugated with phosphatidylethanolamine to form the lipidated form LC3B, which is recruited to the inner and outer surfaces of the autophagosome membrane. Then, during vesicle fusion, LC3B from the outer surface is dissociated and the autophagosome fuses with the lysosome to form the autophagolysosome. Finally, the acidic pH of the lysosome causes the degradation of the autophagolysosome cargo as well as the LC3B from the inner surface.

Autophagy can be pharmacologically targeted at several steps, preventing phagophore elongation with ULK1 inhibitors, vesicle elongation by blocking Beclin-1 activation, or lysosome fusion by chloroquine treatment[40]. We would like to outline the role of Beclin-1 and LC3B as they are two of the most important proteins studied during autophagy.

1.5.2 Beclin-1

Beclin-1, known in mammals as the orthologue of yeast Atg6, is a member of the Bcl-2 family of proteins directly related to the initiation of autophagy. Beclin-1 is a Bcl-2 homology 3 (BH3) only domain protein expressed in most many human tissues. Its cellular expression is mainly distributed within cytoplasmic structures as the endoplasmic reticulum or the mitochondria but it can also be found within the plasma membrane, perinuclear membrane and the nucleus[41].

In NSCLC studies, Beclin-1 has been vastly described as a biomarker of autophagy, in most of them acting as a tumor suppressor but also as a treatment resistance biomarker[41]. A meta-analysis from 2018, which analyzed a total of 1159 patients from 8 studies, reported that high levels of Beclin-1 predicted better OS[42]. On the other hand, EGFR and Beclin-1 interaction, downregulating autophagy, has been described to enhance TKI resistance in EGFR mutated NSCLC[43].

1.5.3 LC3B

LC3B is found in the internal and external compartments of the autophagosome after LC3A lipidic extension[44] and proposed as an important regulator in the selection of the autophagosome cargo. Detection of LC3B commonly used to assess autophagy activity in *in vitro* and *in vivo* assays[40].

As well as Beclin-1, many studies have reported a dual role in cancer. Higher expression of LC3B has been associated to tumor dissemination, lymph node metastasis and metastasis is several solid carcinomas[45]. Interestingly, the upregulation of LC3B and Beclin-1 has been associated to radiotherapy resistance in NSCLC by the downregulation of specific miRNAs[38].

1.6 Metastasis

Despite huge advances in lung cancer diagnosis and treatment, metastasis is present, either at diagnosis or during the course of the disease, in a high percentage of NSCLC patients, being responsible for most of their deaths. Metastasis, or the process of tumor dissemination, could be simply defined as the movement of tumor cells from a primary mass to a second site where they may form a second neoplasia.

The metastasis process is classically divided in sequential steps. First, the enhanced growth of tumor tissues increases hypoxia and metabolic deficiencies in the central areas of the tumor. As a consequence, the process of angiogenesis is activated to support the blood supply in those areas. Then, tumor cells that detach from the mass can intravasate into these new blood vessels, reaching the circulation where they are known as circulating tumor cells (CTCs). In addition,

tumor cells may leave the tumor via the lymphatic system, invading lymphatic nodes from where they can also reach the blood circulation.

In the process of tumor dissemination, CTCs have to evade the attack of the immune system and the applied treatments, finally extravasating from the circulation and colonizing the secondary organ. There, CTCs proliferate forming micrometastasis that could later develop the metastasic tumor[46]. In general, the metastatic process is highly inefficient. The initial steps of hematogenous metastasis and extravasation are quite effective but the survival of CTCs in the circulation, the micrometastasis formation, growth and angiogenesis are quite difficult. This way, to form a metastasis, CTCs must survive the selective forces applied during each step of the dissemination, starting from the primary tumor detachment to the survival in the media and the final metastasis formation[47].

In comparison to other solid tumors as breast or prostate carcinomas, lung cancer metastasis is a rapid process. In lung carcinomas, tumor cells often acquire a semi-mesenchymal state that confers them increased invasive properties. This allow them to infiltrate and colonize other organs in a short period of time, causing short relapse-free survival (RFS)[48]. On the other hand, lung cancers principally metastasize to contralateral lung, brain, bones, adrenal gland, and the liver. The infiltration and homing into specific target organs can be partly explained by the blood circulation, the size and structural features of the capillary walls in different organs and the plasticity of the cells to cross the endothelium in each organ[48]. However, there is also evidence of a preferential metastasis due to specific molecular interactions that promote the homing of CTCs into these organs. The most accepted explanation to this selective metastasis is the “seed and soil” hypothesis[46].

1.6.1 Seed and soil hypothesis:

This theory was postulated by the English surgeon Stephen Paget in 1889. He suggested that tumor cells would be like seeds liberated from a plant, which being carried everywhere, only those falling in compatible and fertile soil would grow. According to this theory, there are several factors that contribute to metastasis: Extrinsic factors such as tumor-secreted factors via extracellular vesicles (EVs), cytokines, etc. that modulate the extracellular matrix of the primary and secondary “soil”. Intrinsic factors such as the epithelial-mesenchymal transition (EMT) or the autophagy mechanism that are involved in CTC survival and colonization. These two processes have been associated to the acquisition of stem properties[49].

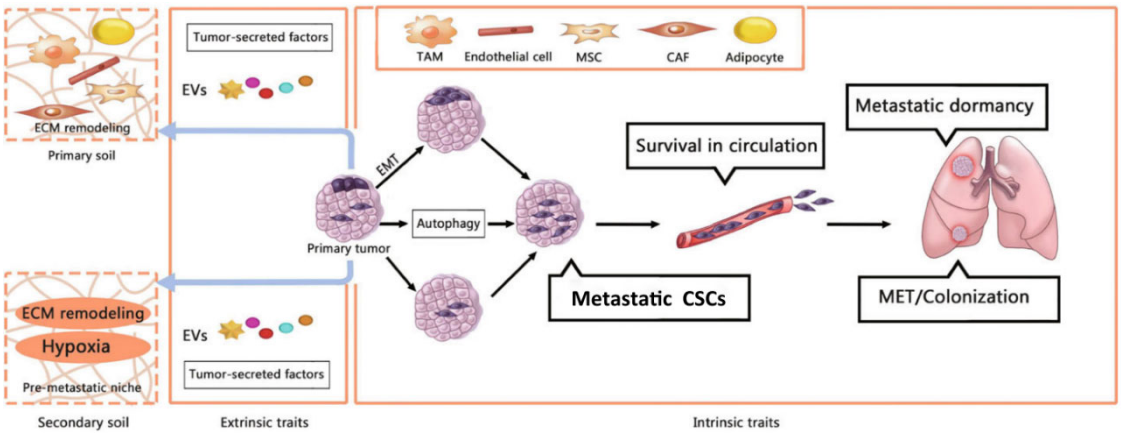

Figure 4: Factors involved in cancer metastasis[49]. Extracellular matrix (ECM), tumor-associated macrophage (TAM), mesenchymal stem cell (MSC), carcinoma associated fibroblast (CAF), mesenchymal-epithelial transition (MET).

1.7 Tumor heterogeneity

We know that histologically similar tumors can show different features and behave in a completely different way, or even tumors found in the same patient may be very distinct, not responding to the same treatment. Cancer is a dynamic and constantly evolving process that from the initial genetic diversity during tumorigenesis, till clonal selection and expansion is modulated by the microenvironment, what leads to tumor heterogeneity.

Tumor heterogeneity can be defined as the divergence of the molecular profile from tumors either between individuals or within themselves. This term has been described for decades[50] but it is nowadays with the recent advances in next-generation sequencing (NGS) technologies that we are really aware of its full extent, realizing how complex and different can tumors be. NGS had helped to change the paradigm of resistance mutations, from the old idea of a binary behavior of tumors towards the notion of intricated and dynamic tumors composed by different cell subpopulations.

Tumor heterogeneity can be divided into intertumoral and intratumoral heterogeneity. Intertumoral heterogeneity is defined by the differences found between patients with the same histological tumor subtype. To the contrary, intratumoral heterogeneity refers to the presence of different cells within one neoplasm (**Figure 5**). Intratumoral heterogeneity may be subclassified into spatial or temporal heterogeneity. Spatial heterogeneity is characterized by the uneven distribution of molecularly distinct cell subpopulations within a single neoplasia or across different locations in a single patient. Temporal heterogeneity would refer to the dynamic modifications of the molecular profile of a single neoplasia over time. For instance, intratumoral heterogeneity can be caused by the natural clonal evolution of the tumor or by the cells ability to adapt to a wide variety of exogenous and endogenous selective pressures.

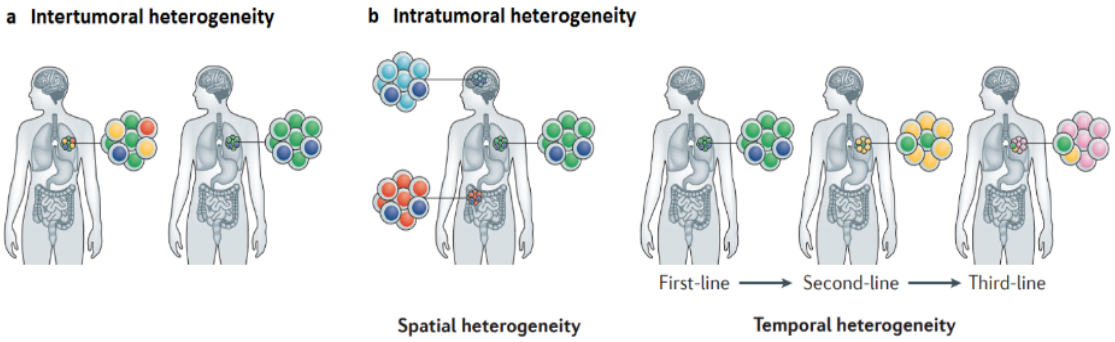

Figure 5: Tumor heterogeneity[51]

Several mechanisms as genomic instability or clonal evolution and selection have been described to cause tumor heterogeneity.

Genomic instability: In normal tissues, the cellular machinery is highly able to avoid and repair errors during DNA replication, producing a low rate of spontaneous mutations that appear during each cellular generation. However, during tumorigenesis, cancer cells lose part of this mutational resistance by, for example, compromising *TP53*, and acquire spontaneous alterations. *TP53*, commonly known as the "guardian of the genome", is a tumor suppressor gene critical for cell cycle arrest, DNA repairing and apoptosis initiation in response to DNA damage[52]. The mutation rate of cancer cells can also be increased due to exposure to carcinogenic agents such as tobacco smoke, radiation or chemotherapy. Indeed, chemotherapy

and other therapies are associated to increase genomic instability within tumors and the emergence of new mutations that were not present before therapy[53].

Clonal evolution and selection: In addition to genomic instability, tumors have other mechanisms to maintain an promote their heterogeneity. The most accepted model for the generation of clonal diversity is the model of clonal evolution and selection proposed by Peter Norwell in 1976[54]. This model could be understood as a cellular example of the Natural Selection model of the best fit. The initial alteration of a single or a bunch of non-malignant cells could confer them a selective advantage over nearby cells that allows them to proliferate more. This growing subpopulation would generate additional genomic instability, that subjected to evolutionary selective pressures, creates different subpopulations of tumor cells. As in the natural selection models, we should not forget the important role of the microenvironment. The microenvironmental pressure of each cell within a single tumor might be different depending on the regional localization. For example, cells found in the inner region of the tumor are more exposed to hypoxia and nutrient deprived than those in the peripheral area what could trigger a transformation into a different phenotype.

Intratumor heterogeneity is the keystone of tumor evolution and important in the development of therapy resistances. In tumor characterization, the analysis of single-site tissue biopsy might not reflect the reality of the clonal spatial heterogeneity of a tumor. In consequence, treatments might fail, finally giving room to tumoral progression and metastasis.

Multiregional and sequential sampling could be the solution for spatial and temporal intratumor heterogeneity, however, most cancers are diagnosed at an advanced stage, when multiple tissue sampling might be risky for the patient. Moreover, longitudinal biopsies over time are not possible in some cases or not well tolerated by the patient, being not accurate biomarkers for the administration of a targeted therapy[51].

1.8 Liquid biopsy

Tissue biopsies have been clinically used for centuries, being the gold-standard for the diagnosis and assessment of cancer patients. However, NSCLC patients presents one of the latest diagnosis among solid tumors with high rates of treatment failure, metastasis and mortality. Tissue biopsies has many drawbacks caused by its invasive nature and also due to tumor heterogeneity. In addition, some tumors might be not accessible or impossible to perform multiple, accurate and sequential biopsies to follow the evolution during the treatment.

In this scenario, liquid biopsy emerged as the potential tool that could enable a real-time longitudinal analysis of the tumors without the disadvantages of tissue biopsy. Liquid biopsy can be defined as a non-invasive and dynamic analysis of molecular biomarkers in body fluids, normally peripheral blood. The use of liquid biopsy could address the challenges in treatment selection during the course of the disease thanks to its repeatable and harmless potential[55]. The most studied biomarkers in liquid biopsy are circulating tumor cells, extracellular vesicles, and cell-free nucleic acids such as circulating tumor DNA but, in this work, we only focused on the role of circulating tumor cells and extracellular vesicles.

1.8.1 Circulating tumor cells

Circulating tumor cells (CTCs) can be defined as those cells disseminated from the primary or metastatic tumor that can be found in the blood traveling to a secondary organ to establish metastasis[56]. CTCs were described for the first time by Thomas Ashworth in 1869, who postulated that “cells identical with those of the cancer itself being seen in the blood may tend to throw some light upon the mode of origin of multiple tumors existing in the same person”[57].

(Ashworth TR (1869) A case of cancer in which cells similar to those in the tumors were seen in the blood after death. Australian Medical Journal 14: 146–147. As it has been reported in the metastasis section, we know that tumor dissemination can occur in different ways. Tumor cells can disseminate directly through blood vessels to a secondary organ or they can invade the lymphatic circulation reaching the regional lymph nodes[58] **(Figure 6).**

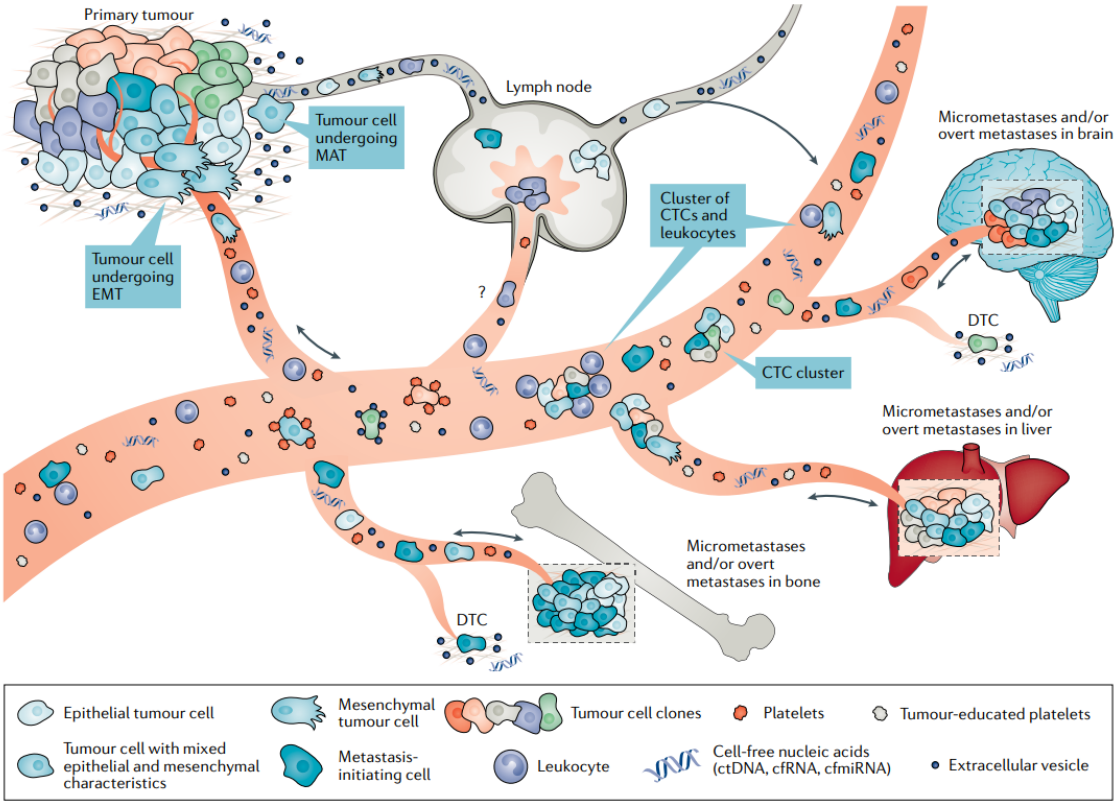

Figure 6: Circulating tumor cell dissemination[58].

CTCs from the same patient can show different phenotypes as they can detach from different areas within the tumor and also suffer phenotypical changes in the circulation that make them survive, such as the EMT. Thus, CTCs found in the blood may reflex the complex tumor heterogeneity or indeed the nature of the potential metastasis.

To date, the molecular diagnosis of cancer patients is based on the biopsy of the primary tumor. However, as it has been described above, the primary tumor is composed by different subpopulations of cells and only some might have metastatic properties that make them clinically relevant. The CTCs found in blood represent a pool of those cells that have at least invasive properties that allowed them to migrate to the circulation. Thus, these cells could represent a good surrogate of the tumor population that would clinically important for therapy selection. However, several studies have reported dissimilarities between CTCs and primary tumors[59].

The detection and characterization of CTCs found in peripheral blood can contribute to the understanding of tumor evolution during its natural course or in response to therapies, as well as of the spatial and temporal heterogeneity. In a recent study, sequential CTC-xenograft modeling revealed an organ-specific gene signature for triple-negative breast cancer as well as biomarkers of clinically available drugs. In this manner, combination of new therapies and CTC-targeted drugs could improve the clinical outcome of NSCLC patients[60].

1.8.1.1 EMT

The phenotypical differences found in CTCs may be partially caused by the EMT. The epithelial-mesenchymal transition (EMT) is the process by which epithelial cells lose their epithelial characteristics in exchange of mesenchymal ones. It plays a role not only during cancer progression and metastasis, but also along embryonic development, regulating organ formation, or wound healing[61].

Epithelial cells are characterized by polygonal/epithelial morphology with an apical-basal polarization, strong intercellular and cell-matrix adhesions. During the EMT, these cells lose these properties, acquiring a mesenchymal phenotype characterized by higher invasive and migration ability associated to a morphological shift to a spindle/fibroblastic shape that aid them to detach from the tumor[62] (**Figure 7**).

The molecular analysis of EMT revealed a loss of epithelial markers such as E-cadherin, the epithelial cell adhesion molecule (EpCAM) or cytokeratin while an increase of vimentin, N-cadherin or fibronectin mesenchymal markers. The transformed cells can also express cancer stem cell markers as CD44, Bmi1 or aldehyde dehydrogenase that confer them auto-repairing ability, high tumorigenicity and chemoradiotherapy resistance[63,64].

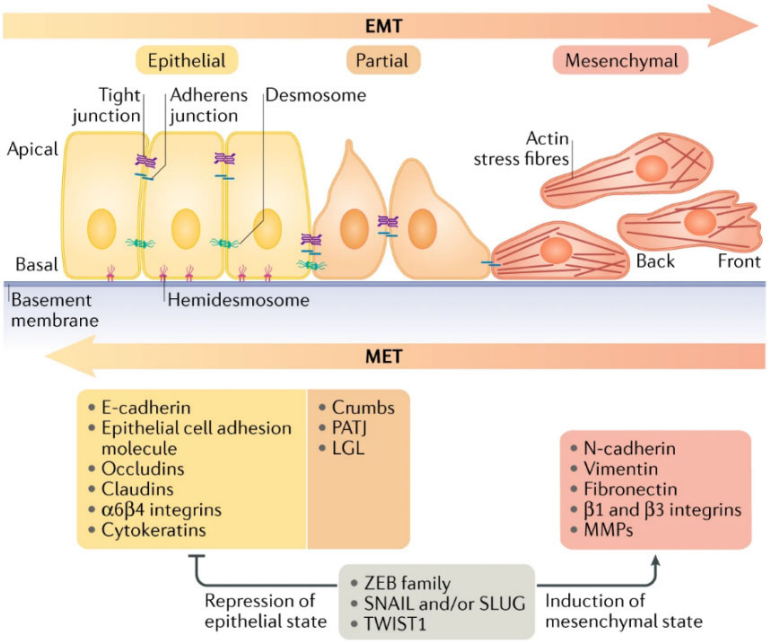

Figure 7: Epithelial-mesenchymal and mesenchymal-epithelial transition. Mesenchymal-epithelial transition (MET)[65].

EMT regulation: The EMT is regulated by EMT-inducing transcription factors, which regulate the expression of genes that promote either the mesenchymal or the epithelial state. Evidence suggests that the EMT is orchestrated as an epigenetic mechanism and it cannot be determined by sequencing cancer cell genomes[65]. Thus, transcription factors are modulated in response to mechanism as hypoxia, cytokine and growth factor secretion by the tumor microenvironment, immune responses, and treatment with antitumor drugs, among others[66]. The transition in gene expression is modulated by the regulatory network including Snail, Slug, Twist, Zeb1, and Zeb2 transcriptional factors and also several miRNAs[33]. Moreover, within the tumor microenvironment, tumor-associated macrophages, fibroblast and other blood components as platelets secrete TGF-β, TNF-α, miRNAs, etc. either alone or enclosed in vesicles that can be

absorbed by tumor cells and regulate the EMT. In the same way, tumor cells can interact and modulate the function of other cells from the tumor microenvironment[67].

EMT in tumor dissemination: In cancer, the EMT has been widely associated to the mechanism of metastasis, being essential for CTC detachment and dissemination[68] and it is reported that CTCs must undergo at least partially the process or mesenchymal-epithelial transition, acquiring cell adhesion and proliferative properties that allow them to form the new tumor[65,69]. We actually know that not all CTCs undergo complete EMT, indeed many lung cancer CTCs are found in a semi-mesenchymal state[70]. Nevertheless, the role of the EMT in the consecution of metastasis has been recently questioned describing that some types of tumors might metastasize in an EMT independent way and EMT is only is associated to CTC resistance to apoptosis, immune and other drug treatments[71]. However, these studies have potential limitations such as cell identification based on a single gene, what could lead to miss EMT events. In addition, when metastasis was developed in mouse models, the results were unable to fully demonstrate EMT inhibition[49,72]. Hence, further evidence is necessary to conclude if the EMT is dispensable during metastasis.

Partial EMT or semi-mesenchymal CTCs: Hybrid CTCs with a semi-EMT phenotype has been detected in several tumors including NSCLC and interestingly, some studies linked the presence of this phenotype, rather than the fully epithelial or mesenchymal, to poor prognosis[70,73]. During EMT, EpCAM experience a dramatic decrease in comparison to cytokeratin proteins[74]. Indeed, there is evidence that cytokeratin-7 could not be reduced during EMT[75].

1.8.1.2 CTC clusters

Circulating tumor cells can be found not only as single cells but also as aggregates of two of more cells, called clusters[76]. Clusters, or microemboli, have emerged as another way of CTC migration and metastasis in an EMT independent-way. Recent studies have observed that these clusters do not lose their epithelial characteristics and generally do not express vimentin or other EMT markers[77]. CTC clusters are oligoclonal tumor cell aggregates than are shred together from the primary tumor and not grouped within intravascular circulation. This could enhance the intratumoral spatial heterogeneity of the metastasis in which several clones are present and more diversity is potentially developed, providing a potential survival advantage for metastasis colonization[78].

CTCs can also form cluster with other non-malignant cells such as leukocytes, cancer-associated fibroblast, platelets and extracellular vesicles. These blood components can confer them survival advantage versus single cells in the blood. In a novel study, CTC-associated neutrophils expressed IL-6 and IL-1β while the CTCs expressed the corresponding receptors. CTCs that clustered with neutrophils expressed higher levels of cell-cycle progression and higher proliferation marker protein Ki67 compared to single CTCs[79]. In clusters, CTCs might be surrounded and protected from the immune surveillance[48]. In addition, these cells may help during extravasation by liberating cytokines that induce the dissociation of cell junctions, facilitating the infiltration of CTCs in the tissue through the vascular endothelium[80]. We know that these cytokines can also induce the EMT. For example, activated platelets secrete TNFα and TGFβ that regulates the EMT and are also associated with the inflammatory process[81].

1.8.1.3 Clinical impact of CTCs in lung cancer:

CTCs in early NSCLC: The prognostic value of CTCs in early NSCLC has been evaluated only in a few studies to date. Among them, one study in resectable in 210 NSCLC patients reported that preoperative CTCs, isolated with CellSearch Assay™ and the Isolation by size of tumor cells (ISET), were prognostic factors for disease-free survival (DFS)[82]. Moreover, our group demonstrated first in 56 [83] and then in 102 NSCLC patients that CTCs found after surgical resection were significantly correlated with shorter RFS[84]

Interestingly, most studies performed in resectable NSCLC patients evaluated the presence of CTCs in the pulmonary vein, showing similar results[85–88]. One study compared the CTCs and CTC clusters found in the pulmonary vs. peripheral blood[89]. This study showed not only the prognostic value of CTC microemboli but also that CTC clusters display activated immune and invasion pathways. This suggested a survival advantage in the circulation and an enhanced therapeutic resistance.

CTCs in advanced NSCLC: Similar studies have been conducted in locally advanced NSCLC, where there is further evidence of the prognostic role of these cells, as some meta-analysis have reported[90]. CellSearch and ISET have been also compared in a cohort of 40 locally advanced and metastatic NSCLC patients. In this case, ISET detected higher number of CTCs including EMT CTCs and clusters[74]. Most studies several studies have evaluated the presence CTCs in different populations across the globe and its association to chemotherapy response and worse prognosis[91–94].

Methodological issues: Most of these studies have evaluated the role of CTCs in advanced NSCLC, reporting little evidence in early NSCLC. Moreover, high percentage of them rely on the CellSearch technology, which use has been approved by the US Food and drug administration in breast, prostate or colorectal cancers, is not so well accepted in NSCLC[95]. This system isolates CTCs by immunomagnetic selection of EpCAM expressing cells[96]. A membranous protein which levels are highly decreased during the EMT. Due to the common EMT phenotype in lung cancer, low EpCAM CTCs might escape this isolation and as a result, highly different rates of CTC are observed in NSCLC patients[93]. As an EpCAM non-reliant methodology, ISET has been reported to outperform CellSearch. This technology separate CTCs from white blood cells, which are smaller, based on size filtration of blood cells through 8µm pores[97]. CTC size have been usually reported to range from 10-25µm diameter[98]. However, some studies have reported the presence of smaller CTCs with the same size as white blood cells[93], or even CTCs of 4-6µm diameter that could be lost during the ISET selection[96,99].

In consequence, there is a considerable need to perform further research in NSCLC, especially in early stages, as well as to improve CTC isolation technologies. This would allow researchers to identify higher number of CTCs with a wider range of phenotypes to finally prove their clinical validity and utility.

1.8.2 Extracellular vesicles

The extracellular vesicles (EVs) are another interesting biomarker of the liquid biopsy family. EVs are double-membrane structures of 20 – 2000 nm liberated by cells into the extracellular media. These vesicles are involved in intercellular communication by the transmission of the molecular cargo from the donor to the receptor cell. Most cells are able to release EVs of heterogeneous size, composition and intracellular origin.

Initially, EVs were simply considered as a mechanism by which cells would dispose waste and unwanted compounds or as vesicular remains of apoptotic cells. Now, we know that EVs are implicated in a wide spectrum of cellular processes in perfectly healthy cells, apart from other secretory vesicles of specialized cells[100]. EVs can be divided into two broad subgroups based on the mechanism of generation and their size. The major subgroup includes vesicles from 150 nm to 1-2 µm in diameter, commonly known as microvesicles (MVs) while the second comprises vesicles from 20 to 150 nm in diameter, referred as exosomes.

1.8.2.1 EVs formation and release

MVs are directly generated by outward budding of the plasma membrane while exosomes are formed as intraluminal vesicles (ILVs) by the invagination of the early endosome membrane and multivesicular endosomes (MVEs). MVEs can fuse either to the lysosome, for content degradation, or to the plasma membrane for exosome release[101]. MVEs are trafficked to the membrane in a Rab27 dependent manner while lysosome fusion is mediated by Rab7. This way, MVEs can be regulated by Rab7-27 inhibitors to increase or reduce exosome production[102] (**Figure 8)**.

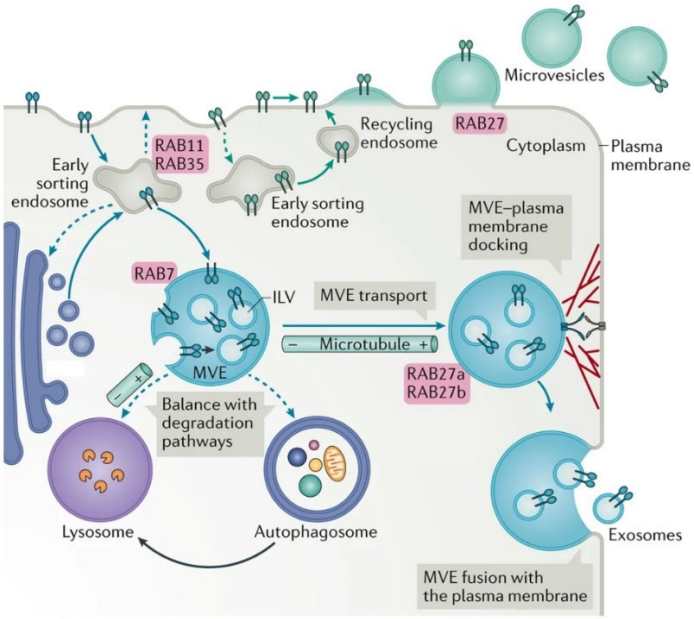

Figure 8: Origin and release of EVs[100].

1.8.2.2 Molecular composition of EVs and cargo:

The content of EVs may vary with respect to the cells of origin and the conditions. EVs contain proteins, lipids, and nucleic acids, usually reflecting the content of the cell. Commonly found proteins are Alix, Tsg101, and Hsp70 that are associated to the endosomal pathway and EV biogenesis, tetraspanins such as CD9 or CD63, or proteins involved in antigen presentation, including MHCI and MHCII. Normally, lipid composition is also shared with the cell of origin, however, it depends on the type of vesicle and the mechanism of biogenesis. Exosomes are usually enriched in phosphatidylserine but have less phosphatidylcholine in comparison to the cell membrane[103]. EVs can also transport nucleic acids, in particular, EVs are enriched in small RNAs such as miRNAs.

In general, EVs cargo is selectively incorporated by an active incorporation or proteins, nucleic acids, or proteins into ILVs and MVEs[104]. Post-transcriptional modifications of miRNAs also contribute to their packaging. Indeed, some studies have shown that miRNAs are packaged into EVs by mechanisms that rely on own miRNA levels. Thus, reflecting the levels of the cytoplasmic content of the cell[103]. Moreover, EV composition is known to regulate their own function and fate[100].

1.8.2.3 EV fate and cellular targeting:

Once the EVs are charged and released they can travel in the biological fluids to deliver their content into other cells. EVs uptake is not yet well understood but it is thought to rely on the ability of EVs to bind to target cells. EVs can attach to the surface or they can be uptaken into endosomes. In both situations, EVs release their content into the cytoplasm by membrane fusion[105]. Exosome tropism to a specific type of cell has been related to the proteins enriched in the exosome and the cell plasma membrane such us tetraspanins, integrins, or proteoglycans. Evidence suggest that these molecules direct organ-specific adhesion by mutual recognition. Indeed, they have been related to the preformation of the metastatic niche, helping in the future colonization by CTCs[106].

1.8.2.4 EV as biomarkers in cancer:

In cancer, EVs play a role in different aspects as tumor promotion, invasion, angiogenesis, or apoptosis resistance[107]. EVs production is increased due to instability of oncogenes, or as a result of stress responses due to hypoxia, acidosis or immune inflammation. In addition, chemotherapeutic drugs and radiotherapy treatment increase the production of EVs in cancer cells[102]. As mentioned above, EVs can modulate the tumor microenvironment and the pre-metastatic niche by the specific delivery of proteins, cytokines, or miRNAs that regulate angiogenesis, EMT, or contribute to the tropism for the metastatic disease[108].

The clinical utility of EV miRNA as lung cancer biomarkers has been extensively assessed during the last decade as this review summarize[109]. For example, EVs miRNAs extracted from plasma have been proposed as lung cancer diagnostic and prognostic biomarkers in many studies. One of the largest, including 141 ADC and 124 healthy controls, found differential expression of miR-19, 21, 221, 30a between both populations, potentially acting as diagnostic biomarkers[110]. EVs can act as biomarkers of the tumor activity due to the specific selection of their cargo. High similarity was observed between the expression signature of miRNAs in the tumor tissue and in circulating EVs, suggesting that EVs might be useful tissue surrogates[111]. Other study reported that expression of EV-derived miR-30e and Let-7f identified patients with shorter survival[112].

Liquid biopsy studies usually study circulating MVs and exosomes as current purification methods and biomarkers do not fully discriminate between the two types[101]. This way, the term “exosomes” has been widely confused across the literature, with studies reporting exosomal results when actually isolating general EVs. The exact origin of EVs is only determined when the molecular machinery required for formation or cargo is interfered[102]. To fix these problems, the International Society of Extracellular Vesicles (ISEV) has elaborated a guide with rules for a good EVs classification. These guidelines are an update from the ones from 2014 with the necessary considerations to perform proper EV enrichment, protein characterization, and functional assays[113]. The publication of these guidelines and the standardization of the EV assays open the possibility for a promising use of EVs as liquid biopsy biomarkers in NSCLC.

1.9 Lung cancer biomarkers

Many genes have been classically studied in NSCLC tissues due to their role in proliferation, invasiveness, EMT, metastasis or therapy resistance. In this work, we focus on four genes:

Axl receptor tyrosine kinase (*AXL*): *AXL* is involved in tumor growth and invasiveness by regulating processes as the EMT. This gene is overexpressed in solid tumors including lung cancer[114] and it has been linked to lymph node involvement and more advanced stages[115]. Moreover, it plays an important role in the modulation of the antitumor immune response[116].

Interleukin-6 receptor (IL-6R)*: IL-6* is an immune cytokine regulator that when binds the IL-6R modulates immune and inflammatory responses. Moreover, they act in the STAT3 pathway promoting proliferation and migration of lung cancer cells[117] and it has been linked also to the activation of the EMT[118]. Its up-regulation has been associated to the progression, therapy resistance and worse survival in NSCLC[119].

MET proto-oncogene receptor tyrosine kinase (*MET*): This gene encodes a transmembrane receptor tyrosine kinase protein, activated by the hepatocyte growth factor (HGF) ligand and involved in several important cancer pathways as the PI3K/AKT or the STAT signaling pathways[120]. In lung cancer, its overexpression increases proliferation, motility, angiogenesis and the EMT. In particular, overexpression of *MET* has been associated with poor prognosis in NSCLC patients[121]. MET signaling dysregulation in NSCLC occur through several mechanisms as MET or HGF protein overexpression, *MET* mutations, amplification, or rearrangements. Targeting MET is a promising strategy to control the EMT and the metastasis in NSCLC tumors[120].

Glyceraldehide-3-phosphatase dehydrogenase (*GAPDH*): This gene plays an important role in glucose metabolism and had been classically used as a housekeeping gene in expression studies. Nevertheless, it is overexpressed in tumors such as NSCLC and it has been associated to worse survival in resected NSCLC patients[122]. *GAPDH* has also been described to interact with the transcriptional factor Sp1, enhancing Snail expression, thus boosting the EMT[123].

β2-Microglobulin (*B2M*)*: B2M* is a well-known housekeeping gene expressed in all cells that encodes one HLA-I unit. It has been extensively used as a housekeeping gene in early NSCLC expression studies[124,125].

1.10 miRNAs

microRNAs are small non-coding RNAs of approximately 22 nucleotides in length. Genes that encode miRNAs represent around 1% of the genome and they can be found as individual genes or as groups that can encode up to hundreds of miRNAs. High percentage of miRNAs are located in fragile chromosomic sites, frequently deleted or amplified in cancer. This way, the aberrant expression of miRNAs has been also associated to genomic changes caused by carcinogenesis, suggesting their potential role as cancer biomarkers.

miRNAs are important modulator of cancer processes. Indeed, they are involved in most biological processes, from cell cycle or cellular differentiation up to autophagy and apoptosis. miRNAs regulate gene expression of genes at the post-transcriptional level. They are predicted to regulate 60% of all human genes by binding to specific target sites[126]. When miRNAs targets oncogenes are called tumor suppressor miRNAs and if they target tumor suppressor genes are denoted oncomiRNAs[127].

1.10.1 miRNA biogenesis

In general, miRNAs encoded as monocistronic, polycistronic, or intronic genes are first processed in the nucleus by the RNA polymerase II into primary miRNA (pri-miRNA) transcripts containing a 5' 7-methilguanosine cap structure and the 3' poli-adenine tail (**Figure 9**). These transcripts are kilobases long and have a hairpin structure. Then, the pri-miRNA is cropped by the RNase III enzyme Drosha, liberating the stem of the hairpin. This enzyme functions as a complex with the double-stranded RNA-binding protein DiGeorge critical region 8 (DGCR8), that recognizes the proximal 10 base pair of the pri-miRNA. As a result, the complex liberates the precursor miRNA (pre-miRNA), with ≈65 nucleotides long that it is characterized by a 5' phosphate and a 3' OH with overhanging 2-3 nucleotides. These nucleotides are recognized by the Exportin-5 and Ran-GTP that enable the transport of the pre-miRNA to the cytoplasm for its maturation (**Figure 9**)[126].

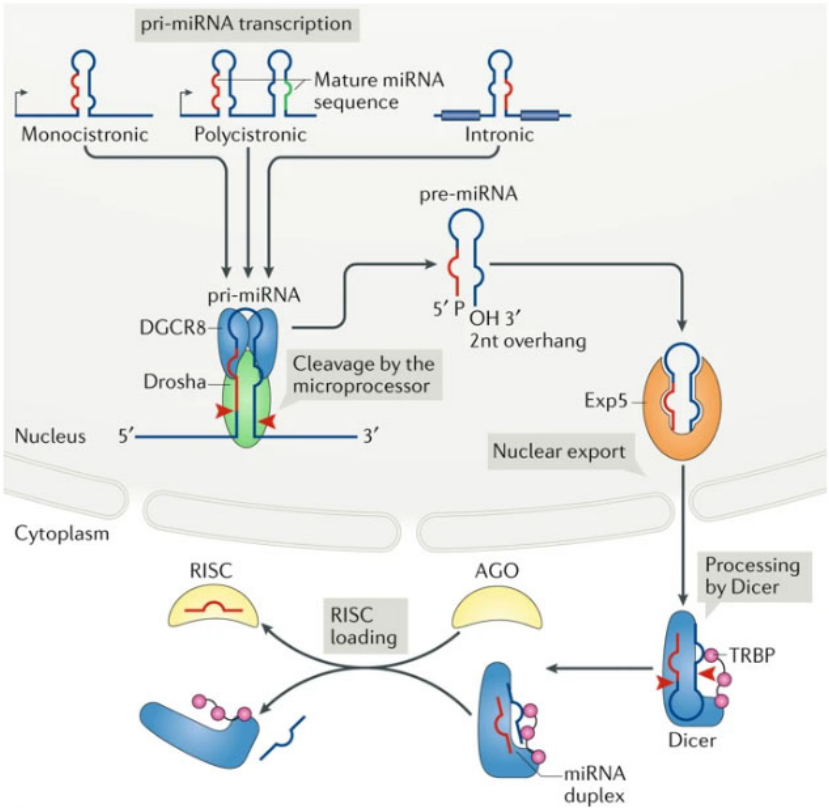

Figure 9: miRNA processing[128].

In the nucleus, the pre-miRNA is processed into a ≈22 nucleotide double-stranded miRNA by the RNase III enzyme Dicer that cleaves the stem close to the terminal loop. Dicer interacts with the transcriptional response RNA-binding protein (TRBP), which contribute to the activity of the miRNA. Afterwards, Dicer and TRBP also associates with Argonaute (Ago) proteins that will separate the two strands of the miRNA duplex. One strand, deemed as the guide strand and mature miRNA, will be selected to form the RNA-induced silencing complex (RISC) with Ago; while the other (known as passenger strand) will be degraded (**Figure 9**)[105]. This selection is partly based on the thermodynamic stability at the 5' end of the miRNA duplex. Generally, the strand with lower 5' stability or 5' uracil is selected as the guide strand. This miRNA will guide the RISC to target sequences of mRNAs of imperfect complementarity[129].

1.10.2 miRNA function

There are four Ago proteins (Ago1-4) in mammals, being Ago2 the most abundant and the only one able to degrade the mRNA when the guide miRNA and mRNA sequences are fully complementary. The nucleotides 2-8 in the 5' end of the miRNA are called the "seed" and are considered the main criterion in the mRNA recognition. Moreover, nucleotides ≈13-16 are called the "supplementary region" and generally add some complementarity to the mRNA. miRNAs target sites usually located in the 3' UTR of the mRNA due to high complementarity with the seed region. The degree of complementarity between the two sequences determines the fate of the mRNA. When the miRNA-mRNA complementarity is full, Ago2 endonuclease activity is enhanced and the mRNA is cleaved. However, this full interaction destabilizes the union between Ago2 and the miRNA guide 3' end, leading to the miRNA degradation. On the other hand, most miRNA-mRNA interactions are not fully complementary due to central mismatches. In consequence, Ago2 endonuclease cleavage is scarce, the RISC complex can be formed by all Ago proteins, and mRNA translation is inhibited by blocking ribosome access[105].

miRNAs have a huge impact on gene expression as a single miRNA can target hundreds of mRNAs. Thus, the modulation of a single miRNA can have a significant impact on processes as cancer by the post-transcriptional regulation of specific related mRNAs[130]. The identification of miRNA targets is essential to the identification of its function. To date, the prediction of those mRNAs is still challenging since miRNA-mRNA interactions are highly complex and further research is needed to fully understand how they are regulated[129].

1.10.3 miRNA subcellular compartmentalization

Besides their location in the cytoplasm, miRNAs and RISC complexes can be found in the nucleus and other cellular compartments. As reported in EVs biogenesis, miRNAs can be observed in MVEs and be exocytosed in EVs to mediate cell-to-cell communication[105]. miRNAs can be secreted and found in body fluids, either as free miRNAs due to passive liberation after cell death, encapsulated into EVs, or associated with proteins such as Ago or HDL[131].

1.10.4 miRNAs as biomarkers in lung cancer

Most studies have analyzed miRNAs expression in the tissue with lesser extent in free-miRNAs and EV miRNAs. We know about the disadvantages of tissue sampling but no real consensus has been reached if free-miRNAs or EV miRNAs are better biomarkers. To the contrary, the lipid membrane is thought to exert more protection to miRNA from RNases found in the blood. EV production is a purpose-driven communication process increased in cancer cells which involves the selective package of miRNAs, in contrast to free-miRNAs that might just be released during apoptosis. For these reasons, we believe that EV miRNAs are more stable and tumor-specific than circulating miRNAs to be used as liquid biopsy biomarkers in NSCLC.

Here, we summarize the described roles of the selected miRNAs that will be studied in NSCLC patients (**Table 1**):

miR-21: This miRNA is one of the most studied miRNAs and its overexpression has been associated with poor survival[132] and platinum resistance in resected tissues. It has been also linked to the radioresistance mechanism by suppressing PTEN and PDCD4 signaling pathways, increasing migration, proliferation and invasiveness in NSCLC cell lines[30,133]. Mouse models showed that EV miR-21 binds to macrophages TLR-8 and activate the inflammatory response mediated by IL-6 and TNF-α, promoting tumor metastasis[134].

miR-222: This miRNA has been linked to an increased resistance to EGFR TKIs by the overexpression or amplification of *MET* and the initiation of the EMT[135]. However, one study

reported an anti-oncogenic role of this miRNA. In this study, miR-222 reduced growth in NSCLC cell lines by inducing apoptosis or a S-phase arrest during mitosis, also enhancing the sensitivity to s-phase drugs such as cisplatin but not to M-phase drugs as paclitaxel[136].

miR-24: The down-regulation of this miRNA suppressed proliferation and invasion in NSCLC cell lines[137]. Indeed, its down-regulation has been associated to enhanced cisplatin chemosensitivity[138].

miR-30c: As miR-222, miR-30c was associated to EGFR TKIs resistance associated with *MET*[135]. On the other hand, other study attributed a tumor suppressive role to this miRNA, where its down-regulation promoted NSCLC invasion[139].

MiR-155: As miR-21, it has been associated to worse prognosis, promoting proliferation and invasion in NSCLC tissues by targeting *PDCD4*[140]. It also plays a role in radioresistance, switching cell metabolism from normal oxidative metabolism to anaerobic glycolysis, even in the presence of oxygen[141]. Interestingly, other studies have reported a tumor-suppressor role of miR-155 in NSCLC[142]. miR-155 expression in tissues was a prognostic biomarker of bad response in ADC while of good response in SCC[143]. In addition, this miRNA plays an important role in different steps of innate and acquired immune responses[144]

miR-218: miR-218 is downregulated in lung cancer tissues and correlates with good prognosis, acting as a tumor suppressor by targeting the IL-6/STAT3 pathway[145], *HMGB1*, an important promotor of the autophagic process[146], and *EGFR*[147]. This way, its overexpression has been associated to the inhibition of proliferation, migration and invasion in NSCLC cell lines. It has also been associated to carboplatin resistance via the regulation of apoptosis through Mcl-1 and survivin[148].

miR-200c: This miRNA, as other members of the miR-200 family, has been related to the repression of EMT by targeting Zeb1, reducing the invasive and metastatic capacity of lung cancer tumors[149].

miR-375: This miRNA have a tumor-suppressive role with an associated good prognosis[150].

miR-129: miR-129 is downregulated in NSCLC tissues and a prognostic factor for good prognosis, showing lower levels in patients with shorter OS. It has also been reported to target *HMGB1* in lung cancer cells[151].

miR-186: The expression of this miRNA is reduced in NSCLC as well as in other solid tumors. The downregulation of this miRNA was associated to the inhibition of proliferation and apoptosis induction in NSCLC[152]. To the contrary, it's up-regulation has also been associated to ADC and SCC carcinoma tissues and the promotion of tumor proliferation, invasion and migration by targeting *PTEN* in ADC cell lines[153].

miR-16: miR-16 has been widely used as a housekeeping in miRNA studies in several carcinomas and EV-miRNAs including NSCLC[154,155].

As we can observe in the **table 1**, most miRNAs have been reported to have a dual role in lung cancer regarding the targeted gene.

Table 1: The role of miRNAs in NSCLC.

miRNA	Role	OncomiRNA and tumor suppressor miRNA.
miR-21	Poor survival, platinum and radio resistance, and pro-tumoral inflammatory response	OncomiRNA
miR-222	- Increased EGFR TKI resistance and EMT. - Growth suppression by S-phase arrest.	OncomiRNA and tumor suppressor miRNA.
miR-24	Enhanced proliferation and invasion. Cisplatin resistance.	OncomiRNA
miR-30c	- Increased EGFR TKI resistance. - Reduced cell invasion. Target*s Beclin-1, CDK1* and *MAP1LC3B*	OncomiRNA and tumor suppressor miRNA.
miR-155	- Poor survival, enhanced radioresistance. Immune responses. - Predictor of good response	OncomiRNA and tumor suppressor miRNA.
miR-218	Good prognosis by inhibiting autophagy and EGFR. Carboplatin sensitivity.	Tumor suppressor miRNA
miR-200c	EMT, invasion and metastasis inhibition.	Tumor suppressor miRNA.
miR-375	Good prognosis	Tumor suppressor miRNA.
miR-129	Reduced proliferation and invasion through autophagy inhibition. Good prognosis. Target*s Beclin-1, CDK1, HMGB1* and *MAP1LC3B*	Tumor suppressor miRNA
miR-186	- Reduced proliferation and metastasis - Promoting proliferation by targeting *PTEN.* Targets *RAF1, CDK1, KIF11*	OncomiRNA and tumor suppressor miRNA.
miR-16	House-keeping	

2. Hypothesis

Lung cancer is the most frequent neoplasia and the leading cause of cancer related death in the world. NSCLC is the most common form covering 80% of all lung cancer cases. Surgical techniques, chemotherapy, radiotherapy, targeted therapies and immunotherapy treatments have evolved enormously during the last years. However, local progression and metastasis are still highly present and the survival rates of NSCLC patients are low. In order to improve the survival, the current WHO guidelines recommend a more personalized strategy, starting from an accurate subclassification of NSCLC as well as the discovery and validation of new prognostic and predictive biomarkers that would stratify patients for a better management and treatment selection.

New NGS studies have revealed very different molecular behavior between histological subtypes and the importance of the intratumoral heterogeneity with its therapeutic potential. We know that tumors are composed by different subpopulations of cells and only some of them might have metastatic potential.

CTCs have been described to contribute to the metastatic process in many solid tumors, including NSCLC. We know that these cells, shred from different regions within the tumor and may suffer phenotypical changes as the EMT. As a consequence, heterogeneous populations of these cells can be found in a patient. This way, CTCs could act as surrogates of the clinically relevant tissue subpopulations and face the challenges of tissue biopsies and both the spatial and the temporal intratumoral heterogeneity. To date, many studies have evaluated the presence of CTCs and its association to chemotherapy resistance in advanced NSCLC. However, to the best of our knowledge, only a few have reported their prognostic role in early stages and none in advanced patients under concomitant ChT-RT. Thus, further evidence is needed to validate the clinical use of CTCs in NSCLC.

In fact, most of the reported studies were based on immunomagnetic isolation of EpCAM positive cells. A membranous protein lost during the EMT. As a result of the EMT, which is particularly common in NSCLC, CTCs lose epithelial markers in exchange of mesenchymal ones. However, there is evidence that the cytoplasmic cytokeratin-7 is not reduced, or only in a lesser extent, in pulmonary adenocarcinomas. Thus, we thought that the use of an isolation methodology based on multi-cytokeratin antibodies, such as the one from Miltenyi Biotec, would be more appropriate. On the other hand, miRNAs are important modulators of cancer processes, they regulate gene expression in a broad and fast way and are therefore responsible for phenotypical changes of tumor cells. miRNAs have been vastly studied in the tissue but they can also be selectively encapsulated and found in EVs circulating in the blood, also acting as tissue surrogates. This way, EV derived miRNAs are potential liquid biopsy biomarkers in NSCLC.

In this context, this thesis encompasses two independent studies, one including early stage NSCLC patients undergoing surgical resection and a second study enrolling advanced NSCLC patients with concomitant ChT-RT.

2.1 Early NSCLC patients

In early stages of NSCLC (I-IIIA) surgery is the mainstay of treatment and the addition of adjuvant platinum-based chemotherapy is associated with only little benefit in the survival of these patients. Even after complete resection, relapse is developed in a high percentage of them. For these reason, new prognostic biomarkers are highly needed.

Despite recent studies have revealed the different molecular behavior between ADC and SCC subtypes the reason of their differences in prognosis and progression are not clear yet. miRNAs are probably involved in this heterogeneity as they responsible for phenotypic changes in the tissue. Moreover, heterogeneous populations of CTCs can be found in the blood and they may have different metastatic ability and prognostic potential. Hence, we hypothesize that there are the specific genetic and miRNA profiles in ADC and SCC responsible of generating the diversity of CTCs found in these patients. Finally, the presence of specific subtypes of CTCs will be associated with the relapse, acting as prognostic biomarkers in early ADC and SCC patients.

2.2 Advanced NSCLC patients

Most NSCLC patients are diagnosed at an advanced stage, when surgery is not an option. In these cases, the standard first line treatment is platinum-based chemotherapy combined with radiotherapy. However, treatments usually fail and PFS and OS rates are especially low. Then, there is an urgent need to find and validate new prognostic biomarkers. Despite there is still controversial evidence about how autophagy acts during tumor cell survival, recent evidence has linked the upregulation of autophagy to an increased resistance to cisplatin, vinorelbine or radiotherapy treatments.

In this context, we hypothesize that the expression not only of autophagic proteins in the heterogeneous populations of CTCs, but also of EV miRNAs will reveal the autophagy status and the molecular complexity of the tumors. This way, CTCs and EV miRNAs during the follow-up will shed light upon the mechanism of resistance and act as as prognostic biomarkers in advanced NSCLC patients.

3. Objectives:

3.1 Objectives study 1 (Early NSCLC population):

Main objective: The main objective of this sub-study was to identify tissue gene and miRNA signatures related to the release of different CTC subpopulations and their role as prognostic biomarkers in ADC and SCC patients undergoing surgical resection.

Specific objectives:

- Investigate the association between different subpopulations of CTCs before and after surgical resection and the clinical-pathological characteristics.

- Evaluate the CTC dynamics before-after surgical resection and adjuvant treatment.

- Identify specific tissue gene and miRNA signatures related to the presence of different subpopulations of CTCs.

- Evaluate the prognostic role of different subpopulations of CTCs along the treatment.

- Evaluate the prognostic role of the expression of specific tissue genes and miRNAs.

3.2 Objectives study 2 (Advanced NSCLC population)

Main objective: The main objective of this second sub-study was to identify miRNA signatures in extracellular vesicles related to the presence of different CTC subpopulations and their role as prognostic biomarkers in advanced NSCLC patients undergoing concomitant ChT and RT.

Specific objectives:

- Investigate the association between different subpopulations of CTCs before, during and after the ChT-RT treatment and the clinical-pathological characteristics.

- Evaluate the CTC and dynamics along the follow-up.

- Evaluate the EV miRNA dynamics along the follow-up.

- Identify specific EV miRNA signatures related to the presence of different subpopulations of CTCs.

- Evaluate the prognostic role of different subpopulations of CTCs along the treatment.

- Evaluate the prognostic role of the expression of specific EV miRNAs.

4. Material and methods

4.1 Study design and patient population

4.1.1 Study 1: Early NSCLC population

We conducted a prospective observational cohort study in NSCLC patients who underwent anatomical pulmonary resection and systematic lymph node dissection with curative intent. Lung tissue was extracted at tumor resection and peripheral blood was collected before surgery, one month later and 6 months later (**Figure 10**). The study population consisted in early stage (I-IIIA) NSCLC patients diagnosed with resectable tumors and who were subjected to a complete tumor resection in the Thoracic Surgery Unit of the University Hospital Virgen de las Nieves, Granada (Spain), between November 2012 and February 2015. The study also included a group of lung cancer initially suspicious patients, that were confirmed as non-tumor lung malignances at the resection, and were considered as the control group for tissue characterization and CTC negative group.

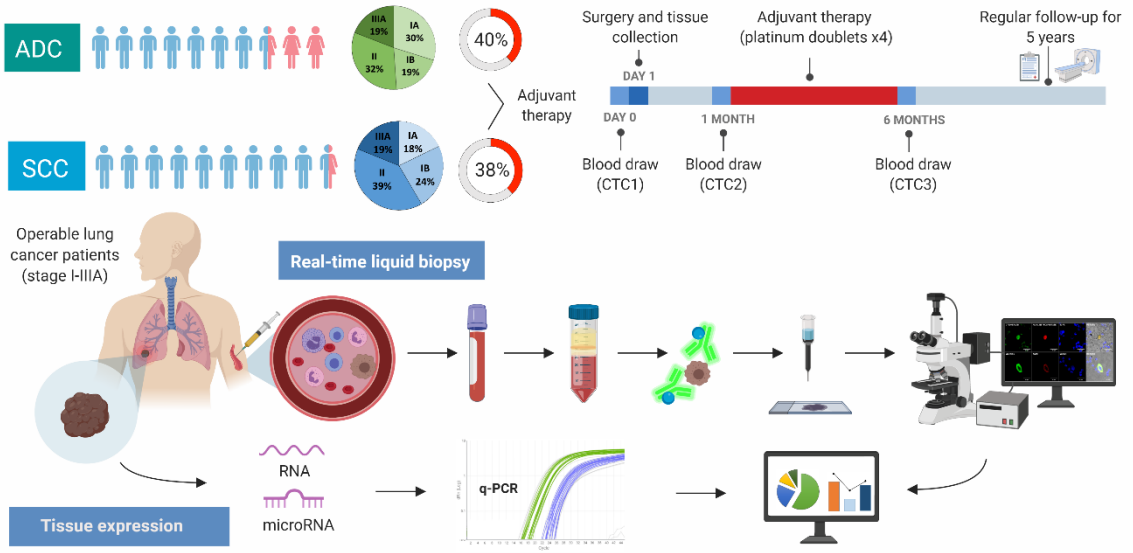

Figure 10: Study design 1. Early NSCLC population. The study 1 enrolled a cohort of ADC (n=47) and other of SCC (n=50) patients with similar distribution by gender, stage and percentage of patients receiving adjuvant treatment. Baseline blood samples (CTC1) were collected before the surgery, beside the tissue collection, one month after (CTC2) and 6 months later (CTC3) during the adjuvant treatment in those susceptible cases. Presence of different subpopulations of CTCs and the tissue RNA and miRNA expression were statistically compared with the clinical variables and the prognosis [Created with BioRender] [156].

This prospective study was approved by the Institutional Ethical Committee (Comité de Ética de la Investigación de Centro de Granada, CEI-GRANADA) on July 26, 2012. Written informed consent was signed by all patients prior to the inclusion in the study. Clinical and laboratory procedures were completed under good clinical practice and laboratory practice conditions in accordance with local standards. Inclusion criteria were patients older than 18 years old at the time of diagnosis, stage I-IIIA NSCLC, ECOG Performance Status ≤2, and in which complete resection was possible. Briefly, complete resection was defined as demonstrating cancer-free surgical margins microscopically and systematic ganglionic dissection. Exclusion criteria were concurrent or previous tumor history, prior induction chemotherapy or radiotherapy, or death within 30 days from the surgery.

Study protocol

Pathological stage was defined according to the international tumor-node-metastasis (TNM) system seventh edition[157] that was the current version at the time of sample collection and histological diagnosis was posed using the World Health Organization classification. Indication for adjuvant treatment was evaluated according to Local Tumor Committee and the ASCO guidelines[158] one month after the surgery. In those susceptible cases, adjuvant treatment started always after second CTC evaluation and consisted in 4 cycles of platinum doublets. Follow-up schedule was usually performed for this type of patients, consisting in a first evaluating one month after surgery, then one every 3-6 months with at least a positron emission tomography - computed tomography (PET-CT) of the thorax and abdomen per year. Recurrence was diagnosed based on radiological criteria and (PET), with histological confirmation when possible. Clinical outcomes were evaluated in terms of RFS and OS. RFS was defined as the time elapsed from surgical resection until first recurrence (loco-regional or distant metastasis) or death due to any cause, while OS was the time elapsed from surgical resection until death due to any cause.

Samples

Samples from every patient consisted in fresh tissue from the tumor pulmonary surgical resection, that was stored at -80°C in RNA later Tissue Protect Tubes (Qiagen), and 15 mL of peripheral blood, collected in EDTA tubes, stored at room temperature, and processed within 4 hours.

4.1.2 Study 2: Advanced NSCLC population

We also conducted a prospective observational cohort study in unresectable advanced NSCLC patients. In this case, individuals were enrolled and subjected to concomitant radiotherapy and chemotherapy. Peripheral blood samples were collected before the initiation of the treatment, three weeks after it (during the treatment), at the end of the treatment (2 months), and finally 10 months later (**Figure 11**). The study population included locally advanced inoperable (IIIA-IIIB) NSCLC patients and metastatic NSCLC patients (IV), who were treated with concomitant radiotherapy (RT) chemotherapy (ChT) (vinorelbine plus cisplatin or taxol plus carboplatin in the University Hospital Virgen de las Nieves, Granada (Spain) between July 2015 and May 2019. Moreover, the study enrolled a group of 15 healthy donors, with no history of tumor malignances, who were used control branch for standard EV miRNA expression.

Inclusion criteria were patients older than 18 years old at the time of diagnosis, unresectable stage IIIA-IV NSCLC confirmed by histology, ECOG Performance Status ≤2, and acceptance to receive concomitant ChT and RT. Exclusion criteria were patients susceptible to palliative treatment, resectable but medically inoperable patients treated with radical radiotherapy. In the same way, this prospective study was approved by the Ethical Committee of the University Hospital of Granada, Spain. Written informed consent was signed by all patients prior to the inclusion in the study. Clinical and laboratory procedures were completed under good clinical practice and laboratory practice conditions in accordance with local standards.

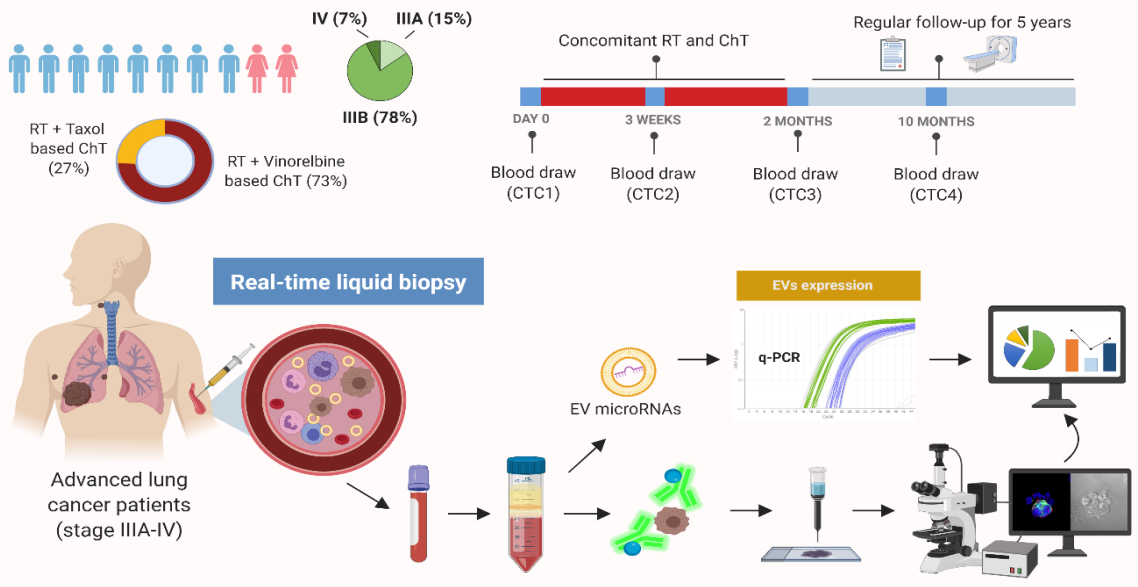

Figure 11: Study design 2. Advanced NSCLC patients. The study 2 enrolled a cohort of unresectable NSCLC patients (n=41) receiving concomitant RT and ChT. Blood samples were collected before (CTC1), during (CTC2), after the finalization of the treatment (CTC3) and 10 months after the initialization (CTC4). Presence of different subpopulations of CTCs and the EVs miRNA expression were statistically compared with the clinical variables and prognosis [Created with BioRender].

Study protocol

Pathological stage was defined according to the international TNM system seventh edition[157] that was the current version at the time of sample collection and histological diagnosis was posed using the World Health Organization classification. Indication for radiotherapy chemotherapy treatment was evaluated according to the Multidisciplinary Thoracic Pathology Committee or the Oncology Committee. Eligible individuals were treated with total dose of 60 Gy 3D radiotherapy (2Gy per day during 3 weeks from Monday to Friday) with concomitant 6 cycles of chemotherapy with cisplatin & vinorelbine (80 & 15 mg/m2) or carboplatin & taxol (45 mg/m2 & AUC 2). Follow-up schedule consisted in weekly evaluation, with a 3-week evaluation, a PET-CT of the thorax and abdomen after the end of the treatment and then according to standard recommendations. Clinical outcomes were evaluated in terms of RFS and OS. RFS was defined as the time elapsed from the start of RT-ChT treatment until first recurrence (loco-regional or distant metastasis or tumoral death, while OS was the time elapsed from the end of RT-ChT treatment until tumoral death.

Samples

Samples consisted in 20 mL of peripheral blood that were collected in EDTA tubes, stored at room temperature, and processed within 4 hours.

4.2 Cell culture

The following human tumor cell lines were acquired from ATCC: Lung adenocarcinoma cell lines A549, H1975, H820, H1299 and the human epidermoid carcinoma A431 cell line. A549 and A431 cells were grown in DMEM culture medium (Biowest), while H1975, H820 and H1299 cells were grown in RPMI-1640 with L-Glutamine (Biowest). Both culture media were supplemented with 10% of fetal bovine serum (Biowest), 100 U/ ml penicillin and 100 ng/ ml streptomycin (Biowest) and cells were grown in a humidified incubator with 5% CO2 at 37°C. When needed, cells were detached using Tryple Express (ThermoFisher), which is more delicate to cells than

trypsin or other dissociation reagents and better preserves the extracellular domains of transmembrane proteins.

4.3 CTC isolation and characterization

4.3.1 CTC enrichment and isolation

Blood samples were processed according to the density gradient centrifugation followed by CTC enrichment and characterization, stablished by our group[83]. Blood was diluted in 10 ml 1X phosphate-buffered saline (PBS) and slowly added to a 50ml tube containing a bottom layer of 10 ml Ficoll Histopaque®-1119 (density=1.119 g/ml) (Sigma-Aldrich), observing two different liquid phases. The tube was centrifuged at 700 x g for 45 minutes at 22°C with no brake, resulting in the formation of a cloudy interphase between the plasma and the Ficoll phases. This layer contained the mononuclear cells, granulocytes, and other cells of similar density as the CTCs (≈1.050 - 1.070 g/ml). This layer was carefully collected and washed with PBS1X in a 350 x g centrifugation during 10 minutes. Following procedures were made according to the adapted protocol of the Carcinoma Cell Enrichment and Detection Kit with MACS Technology (Miltenyi Biotec). Resulting pellet was resuspended in 5ml of 1X Dilution buffer and permeabilized for 5 min and fixed during 15 min with MACS CellPerm and MACS CellFix Solutions respectively. Then, the cell fraction was centrifuged again at 350 x g, for 10 minutes and then washed with 1X CellStain Solution with a similar centrifugation.

The cell pellet was resuspended in the approximately 100 µl remainder 1X CellStain Solution and incubated with 30 µl FcR Blocking Reagent and 30 µl of MACS Cytokeratin microbeads for 45 min at room temperature. These magnetic microbeads were labeled with a multi-cytokeratin-specific antibody (CK3-11D5) that recognizes the cytoplasmic cytokeratins 7, 8, 18 and 19. Afterwards, to detect cytokeratin positive cells by immunocytochemistry or immunofluorescence, 15 µl of Anti-Cytokeratin-FITC were added and the mix was incubated for additional 15 min in the dark. This suspension was washed with 4ml of 1X CellStain Solution and centrifuged again at 350 x g, for 10 minutes. Cell pellet was resuspended in a final volume of ≈150 µl and incubated with 2µl of Anti-FITC Alkaline-Phosphatase for another 15 min in the dark. Sample was adjusted with 1X CellStain Solution to a final volume of 500µl and passed through a previously washed MACS Cell Separation magnetic MS column that was supported by a MiniMACS separator. Then, the column was washed 3 times with 1X Dilution buffer, detached from the magnet separator and the enriched cell fraction was eluted and spun down onto 2 polylysine-coated glass slides using a cytocentrifuge (Hettich).

Samples from advanced NSCLC patients were processed in the same way until magnetic microbeads incubation. However, in this case, the sample was divided in two parts; one was processed as early NSCLC patients resulting in the called “slide 1”, while the other was processed in absence of Anti-Cytokeratin-FITC and Anti-FITC Alkaline-Phosphatase, resulting in called “slide 2”. Finally, all slides were air dried for at least 2 hours at room temperature before being maintained at 4°C for short term or -80°C for long term storage. Furthermore, in baseline samples (CTC1), MACS column elutes during washing, containing non-epithelial cells. These elutes were first centrifuged at 350 x g for 10 min and washed in 1X CellStain with another centrifugation. The pellets were incubated with primary Mouse Anti-Vimentin-FITC (Santa Cruz biotech® sc-6260) antibody in dark at 4°C overnight. Next day, cells were washed with CellStain1X and incubated with secondary Anti-FITC Microbeads (Miltenyi Biotec 130-048-701). Finally, each sample was eluted, as described above, through a MACS Cell Separation magnetic MS column, spun down on a new slide.

4.3.2 Immunocytochemical and chromogenic characterization:

In early NSCLC slides and slide 1 of advanced NSCLC, the area of interest containing the cells was surrounded with a hydrophobic pen (DAKO). Subsequently, it was washed in 1X PBS for 1 min and 100 µl of freshly prepared Fast Red TR/Naphthol AS-MX Substrate Solution was added to cell spot, incubating 15 minutes in humidity chamber. This was the base for CTC visualization, as the Fast-Red TR/Naphthol produced an insoluble red precipitate in reaction to Alkaline-Phosphatase. The slide was washed again, incubated with Mayer's hematoxylin for 30 seconds and finally washed in double-distilled water for 30 seconds and in tap water for another 30 seconds as a bluing reagent.

4.3.3 Microscopy

Early NSCLC slides and slide 1 of advanced NSCLC, which had been prepared for immunocytochemical and chromogenic visualization, were observed under a direct light microscope. After the identification of CTCs, positive slides were subjected to immunofluorescence methods.

4.3.3.1 Immunofluorescence microscope

Slides from early NSCLC patients (study 1) were characterized by immunofluorescence protocols (Nadal et al 2013) to check expression of EGFR. In summary, slides from epithelial CTCs destined to EGFR characterization were blocked in 1X CellStain with 10% Donkey serum and incubated with primary Goat Anti-EGFR (C-20) (Santa Cruz biotech® sc-31157) and secondary antibody Donkey anti-Goat 350 (Invitrogen A-21081). Finally, they were mounted with SlowFade™ Antifade Kit (Invitrogen S2828) and visualized under fluorescence microscope. EMT slides from early NSCLC patients were also incubated with primary Goat Anti-EGFR (C-20) but using Donkey anti-Goat 555 (Invitrogen A-21432) as a secondary antibody and VECTASHIELD mounting medium with DAPI (Vector Labs) to be visualized under fluorescence microscope.

4.3.3.2 Confocal microscope

Slides 1 from advanced NSCLC patients (study 2) were characterized by similar methods to evaluate the expression of Beclin-1. Previously described, they were blocked in 1X CellStain with 10% Goat serum and incubated with rabbit polyclonal anti-Beclin-1 (N-terminal) (Sigma-Aldrich B6061) and with Goat anti-Rabbit 405 (Invitrogen 35551). Finally, they were mounted with SlowFade™ Antifade Kit (Invitrogen S2828) and visualized under under confocal microscope.

Slides 2 from advanced NSCLC patients (study 2) were blocked in 1X CellStain with 10% Donkey serum and incubated with primary antibodies Goat Anti-EGFR (C-20) (Santa Cruz biotech® sc-31157) and Rabbit Anti-LC3B (ThermoFisher Scientific PA1-16930). Then, they were stained with secondary antibodies Donkey anti-Goat 555 (Invitrogen A-21432) and Donkey anti-Rabbit 647 (Invitrogen A-31573). They were mounted with VECTASHIELD mounting medium with DAPI (Vector Labs) and visualized under confocal microscope.

EMT slides from advanced NSCLC patients were processed as the same way as those from early NSCLC patients but observed under confocal microscope.

4.4 EVs isolation and characterization

EVs from cell cultures and patients were extracted by previously established protocols from our group[159,160]. Briefly, culture supernatants were collected and centrifuged at 3000 x g for 15 min, while blood samples were centrifuged at 1500 x g for 15 min for plasma collection. Then, supernatants were centrifuged at 10.000 x g during 30 min to eliminate cellular debris. They were transferred into 6ml polyallomer ultracentrifuge tubes, that were filled up with 1X PBS and ultracentrifuged (Thermo Scientific) in a TFT 80.4 Rotor (Thermo Scientific, UK) at 100.000 x g for 3 h at 4°C. After that, supernatants were removed and cultured EV pellets were directly lysed by adding ice-cold 1X Cell Lysis Buffer (Cell Signaling Technology) into the tube for western blot analysis or resuspended in 1X PBS for transmission-electron microscopy (TEM) and nanoparticle tracking analysis (NTA). EVs from advanced NSCLC patients were lysed with the Maxwell® RSC miRNA Tissue or Plasma and Serum Kit (AS1680) for subsequent miRNA analysis in patients.

According to the ISEV recommendations at that time[161], we characterized the nature of the EVs isolated by electron microscopy, NTA and the identification of specific markers by western blot analysis.

4.4.1 Transmission-electron microscopy characterization

EVs from culture cells were washed using 1% paraformaldehyde/PBS solutions and kept overnight at 4°C. Then, they were mounted onto carbon-coated electron microscopy grids and washed twice during 3 min with 1X PBS. EVs were stained with 2% uranyl acetate for 5 min, washed twice again and finally visualized in the LIBRA 120 PLUS Carl Zeiss SMT transmission electron microscope at the Centre for Scientific Instrumentation (University of Granada, Spain).

4.4.2 Nanoparticle tracking analysis

EVs size distribution and concentration were measured using a NanoSight NS300 system equipped with an LM14 violet 405nm laser module (Malvern Panalytical). EVs were diluted in PBS (1:500) for appropriate analysis and visualized at camera level 9 under control of a script, which included acquisition of 3 movies for 1 min at a fixed temperature of 22°C. Analysis was performed using NTA 3.2 software (Malvern Panalytical). Detection threshold was set at 2 and other settings were kept at default.

4.4.3 Western blot characterization

A549 and H1975 cells were washed with 1X PBS and lysed with ice-cold Cell Lysis Buffer (Cell Signaling Technology). EVs and cell lysates were sonicated for 30 seconds, centrifuged at 14.000 x g for 10 min at 4°C and supernatants were collected and stored for protein determination. Protein concentration was quantified by Pierce™ BCA Protein Assay Kit (Thermo Scientific), according with manufacturer's instructions in the Infinite® 200 PRO NanoQuant plate reader (TECAN).Thirty µg of protein from each sample were loaded into Mini-PROTEAN TGX 4–20% precast gels (Bio-Rad) and run at 120 mV until optimal separation. Then, proteins were transferred to nitrocellulose membranes in the X-Cell II Blot module (Invitrogen). Plotted membranes were blocked with 5% non-fat dry milk in Tris-buffered saline +1% Tween 20 for 1 hour and incubated with primary antibodies at 1:1000 dilutions in 3% non-fat dry milk in Tris-buffered saline +1% Tween 20 at 4°C overnight. Primary antibodies used were: mouse monoclonal anti-CD9 (Thermo Fisher Scientific - 10626D), mouse monoclonal anti-Hsp70 (BD Biosciences - 554243), mouse monoclonal anti-GM-130 (BD Biosciences – 610822). The next morning, the membranes were incubated in blocking buffer with secondary antibody Goat anti-mouse HRP-conjugated (Abcam - ab97023) at 1:5000 for 1 hour at room temperature. Finally, membranes were revealed using Clarity Max™ Western ECL Substrate (Bio-Rad) according to manufacturer protocol in the ImageQuant LAS 4000 (GE HealthCare Life Sciences).

4.5 Molecular characterization of genetic expression

4.5.1 Tissue Total RNA extraction

Frozen tissues were thaw on ice and a portion with the size of a rice grain was cut and used for total RNA extraction with TRIzol™ Reagent (Invitrogen), according to manufacturer's instructions. Briefly, the tissue fraction was incubated for 5 minutes in 400 µl of TRIzol™ and sonicated afterwards for 3 cycles of 30 seconds for tissue disruption in individual cells and homogenization. Mixture was incubated with 160 µl chloroform for 3 minutes and centrifuged at 12.000 x g for 15 min at 4°C, resulting in the separation into a lower red-chloroform phase, an interphase, and a colorless upper aqueous phase containing the RNA. The latter was mixed with 400 µl of isopropanol in a new tube that, when centrifuged again, will allow the RNA to pellet. This pellet was resuspended in 1ml 70% ethanol and centrifuged again to eliminate impurities. Supernatant was discarded, the pellet was air-dried and the RNA was resuspended in 50µl of RNase-free water. Finally, it was incubated at 55°C for 15 minutes and stored at -80°C until further applications.

4.5.2 EVs miRNA extraction

EVs miRNAs were also extracted and analyzed according to previous publications of our group[159,160]. Briefly, EV pellets were directly treated in the ultracentrifuge tubes according to the Maxwell® RSC miRNA Tissue or Plasma and Serum Kit (AS1680). This kit can also be used to purify total RNA, including miRNA, from EVs. Its methodology is based on the EV lysis and RNA binding to magnetic beads that allow the RNA extraction from the sample, with enhanced enrichment of miRNAs. Furthermore, it includes treatments with proteinase K and DNase to eliminate protein and DNA contamination.

4.5.3 Gene and miRNA retrotranscription

Total RNA concentration and purity were determined using NanoDrop 2000c Spectrophotometer (ThermoFisher Scientific). Samples were considered pure when a ≈2 A260/A280 ratio was found. 1µg of total RNA was converted to cDNA according to QuantiTect Reverse Transcription Kit (Qiagen) for subsequent RNA expression analysis. This kit includes a first step for genomic DNA elimination and the standard reverse transcription reaction that results in cDNA synthesis. For the miRNA analysis, 10ng of total RNA was converted to miRNA-cDNA according to TaqMan™ Advanced miRNA cDNA Synthesis Kit (ThermoFisher Scientific). This kit uses a first step of 3' poly-A tailing and 5' adaptor ligation to extend the mature miRNA. In addition, the last step consists in an amplification using Universal miR-Amp Primers, that recognize the universal sequences, added to all mature miRNA, to uniformly increase the amount of miRNA-cDNA, in this way, improving detection of low-expression miRNA targets.

4.5.4 Gene and miRNA selection and primer design

In the study 1, genes and miRNAs genes were selected based on their previously reported association with tumor migration, aggressiveness, treatment resistance, immune response and progression in NSCLC tumors. Genes were *AXL, IL6R, MET* and *GAPDH,* with *B2M* as housekeeping control while miRNAs were miR-21-5p, 222-3p, 24-3p, 30c-5p and 155-5p using 16-p as endogenous control.

In the study 2 including advanced NSCLC patients, some miRNAs were selected by previously reported NSCLC tumor association or by the identification of mRNA targets in important genes of the autophagy and vinorelbine radiotherapy resistance such as *BECN1, MAP1LC3B, CDK1, RAF1, or KIF11*. miRNAs were selected with the computation algorithm ENCORI, that predicts miRNA targets[162].

EVs studied miRNAs were miR-21-5p, 222-3p, 155-5p, 218-5p, 200c-3p, 375-3p, 129-5p, 186-5p and 30c-5p using miR-16-5p as endogenous control. Primers were designed spanning exon-exon boundaries (Sigma-Aldrich) while specific miRNA probes were acquired from ThermoFisher Scientific. Sequences can be found in **table 2**.

Table 2: Primers and probes sequences:

Gene	Primer or probe sequence		
AXL	F: CAATGGGGACTACTACCGCC	R: GAAGGACCACACATCGCTCT	
MET	F: CTGACTTGCTGAGAGGAGGC	R: GGTTTATCTTTCGGTGCCCAG	
IL6R	F: TCAGTGTCACCTGGCAAGAC	R: GGAGGTCCTTGACCATCCAT	
GAPDH	F: ATCACCATCTTCCAGGAGCGAGA	R: CATGGTTCACACCCATGACGAACA	
β2M	F: TGCTGTCTCCATGTTTGATGTATCT	R: TCTCTGCTCCCCACCTCTAAGT	
miR-21-5p	UAGCUUAUCAGACUGAUGUUGA	miR-218-5p	UUGUGCUUGAUCUAACCAUGU
miR-222-3p	AGCUACAUCUGGCUACUGGGU	miR-200c-3p	UAAUACUGCCGGGUAAUGAUGGA
miR-24-3p	UGGCUCAGUUCAGCAGGAACAG	miR-375-3p	UUUGUUCGUUCGGCUCGCGUGA
miR-30c-5p	UGUAAACAUCCUACACUCUCAGC	miR-129-5p	CUUUUUGCGGUCUGGGCUUGC
miR-155-5p	UUAAUGCUAAUCGUGAUAGGGGU	miR-186-5p	CAAAGAAUUCUCCUUUUGGGCU
miR-16-5p	UAGCAGCACGUAAAUAUUGGCG		

4.5.5 Quantitative Real Time PCR for mRNA and miRNA expression

Gene expression was measured using the PerfeCta® SYBR® Green FastMix®, ROX™ (Quanta Biosciences) on an Applied Biosystems 7900HT Fast Real-Time PCR System (Applied Biosystems). Expression levels of miRNAs were analyzed using TaqManTM MicroRNA assays probes and GoTaq® Probe qPCR Master Mix (Promega) in the same PCR system. In this case, the kit includes a CXR reference dye that acts as the ROX dye, maximizing the effectiveness of the reaction. PCR cycling protocol consisted in 2 minutes at 95°C initial denaturation and enzyme activation and 40 cycles including 15 seconds at 95°C for denaturation and 30 seconds at 60°C for annealing and extension. Each test was run in triplicates and included non-template controls (NTC). *B2M* was selected as the endogenous control for gene expression in resected tissue samples while miR-16 for miRNA normalization in tissue and EVs using Normfinder version 20[163]. Expression levels were calculated by the $2^{-\Delta\Delta Ct}$ method[164].

4.6 Statistical methods

Statistical analyses and graphs were performed using SPSS [SPSS Statistics for Windows, Version 22.0 (IBM Corp.) and GraphPad Prism Version 7.00 or 8.02 (GraphPad Software). CTCs and miRNAs were assessed as continuous (absolute number) and dichotomous (CTC: presence/absence and miRNA: high/low) variables. Gene and miRNA expression cut-offs were calculated with the Evaluate Cutpoints application for R[165]. The association between genes, miRNAs and clinical characteristics or CTCs was evaluated using non-parametric Mann-Whitney U and Kruskal-Wallis tests. Dynamics in paired samples were evaluated by Friedman test (continuous variables) and Cochran's Q test (binary variables). Categorical variables were compared by the Fisher's exact test and correlations were measured by Spearman's rank

correlation. Prognostic biomarkers for OS and RFS were evaluated with the univariate Kaplan–Meier (log-rank test) and univariate and multivariate Cox Proportional-Hazards Regression. We applied the criterion of more than a 10% change in the coefficient estimate[166]. *p* values < 0.05 were considered statistically significant.

5. Results

5.1 Study 1: Early NSCLC population

This prospective study enrolled a total of 97 consecutive early NSCLC patients, including 47 ADC (median follow-up 30.5 months, range 3-50) and 50 SCC patients (median follow-up 32 months, range 3-49). All patients were anatomo-pathologically diagnosed as resectable non-small lung cancer (stages I, II or IIIA) with no history of previous malignancy nor previous neoadjuvant treatment.

Clinical-pathological, treatment-related and prognostic characteristics of all the 97 NSCLC patients and divided by histological subtype are summarized in **Table 3**. Both groups had similar distribution of patients by age, smoking habits, and stage. However, the SCC was less common between women (p=0.005), presented larger tumor size (p=0.007) and consequently high positron emission tomography – maximum standardized uptake values (PET SUVmax) (p=0.002). This way, pneumonectomy was more common in SCC than in ADC as the type of surgical resection applied (p=0.024). After surgery, adjuvant chemotherapy was administered in 19 ADC and in 19 SCC patients, while adjuvant radiotherapy only in 3 patients in each group. Finally, during this study, 23 ADC and 19 SCC patients relapsed while 18 ADC and 19 SCC died.

Table 3: Clinical-pathological, treatment-related and prognostic characteristics in early NSCLC patients by histological type.

		NSCLC n = 97 (%)	ADC n = 47 (%)	SCC n = 50 (%)	*p*
Gender	Men	84 (86.6%)	36 (76.6%)	48 (96%)	**0.005***
	Women	13 (13.4%)	11 (23.4%)	2 (4%)	
Age (years)	Mean ± SD	66.13 ± 8.65	65.49 ± 9.64	66.7 ± 7.6	0.646
	<70	58 (59.8%)	28 (59.6%)	30 (60%)	0.966
	≥70	39 (40.2%)	19 (40.4%)	20 (40%)	
Smoking habits	Never smoker	9 (9.3%)	7 (14.9%)	2 (4%)	0.168
	Ex-smoker	62 (63.9%)	11 (23.4%)	15 (30%)	
	Current smoker	26 (26.8%)	29 (61.7%)	33 (66%)	
Stage	I	44 (45.4%)	23 (48.9%)	21 (42%)	0.700
	II	25 (36.1%)	15 (31.9%)	20 (40%)	
	III	18 (18.6%)	9 (19.1%)	9 (18%)	
N status	N0	71 (73.2%)	34 (72.3%)	37 (74%)	0.909
	N1	15 (15.5%)	8 (17%)	7 (14%)	
	N2	11 (11.3%)	5 (10.6%)	6 (12%)	
Tumor size (cm)	Mean ± SD	4.03 ± 2.13	3.52 ± 2.1	4.5 ± 2.1	**0.007***
	≤4 cm	54 (55.8%)	31 (57.4%)	23 (42.6%)	**0.048***
	>4 cm	43 (44.3%)	16 (37.2%)	27 (62.8%)	
PET (SUVmax)	Mean ± SD	11.05 ± 5.67	9.16 ± 5.06	12.74 ± 5.69	**0.002***
	≤9.4	47 (49.5%)	30 (66.7%)	17 (34%)	**0.002***
	>9.4	48 (50.5%)	15 (33.3%)	33 (66%)	
Surgical approach	Thoracotomy	57 (58.8%)	23 (48.9%)	34 (68%)	0.057
	VATS	40 (41.2%)	24 (51.1%)	16 (32%)	

Type of resection	Lobectomy	80 (82.5%)	43 (91.5%)	37 (74%)	**0.024***
	Pneumonectomy	17 (17.5%)	4 (8.5%)	13 (26%)	
Chemotherapy	No	59 (60.8%)	28 (59.6%)	31 (62%)	0.807
	Yes	38 (39.2%)	19 (40.4%)	19 (38%)	
Radiotherapy	No	91 (93.8%)	44 (93.6%)	47 (94%)	0.938
	Yes	6 (6.2%)	3 (6.4%)	3 (6%)	
Relapse	No	55 (56.7%)	24 (51.1%)	31 (62%)	0.189
	Yes	42 (43.3%)	23 (48.9%)	19 (38%)	
Death	No	60 (61.9%)	29 (61.7%)	31 (62%)	0.571
	Yes	37 (38.1%)	18 (38.3%)	19 (38%)	

p: *p*-value of Fisher's exact (Categorical variables) and Mann-Whitney U test (Continuous variables) between ADC and SCC[156].

5.1.1 Circulating tumor cells detection and characterization

The applied methodology allows a 10.000-fold enrichment of tumor cells vs. leucocytes, making possible to detect and quantify CTCs. MACS® are nanosized microbeads that allow an efficient isolation and characterization of epithelial cells due to its minimal labeling, ensuring cellular integrity and without bead aggregation. This way, we were able to identify CTCs due to the red staining and their typical cytomorphology, with an elevated nucleus/cytoplasm ratio[167] and differentiate them from leukocytes due to blue hematoxylin counter-staining[168].

CTCs were analyzed in baseline samples (CTC1) and after surgery samples (CTC2) from the 97 enrolled patients. However, due to exitus, loss during follow-up or technical issues, CTCs at 6 months (CTC3) could be analyzed in 70 patients. EMT CTCs (EMT CTC1) were analyzed only in baseline samples from 54 patients (**Table 4**). No differences were observed in the percentage of patients with CTC positivity, nor the number of CTCs, between the two histological subtypes.

Table 4: Circulating tumor cells in early NSCLC and by histological type.

		NSCLC n = 97 (%)	**ADC n = 47 (%)**	**SCC n = 50 (%)**	***p***
CTC1	Mean (SD) Range	2.13 (± 8.7) 0-84	1.3 (± 2.6) 0-11	2.92 (± 11.9) 0-84	0.178
	Absence	57 (48.8%)	32 (68.1%)	25 (50%)	0.071
	Presence	40 (41.2%)	15 (31.9%)	25 (50%)	
CTC2	Mean (SD) Range	0.74 (± 1.6) 0-10	0.74 (± 1.9) 0-10	0.74 (± 1.2) 0-4	0.525
	Absence	70 (72.2%)	35 (74.5%)	35 (70%)	0.624
	Presence	27 (27.8%)	12 (25.5%)	15 (30%)	
CTC3	Mean (SD) Range	0.7 (± 1.8) 0-9	0.88 (± 2.1) 0-9	0.55 (± 2.8) 0-8	0.665
	Absence	57 (81.4%)	25 (78.1%)	32 (84.2%)	0.514
	Presence	13 (18.6%)	7 (21.9%)	6 (15.8%)	
		NSCLC n = 54 (%)	**ADC n = 22 (%)**	**SCC n = 32 (%)**	
CTC1 EMT	Mean (SD) Range	0.3 (± 0.44) 0-3	0.14 (± 0.4) 0-1	0.41 (± 0.8) 0-3	0.249
	Absence	43 (79.6%)	19 (86.4%)	24 (75%)	0.308
	Presence	11 (20.4%)	3 (13.6%)	8 (25%)	

p: *p*-value of Fisher's exact (Presence vs. Absence) and Mann-Whitney U (Number of CTCs) tests between ADC and SCC.

5.1.2 Circulating tumor cells dynamics

We analyzed the dynamics of the presence and the absolute number of CTCs along the treatment in our 97 NSCLC patients. As a result, we observed not only a reduction in the number of patients presenting CTCs during the follow-up (CTC1-CTC2-CTC3) (p=0.001) (Cochran Q test), but also in the absolute number of CTCs (p=0.001) (Friedman test).

Moreover, when we evaluated this according to the histological subtype, the decrease in the percentage of CTC positive patients was only observed in SCC subtype (p=0.0001), but not in the ADC (p=0.607) cohort. In like manner, when analyzing total number of CTCs, ADC patients showed non-statistically significant differences (p=0.378) while significant dynamics could be observed in SCC patients (p=0.001) (**Figure 12. A & B**).

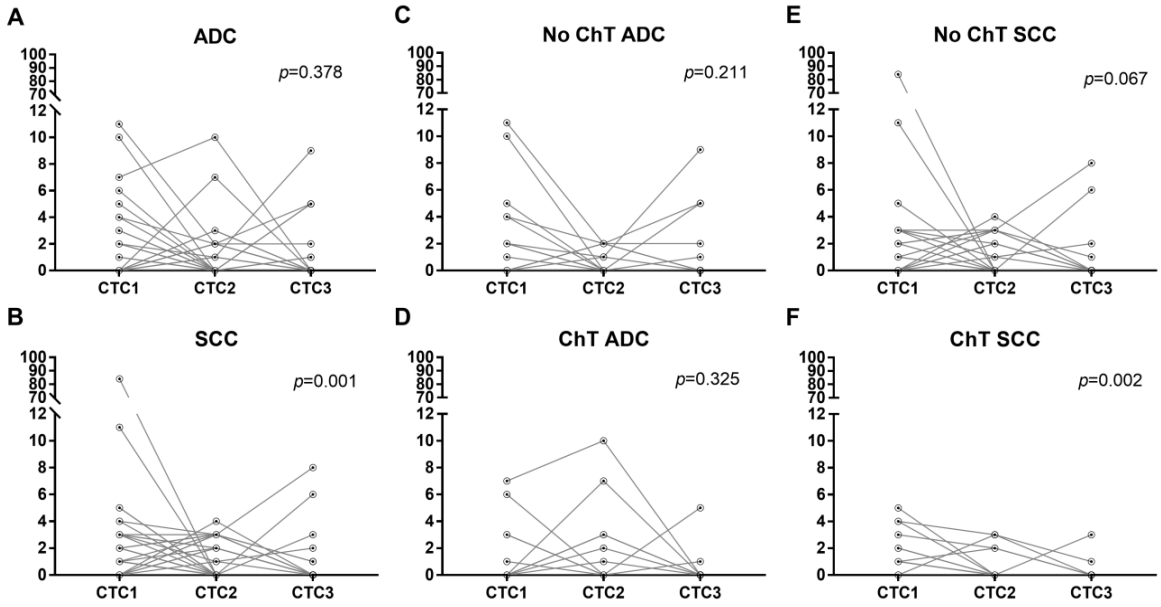

Figure 12: Circulating tumor cells dynamics in ADC and SCC: CTCs dynamics were evaluated in paired samples along the follow-up in the different subtypes. (A) ADC patients experienced no significant change in the number of CTCs during follow-up, while a significant dynamic was observed in SCC patients. When evaluating the impact of adjuvant ChT, ADC patients showed no significant dynamics neither in the treated group nor the untreated group (C & D). To the contrary, an almost significant variation was observed in the number of CTCs in untreated SCC patients (E) and a significant one in the treated group (F). p: p-value of Friedman test.

Deeper analyses were performed to determine the role of the adjuvant ChT treatment in the CTC dynamics. Subgroups were also divided into patients receiving and non-receiving ChT treatment. As previously reported, ADC patients showed no significant variations in the percentage of patients who had CTCs during the follow-up, neither in the group non-receiving (p=0.607) nor in the group receiving ChT treatment (p=0.607). In the same way, no changes were observed in the absolute number of CTCs in both groups (p=0.211 & p=0.325) (**Figure 12. C & D**).

On the other hand, significant reduction in the percentage of CTC positive SCC patients was observed in those receiving adjuvant ChT after surgery (p=0.038) and also in those without adjuvant ChT (p=0.006). When the dynamics of the number of CTCs were analyzed, an almost significant reduction could be observed in the non-adjuvant ChT group (p=0.067) and a clear decrease in the adjuvant group (p=0.002) (**Figure 12. E & F**). No differences were found in the number of patients receiving adjuvant treatment between the two histological subtypes (p=0.807) (**Table 3**).

5.1.3 Circulating tumor cells EGFR expression

EGFR expression was analyzed in epithelial and EMT CTCs (**Figure 13 & 14**). The A431 epidermal (known as highly positive WT EGFR cell line) and the lung adenocarcinoma H1975 (known as a mutated EGFR cell line) cell lines were used as positive and negative controls for EGFR determination. Vimentin expression was also tested in these cell lines, as A431 is a highly epithelial cell line while H1975 is known to have some semi-mesenchymal properties. The EGFR expression of CTCs was considered as positive (EGFR+) or negative (EGFR-) based on those cell line used settings.

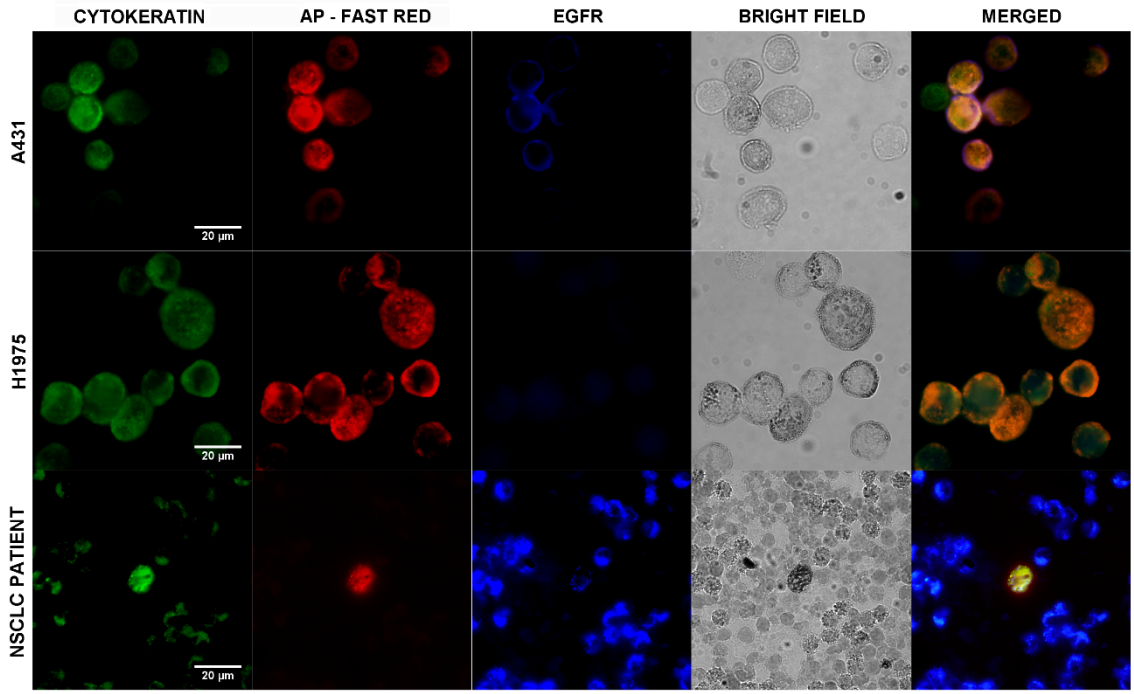

Figure 13: Epithelial CTC characterization in early NSCLC patients. The upper row depicts the epidermal A431 cancer cell line, with high cytokeratin (green and red) and EGFR (blue) expression. Mid row shows the lung H1975 cancer cell line, with high cytokeratin but low EGFR expression. Lower row represents an epithelial CTC from an early NSCLC patient with high cytokeratin and EGFR expression. Last column represents merged green, red and blue channels. Images taken with the Zeiss Epifluorescence Axio Imager A.1 microscope at 63x magnification[156].

In slides from epithelial CTC characterization, which had been previously incubated with Anti-Cytokeratin FITC – Alkaline Phosphatase and then enzymatically revealed with Fast Red (red), EGFR expression was observed in blue. EGFR+ CTCs showed blue signal located only in the plasmatic membrane (**Figure 13**). In slides from mesenchymal CTC characterization, EGFR expression was observed in red due to the availability and the better signal of this fluorophore. (**Figure 14**).

The frequency of patients with EGFR positive epithelial and EMT CTCs are reported in **Table 5**. At baseline status, 25 (62.5%) of NSCLC patients had EGFR positive epithelial CTCs and 11 (100%) EGFR positive EMT CTCs. Surprisingly, all EMT CTCs had high EGFR expression. No significant differences were found in the presence of EGFR CTCs between ADC and SCC at CTC1 (p=0.572), EMT CTC1 (p=0.253), CTC2 (p=0.185) or CTC3 (p=0.617).

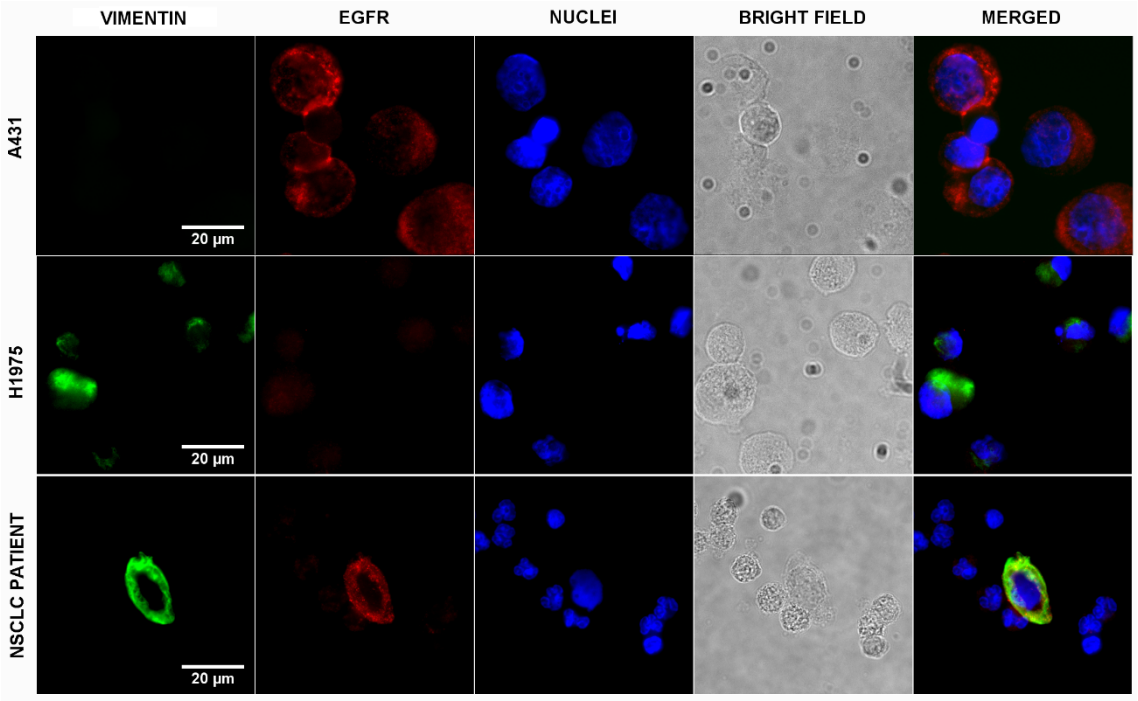

Figure 14: EMT CTC characterization in early NSCLC patients. The upper row depicts the epidermal A431 cancer cell line, showing low vimentin (green) expression but high levels of EGFR (red). Mid row depicts the EGFR mutated lung H1975 cancer cell line, with high vimentin expression while low expression of EGFR. Lower row represents an EMT CTC from an early NSCLC patient with high vimentin and EGFR expression and some PBMCs. Last column represents merged green, red and blue channels. Images taken with the Zeiss Epifluorescence Axio Imager A.1 microscope at 63x magnification[156].

Table 5: EGFR expression in CTCs[156]

	NSCLC		**ADC**		**SCC**	
CTC (+) patients	EGFR+	EGFR-	EGFR+	EGFR-	EGFR+	EGFR-
CTC1 (+) (n=40)	25 (62.5%)	15 (37.5%)	12 (80%)	3 (20%)	13 (52%)	12 (48%)
EMT CTC1 (+) (n=11)	11 (100%)	0 (0%)	3 (100%)	0 (0%)	8 (100%)	0 (0%)
CTC2 (+) (n=27)	10 (37%)	17 (63%)	3 (25%)	9 (75%)	7 (46.7%)	8 (53.3%)
CTC3 (+) (n=13)	6 (46.2%)	7 (53.8%)	3 (42.9%)	4 (57.1%)	3 (50%)	3 (50%)

5.1.4 Circulating tumor cells and their clinical association

The presence of epithelial CTCs along the follow-up (CTC1, CTC2, CTC3) was correlated to the clinical-pathological, treatment-related and the prognostic variables in both histological subtypes. In ADC, the presence of CTC1 showed non-statistical association to any of those variables. However, the presence of CTC2 was associated to higher clinical stage (p=0.006), thoracotomy vs. VATS as surgical approach (p=0.038), and the relapse (p=0.038). The presence of CTC3 in these patients correlated with N1 lymph node status (**Table 6**).

In the same way, the presence of CTC1 in SCC patients was not associated to any clinical-pathological nor other variable. Nevertheless, the presence of CTC2 in these patients was related to higher PET (SUVmax) values (p=0.007) and interestingly, lobectomy versus pneumonectomy as the type of resection (p=0.039). No correlation was found between the presence of CTC3 and these variables in SCC patients (**Table 7**).

The presence of EMT CTCs before surgery (EMT CTC1) was also correlated to the clinical-pathological, treatment-related and the prognostic variables in both histological subtypes (**Table 8**). However, no significant associations with other variables were obtained and the table only represents the comparison with stage and N status. The presence of EMT CTC1 was only correlated with higher N stage (p=0.007).

Table 6: Association between CTCs and clinical-pathological, treatment-related and prognosis characteristics in early ADC.

		ADC								
		CTC1			**CTC2**			**CTC3**		
		N (%) -	N (%) +	*p*	N (%) -	N (%) +	*p*	N (%) -	N (%) +	*p*
Gender	Men	23 (63.9%)	13 (36.1%)	0.232	27 (75%)	9 (25%)	0.582	20 (80%)	5 (20%)	0.489
	Women	9 (81.8%)	2 (18.2%)		8 (72.7%)	3 (27.3%)		5 (71.4%)	2 (28.6%)	
Age (years)	<70	22 (78.6%)	6 (21.4%)	0.061	20 (71.4%)	8 (28.6%)	0.410	16 (84.2%)	3 (15.8%)	0.281
	≥70	10 (52.6%)	9 (47.4%)		15 (78.9%)	4 (21.1%)		9 (69.2%)	4 (30.8%)	
Smoking habits	Never smoker	7 (100%)	0 (0%)		7 (100%)	0 (0%)		5 (100%)	0 (0%)	
	Ex-smoker	7 (63.6%)	4 (36.4%)	0.145	7 (63.6%)	4 (36.4%)	0.208	6 (66.7%)	3 (33.3%)	0.351
	Current smoker	18 (62.1%)	11 (37.9%)		21 (72.4%)	8 (27.6%)		14 (77.8%)	4 (22.2%)	
Stage	I	15 (65.2%)	8 (34.8%)		20 (87%)	3 (13%)		15 (83.3%)	3 (16.7%)	
	II	10 (66.7%)	5 (33.3%)	0.783	12 (80%)	3 (20%)	**0.006***	5 (71.4%)	2 (28.6%)	0.721
	III	7 (77.8%)	2 (22.2%)		3 (33.3%)	6 (66.7%)		5 (71.4%)	2 (28.6%)	
N status	N0	24 (70.6%)	10 (29.4%)		28 (82.4%)	6 (17.6%)		20 (83.3%)	4 (16.7%)	
	N1	4 (50%)	4 (50%)	0.443	5 (62.5%)	3 (37.5%)	0.089	1 (25%)	3 (75%)	**0.017***
	N2	4 (80%)	1 (20%)		2 (40%)	3 (60%)		4 (100%)	0 (0%)	
Tumor size	≤4 cm	22 (71%)	9 (29%)	0.393	25 (80.6%)	6 (19.4%)	0.159	19 (86.4%)	3 (13.6%)	0.115
	>4 cm	10 (62.5%)	6 (37.5%)		10 (62.5%)	6 (37.5%)		6 (60%)	4 (40%)	
PET (SUVmax)	≤9.4	20 (66.7%)	10 (33.3%)	0.635	25 (83.3%	5 (16.7%)	0.090	17 (77.3%)	5 (22.7%)	0.623
	>9.4	10 (66.7%)	5 (33.3%)		9 (60%)	6 (40%)		6 (75%)	2 (25%)	
Surgical approach	Thoracotomy	16 (69.6%)	7 (30.4%)	0.540	14 (60.9%)	9 (39.1%)	**0.038***	11 (73.3%)	4 (26.7%)	0.424
	VATS	16 (66.7%)	8 (33.3)		21 (87.5%)	3 (12.5%)		14 (82.4%)	3 (17.6%)	
Type of resection	Lobectomy	28 (65.1%)	15 (34.9%)	0.202	32 (74.4%)	11 (25.6%)	0.734	23 (76.7%)	7 (23.3%)	0.605

	Pneumonectomy	4 (100%)	0 (0%)		3 (75%)	1 (25%)		2 (100%)	0 (0%)	
Chemotherapy	No	18 (64.3%)	10 (35.7%)	0.363	22 (78.6%)	6 (21.4%)	0.327	16 (76.2%)	5 (23.8%)	0.544
	Yes	14 (73.7%)	5 (26.3%)		13 (68.4%)	6 (31.6%)		9 (81.8%)	2 (18.2%)	
Radiotherapy	No	31 (70.5%)	13 (29.5%)	0.235	33 (75%)	11 (25%)	0.596	23 (76.7%)	7 (23.3%	0.605
	Yes	1 (33.3)	2 (66.7%)		2 (66.7%)	1 (33.3)		2 (100%)	0 (0%)	
Relapse	No	18 (75%)	6 (25%)	0.234	21 (87.5%)	3 (12.5%)	**0.038***	12 (80%)	3 (20%)	0.576
	Yes	14 (60.9%)	9 (39.1%)		14 (60.9%)	9 (39.1%)		13 (76.5%)	4 (23.5%)	
Death	No	21 (72.4%)	8 (27.6%)	0.311	24 (82.8%)	5 (17.2%)	0.096	18 (85.7%)	3 (14.3%)	0.162
	Yes	11 (61.1%)	7 (38.9%)		11 (61.1%)	7 (38.9%)		7 (63.6%)	4 (36.4%)	

p: *p*-value of Fisher's exact test.

Table 7: Association between CTCs and clinical-pathological, treatment-related and prognosis characteristics in early SCC.

		SCC								
		CTC1			**CTC2**			**CTC3**		
		N (%) -	N (%) +	*p*	N (%) -	N (%) +	*p*	N (%) -	N (%) +	*p*
Gender	Men	23 (47.9%)	25 (52.1%)	0.245	34 (70.8%)	14 (29.2%)	0.514	32 (86.5%)	5 (13.5%)	0.158
	Women	2 (100%)	0 (0%)		1 (50%)	1 (50%)		0 (0%)	1 (100%)	
Age (years)	<70	16 (53.5%)	14 (46.7%)	0.387	19 (63.3%)	11 (36.7%)	0.173	20 (83.3%)	4 (16.7%)	0.615
	≥70	9 (45%)	11 (55%)		16 (80%)	4 (20%)		12 (85.7%)	2 (14.3%)	
Smoking habits	Never smoker	0 (0%)	1 (100%)	0.584	0 (0%)	1 (100%)	0.172	0 (0%)	1 (100%)	0.184
	Ex-smoker	8 (53.3%)	7 (46.7%)		9 (60%)	6 (40%)		9 (69.2%)	4 (30.8%)	
	Current smoker	16 (48.5%)	17 (51.5%)		25 (75.8%)	8 (24.2%)		22 (91.7%)	2 (8.3%)	
Stage	I	9 (42.9%)	12 (57.1%)	0.490	16 (76.2%)	5 (23.8%)	0.450	12 (85.7%)	2 (14.3%)	0.280
	II	10 (50%)	10 (50%)		12 (60%)	8 (40%)		12 (75%)	4 (25%)	

	III	6 (66.7%)	3 (33.3%)		7 (77.8%)	2 (22.2%)		8 (100%)	0 (0%)	
N status	N0	18 (48.6%)	19 (51.4%)		24 (54.9%)	13 (35.1%)		22 (81.5%)	5 (18.5%)	
	N1	3 (42.9%)	4 (57.1%)	0.658	7 (100%)	0 (0%)	0.174	5 (83.3%)	1 (16.7%)	0.579
	N2	4 (66.7%)	2 (33.3%)		4 (66.7%)	2 (33.3%)		5 (100%)	0 (0%)	
Tumor size	≤4 cm	11 (47.8%)	12 (52.2%)	0.500	17 (73.9%)	6 (26.1%)	0.404	14 (82.4%)	3 (17.6%)	0.560
	>4 cm	14 (51.9%)	13 (48.1%)		18 (66.7%)	9 (33.3%)		18 (85.7%)	3 (14.3%)	
PET (SUVmax)	≤9.4	8 (47.1%)	9 (52.9%)	0.500	16 (94.1%)	1 (5.9%)	**0.007***	10 (90.9%)	1 (9.1%)	0.429
	>9.4	17 (51.5%)	16 (48.5%)		19 (57.6%)	14 (42.4%)		22 (81.5%)	5 (18.5%)	
Surgical approach	Thoracotomy	18 (52.9%)	16 (47.1%)	0.381	23 (67.6%)	11 (32.4%)	0.428	22 (81.5%)	5 (18.5%)	0.429
	VATS	7 (43.8%)	9 (56.2%)		12 (75%)	4 (25%)		10 (90.9%)	1 (9.1%)	
Type of resection	Lobectomy	17 (45.9%)	20 (54.1%)	0.260	23 (62.2%)	14 (37.8%)	**0.039***	21 (77.8%)	6 (22.2%)	0.107
	Pneumonectomy	8 (61.5%)	5 (38.5%)		12 (92.3%)	1 (7.7%)		11 (100%)	0 (0%)	
Chemotherapy	No	16 (51.6%)	15 (48.4%)	0.500	20 (64.5%)	11 (35.5%)	0.225	17 (81%)	4 (19%)	0.440
	Yes	9 (47.4%)	10 (52.6%)		15 (78.9%)	4 (21.1%)		15 (88.2%)	2 (11.8%)	
Radiotherapy	No	24 (51.1%)	23 (48.9%)	0.500	33 (70.2%)	14 (29.8%)	0.666	30 (83.3%)	6 (16.7%)	0.706
	Yes	1 (33.3%)	2 (66.7%)		2 (66.7%)	1 (33.3%)		2 (100%)	0 (0%)	
Relapse	No	15 (48.4%)	16 (51.6%)	0.500	22 (71%)	9 (29%)	0.546	21 (91.3%)	2 (8.7%)	0.152
	Yes	10 (52.6%)	9 (47.4%)		13 (68.4%)	6 (31.6%)		11 (73.3%)	4 (26.7%)	
Death	No	14 (45.2%)	17 (54.8%)	0.280	22 (71%)	9 (29%)	0.546	19 (82.6%)	4 (17.4%)	0.556
	Yes	11 (57.9%)	8 (42.1%)		13 (68.4%)	6 (31.6%)		13 (87.6%)	2 (13.3%)	

p: *p*-value of Fisher's exact test.

Table 8: Association between EMT CTC1 and stage and N status in ADC and SCC.

		EMT CTC1					
		ADC			SCC		
		N (%) -	N (%) +	*p*	N (%) -	N (%) +	*p*
Stage	I	9 (100%)	0 (0%)		8 (66.7%)	4 (33.3%)	
	II	7 (87.5%)	1 (12.5%)	0.112	10 (76.9%)	3 (23.1%)	0.638
	III	3 (60%)	2 (40%)		6 (85.7%)	1 (14.3%)	
N status	N0	15 (100%)	0 (0%)		16 (69.6%)	7 (30.4%)	
	N1	3 (75%)	1 (25%)	**0.007***	5 (100%)	0 (0%)	0.363
	N2	1 (33.3%)	2 (66.7%)		3 (75%)	1 (25%)	

p: *p*-value of Fisher's exact test.

5.1.5 Genetic and miRNA tissue characterization of ADC and SCC

Data from tissues expression was available in 87 patients. *AXL*, *IL6R*, *MET* and *GAPDH* showed no differences between early NSCLC tissues and non-tumor lung tissues. However, early NSCLC tissues expressed higher levels of miR-21 and miR-155 than non-tumor tissues (p<0.001 and p=0.001, respectively). (**Figure 15**).

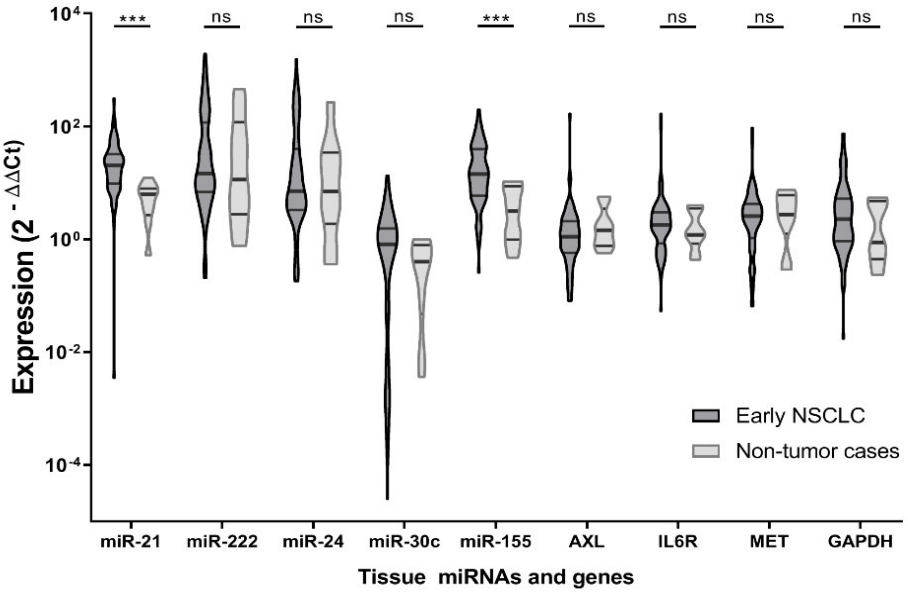

Figure 15: Gene and miRNA tissue expression in early NSCLC and non-tumor patients. NSCLC tissues (dark gray) showed higher expression of miR-21 and miR-155 than tissues from non-tumor lung resected patients (light gray). Data are presented as violin plots (min to max) (median value is represented by a thick black line). Mann-Whitney U test: *** $p < 0.001$, ns: no significant differences.

As we divided our analysis by histological subtypes, we also evaluated the differences expression profiles of ADC and SCC. As a result, we observed no differences in the tissue miRNA expression of both subtypes. On the other hand, higher levels of *MET* were found in ADC in comparison with SCC patients (**Figure 16**).

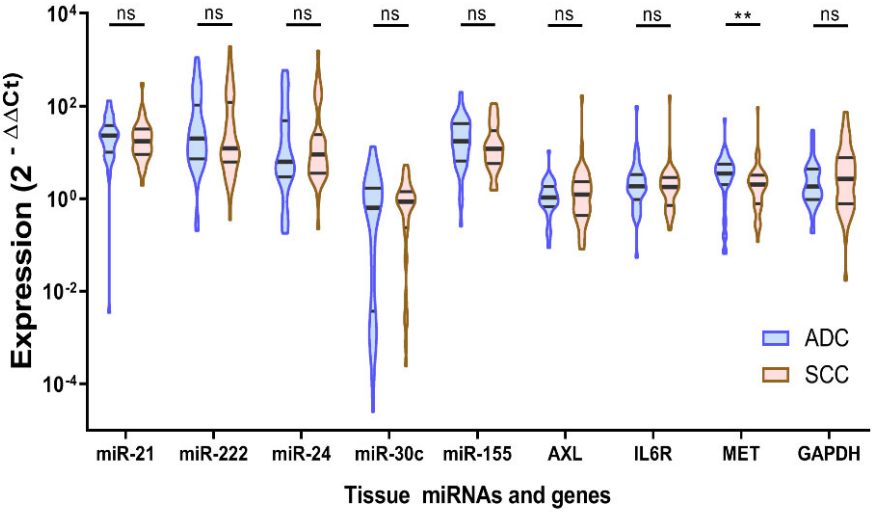

Figure 16: Gene and miRNA tissue expression in early ADC and SCC patients. ADC (blue) and SCC (red) tissues showed similar miRNA expression, while higher levels of *MET* were observed in ADC patients. Data are presented as violin plots (min to max) (median value is represented by a thick black line). Mann-Whitney U test: * $p < 0.05$, ** $p < 0.01$, ns: no significant differences.

Moreover, the analysis of the gene and miRNA correlations revealed specific patterns in ADC and SCC tissues. Besides finding common positive correlations between miR-21, miR-222 and miR-24 in both histological subtypes ($p<0.0001$), we observed ADC-specific miRNA interactions. Thus, miR-155 was positively correlated with miR-21 ($p<0.0001$), and miR-222 ($p=0.018$), and negatively with miR-30c ($p=0.03$) only in ADC. The latter positively correlated with miR-24. Regarding gene expression, there were no specific correlations, as *AXL*, *IL6R* and *MET* were positively correlated with each other in both ADC and SCC tissues (**Figure 17. A**).

On the other hand, we also found specific gene interactions between genes and miRNAs. So, miR-155 was inversely correlated with *AXL* ($p=0.034$) and *IL6R* ($p=0.003$), while *MET* was directly correlated with miR-24 ($p=0.005$) and miR-30c ($p=0.04$) only in ADC tissues. Finally, a negative correlation was observed between miR-21 and *GAPDH* ($p=0.048$) (**Figure 17. A**).

5.1.6 CTCs subpopulations and tissue genetic expression

The presence of different CTC subpopulations and the molecular tissue expression were compared in order to identify the specific miRNA-gene pathways involved in the presence of these CTCs. miRNAs manifested no statistical relation with epithelial or mesenchymal CTC phenotypes in ADC or SCC patients. However, in ADC patients, the presence of EMT+ CTC1 was correlated with higher levels of *IL6R*, *AXL* and *GAPDH* ($p=0.004$, $p=0.014$ & $p=0.021$, respectively) (**Figure 17. B**).

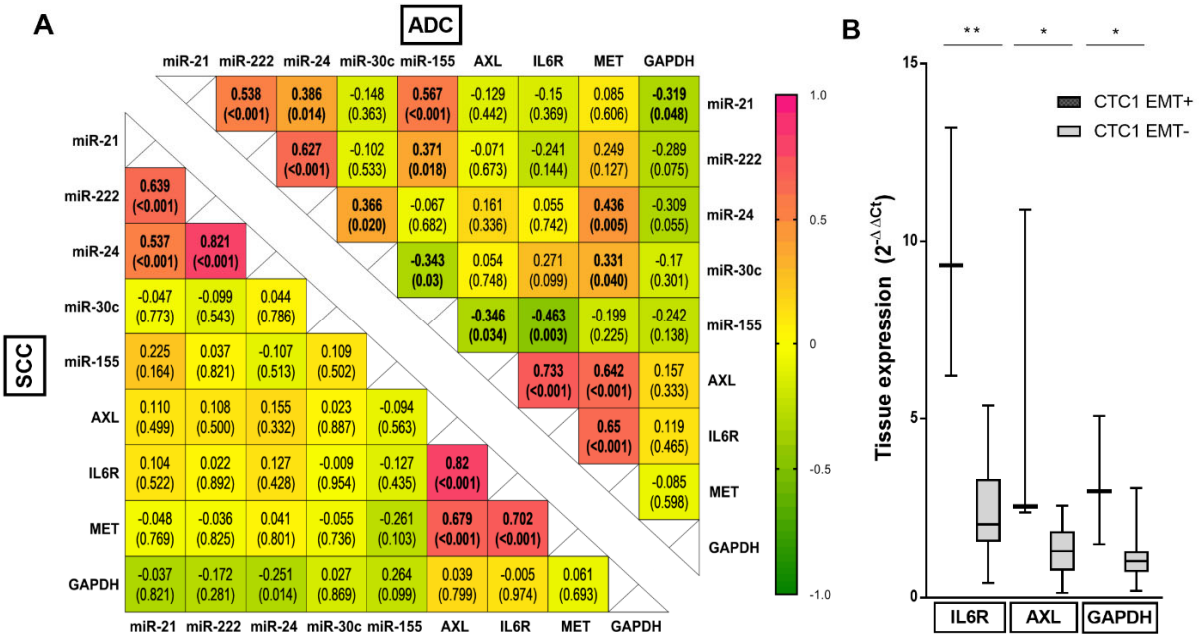

Figure 17: Genetic and miRNA tissue profiling and CTC correlation in ADC and SCC. (A) Heat-map matrix plot displaying correlation between selected miRNAs and genes in ADC (top-right corner) and in SCC (bottom-left corner). Data represent Spearman's rho and (p-value). $p < 0.05$ in bold. Squares in pink tones represent positive correlations, yellow tones neutral correlations while green tones show negative correlations. (B) Blox-plot of gene tissue expression correlation with CTC phenotypes in ADC. Pattern fill colors represent presence of CTC vs. plain colors showing absence. U Mann Whitney test. * $p < 0.05$, ** $p < 0.01$[156].

5.1.7 Prognostic markers of relapse-free survival

During the follow-up of this study, 23 (48.9%) ADC and 19 (38%) SCC patients relapsed (**Table 3**). ADC patients who relapsed had a median RFS of 11 months vs. 32 months in those who experienced no recurrence. In SCC patients, median RFS were 7 vs. 33 months respectively. With a median RFS of 28 months in ADC and 27.5 months in SCC, the RFS was statistically similar in both cohorts (p=0.911).

We analyzed the presence of CTCs along the follow-up in both cohorts with Kaplan-Meier analysis. Presence of CTC1 and CTC3 were not related to the relapse of the patients, however, the presence of CTC2 was associated with worse RFS in ADC patients, with a HR of 4.34 (p=0.037) (**Figure 18. A**). To the contrary, the presence of these CTCs was not associated to the RFS in the SCC cohort (p=0.731) (**Figure 18. B**).

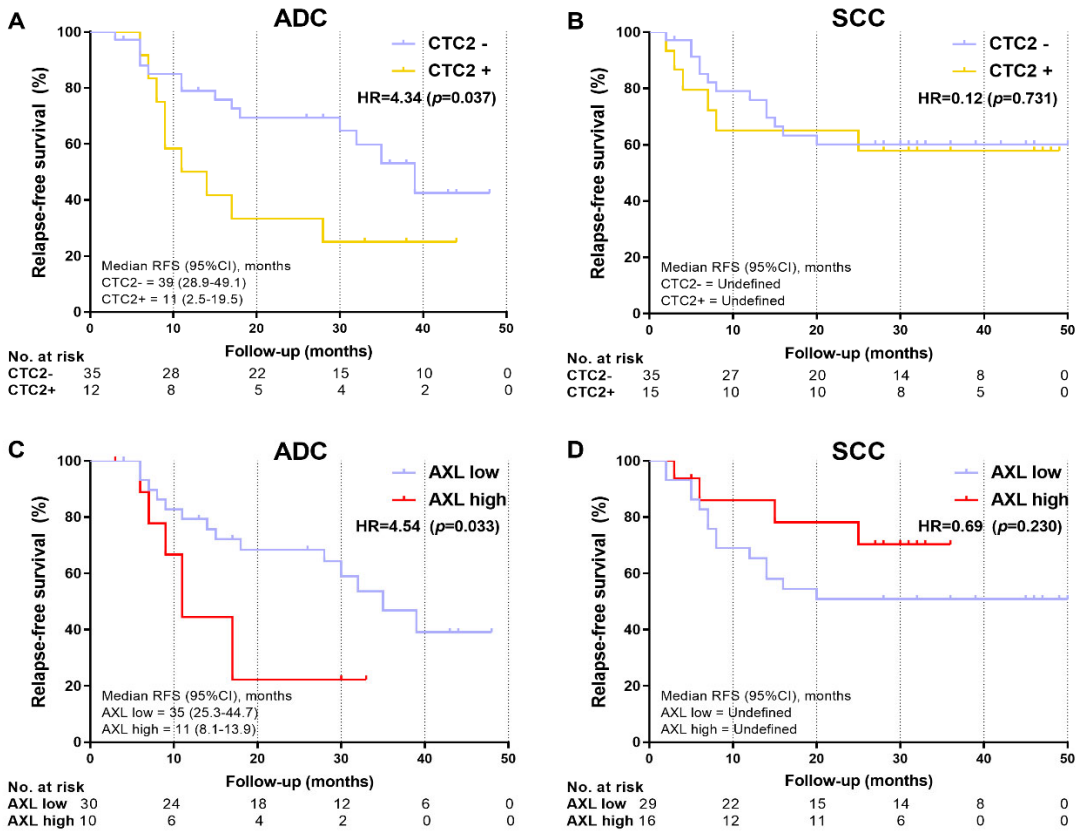

Figure 18: CTCs and tissue *AXL* expression as prognostic biomarkers for relapse-free survival (RFS). Presence of CTC 2 identified patients with higher relapse risk in the ADC cohort (A) but not in SCC (B). Kaplan-meier plots of the RFS according to high/low levels of tissue *AXL* in ADC (C) and SCC (D) cohorts. High AXL expression identified patients with shorter RFS in ADC (C) but not in SCC. *p: p*-value of log-rank (Mantel-Cox) test[156].

We also analyzed the association between high/low levels of genes and miRNAs and their association with the relapse. In this case, ADC patients with high expression of *AXL* showed shorter RFS in comparison with those with lower levels of this gene (HR=4.54, *p*=0.033) (**Figure 18. C**). In SCC patients, the expression of *AXL* was not associated to the RFS (*p*=0.230) (**Figure 18. D**). Furthermore, high expression of *GAPDH* correlated with shorter RFS (HR=6.27, *p*=0.012) in ADC patients (**Figure 19**).

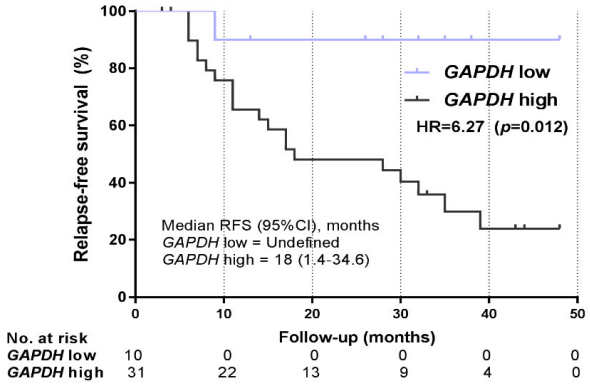

Figure 19: Tissue *GAPDH* expression as prognostic biomarkers for ADC relapse-free survival (RFS). High expression of *GAPDH* correlated with shorter RFS in ADC patients. *p: p*-value of log-rank (Mantel-Cox) test.

In contrast to ADC patients, where miRNAs were not associated to the prognosis, we found that miR-222 and miR-30c were associated to the RFS of SCC patients. High levels of miR-222 (HR=4.72, *p*=0.030) (**Figure 20.A)** and low levels of miR-30c (HR=0.16, *p*=0.011) (**Figure 20.B)** correlated with shorter RFS.

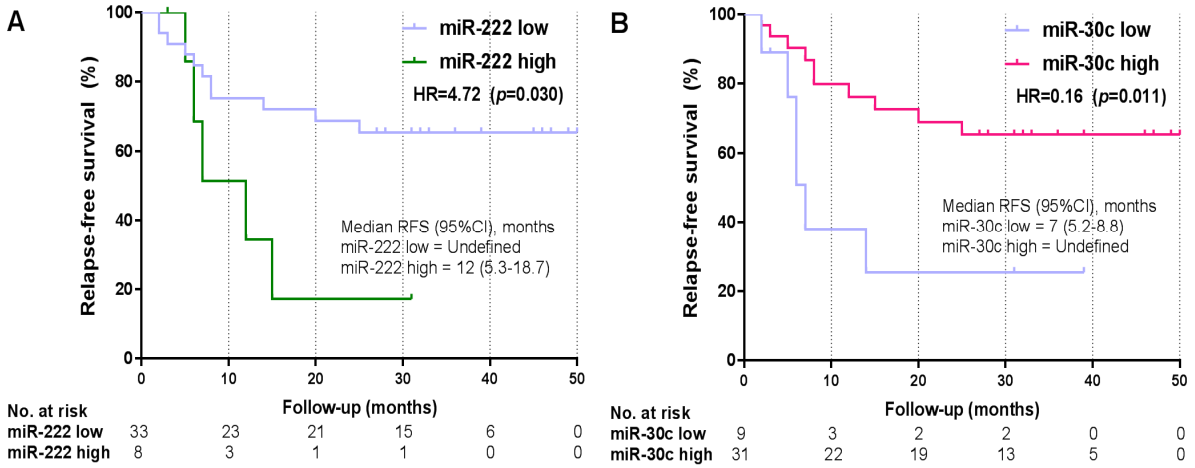

Figure 20: Tissue miR-222 and miR30c expression as prognostic biomarkers for relapse-free survival (RFS) in SCC patients. Kaplan-Meier plots of the RFS according to high/low levels of tissue miR-222 (A) and miR-30c (B) in SCC cohort. High levels of miR-222 (HR=4.72) and low levels of miR-30c (HR=0.16) were associated with shorter RFS. *p: p*-value of log-rank (Mantel-Cox) test.

5.1.7.1 Univariate Cox's proportional hazard regression analysis for RFS

The univariate Cox's proportional hazard regression was performed on every clinical-pathological variable, as well as the studied biomarkers in CTCs and tissue in order to find the potential risk factors involved in the relapse of these patients (**Table 9**). The univariate analyses revealed that several clinical variables as the clinical stage, tumor size, node status, and the resection type were associated with worse relapse prognosis.

From all the CTC extraction points and phenotypes, the presence of CTCs at 1 month after surgery (CTC2) was the only CTC variable associated with the relapse risk in our patients, and specifically in the ADC cohort. Patients with positive CTC2 had 2.4 times higher risk to relapse (95% CI=1.03-6.81, *p*=0.044). As reported in the Kaplan-Meier analysis, the presence of CTC2 in the SCC cohort was not related to the relapse of these patients (**Table 9**).

The univariate Cox's regression also reported that high expression of *AXL* (HR=2.65, *p*=0.044) and *GAPDH* (HR=8.31, p=0.039) were associated to a shorter RFS in ADC patients, while high expression of miR-222 (HR=3.10, *p*=0.041) and low levels of mir-30c (HR=0.29, *p*=0.018) were related to higher risk of relapse in SCC patients (**Table 9**). The presence of EGFR CTCs and the other miRNAs and genes showed no statistical association (*p*>0.05).

Table 9: Univariate Cox's proportional hazard regression analysis for RFS in ADC and SCC cohorts[156].

		Relapse-free survival (RFS)					
		ADC			SCC		
		Univariate			Univariate		
		HR	95% CI	*p*	HR	95% CI	*p*
Age		1.00	0.95-1.04	0.847	1.00	0.95-1.06	0.989
Gender	Men	1.36	0.46-4.01	0.583	0.81	0.11-6.1	0.840
	Women	1.00			1.00		
Stage	I	1.00		**0.046***	1.00		0.087
	II	1.33	0.49-3.56	0.577	2.30	0.78-6.88	0.135
	III	3.53	1.28-9.78	**0.015***	4.04	1.56-14.14	**0.029***
Size (cm)	>4cm	1.55	0.67-3.60	0.307	7.16	2.07-24.7	**0.002***
	≤4cm	1.00			1.00		
PET (SUVmax)	>9.4	1.23	0.5-3.05	0.658	1.47	0.53-4.07	0.463
	≤9.4	1.00			1.00		
N status	N0	1.00		0.143	1.00		0.094
	N1	2.76	0.96-7.94	0.06	3.22	1.16-9.27	**0.031***
	N2	1.93	0.55-6.80	0.307	1.71	0.38-7.65	0.486
Surgical approach	Thoracotomy	1.47	0.64-3.36	0.361	2.68	0.78-9.21	0.117
	VATS	1.00			1.00		
Resection type	Pneumonectomy	3.72	1.02-13.63	**0.047***	1.42	0.54-3.73	0.482
	Lobectomy	1.00			1.00		
Chemotherapy	Yes	1.73	0.77-3.93	0.188	1.56	0.63-3.84	0.335
	No	1.00			1.00		
Radiotherapy	Yes	3.29	0.96-11.33	0.059	2.58	0.59-11.22	0.206
	No	1.00			1.00		
CTC1	Presence	1.44	0.62-3.35	0.395	0.74	0.30-1.82	0.511
	Absence	1.00			1.00		
EGFR+ CTC1	Presence	1.25	0.51-3.04	0.625	0.66	0.22-1.98	0.454
	Absence	1.00			1.00		
CTC2	Presence	2.40	1.01-5.49	**0.046***	1.18	0.45-3.12	0.733
	Absence	1.00			1.00		
EGFR+ CTC2	Presence	1.98	0.46-8.56	0.362	0.27	0.03-1.99	0.197
	Absence	1.00			1.00		
CTC3	Presence	1.60	0.51-5.0	0.418	2.02	0.64-6.34	0.231
	Absence	1.00			1.00		
EGFR+ CTC3	Presence	1.86	0.26-13.51	0.540	1.32	0.18-9.53	0.786
	Absence	1.00			1.00		
EMT CTC1	Presence	2.29	0.46-11.35	0.312	0.19	0.24-1.45	0.108
	Absence	1.00			1.00		

AXL	High	2.65	1.03-6.81	**0.044***	0.52	0.17-1.57	0.243
	Low	1.00			1.00		
IL6R	High	1.70	0.67-4.32	0.264	2.48	0.97-6.30	0.057
	Low	1.00			1.00		
MET	High	1.78	0.73-4.34	0.204	0.50	0.16-1.51	0.216
	Low	1.00			1.00		
GAPDH	High	8.31	1.11-62.03	**0.039***	0.21	0.03-1.57	0.129
	Low	1.00			1.00		
miR-21	High	0.40	0.91-1.74	0.220	0.21	0.03-1.57	0.129
	Low	1.00			1.00		
miR-222	High	2.07	0.80-5.38	0.135	3.10	1.05-9.20	**0.041***
	Low	1.00			1.00		
miR-24	High	1.65	0.69-3.94	0.260	2.40	0.86-6.66	0.093
	Low	1.00			1.00		
miR-30c	High	1.43	0.59-3.46	0.428	0.29	0.10-0.81	**0.018***
	Low	1.00			1.00		
miR155	High	1.68	0.70-4.00	0.243	0.58	0.21-1.60	0.291
	Low	1.00			1.00		

5.1.7.2 Multivariate Cox's proportional hazard regression analysis for RFS

We performed an individual multivariate regression analysis to test the potential risk factors that could influence the relapse for each one of our cohorts of patients. These analyses included all the variables that reported an association ($p \leq 0.1$) in the univariate analysis for ADC or SCC. As previously described in the statistical methods, the criterion of more than a 10% change in the coefficient estimate was considered to include variables in the multivariate model.

The final multivariate models for RFS in ADC and SCC are represented **Table 10**. As a result, in ADC, the presence of CTC2 was an independent prognostic factor for RFS, identifying patients with 2.51 times shorter RFS (95% CI=1.07-5.87, p=0.034). Moreover, pneumonectomy subjected patients also presented higher risk to relapse (HR=4.23, 95% CI=1.13-15.8, p=0.032). In contrast, in SCC, larger size and N1 status were associated to shorter RFS.

Table 10: Multivariate Cox's proportional hazard regression model for RFS in ADC and SCC[156].

	Relapse-free survival (RFS)						
	ADC				**SCC**		
	HR	**95% CI**	***p***		**HR**	**95% CI**	***p***
Resection type				**Size (cm)**			
Pneumonectomy	4.23	1.13-15.8	**0.032***	>4cm	6.77	1.94-23.56	**0.003***
Lobectomy	1.00			≤4cm	1.00		
CTC2				**N status**			
Presence	2.51	1.07-5.87	**0.034***	N0	1.00		0.192
Absence	1.00			N1	2.72	0.92-7.98	0.070
				N2	1.26	0.28-5.84	0.764

CTCs after surgery were associated to worse prognosis in ADC. As represented in **figure 21**, patients with presence of CTC2 showed higher risk of recurrence and shorter RFS independently of the adjuvant therapy.

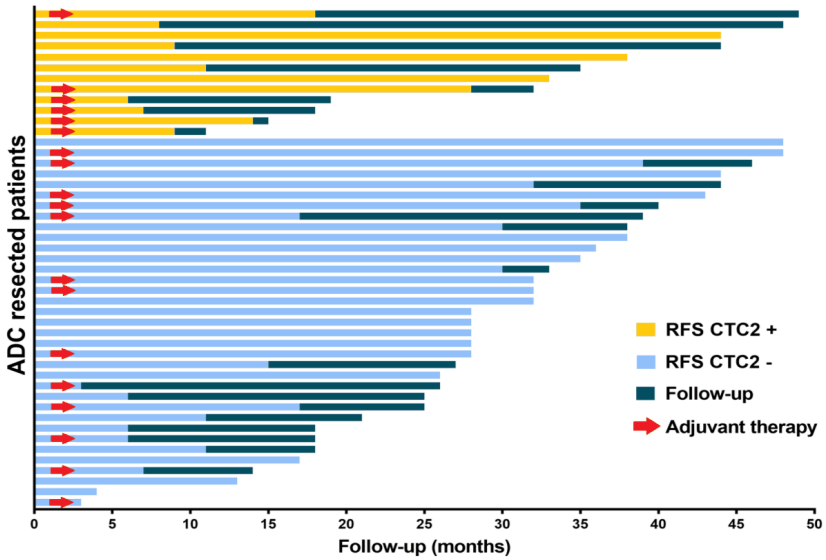

Figure 21: Swimmer plot of the RFS during follow-up according to the presence of CTC2 in ADC patients. Patients with positive CTC2 (orange) presented lower RFS than those with negative CTC2 (light-blue) and independently of the adjuvant therapy administration (red arrows)[156].

5.1.8 Prognostic markers of overall survival

A total of 18 (38.3%) ADC and 19 (38%) SCC patients died during the follow-up of this study (**Table 3**). In the ADC cohort, patients who died had a median OS of 18 vs. 36 months in those who survived. On the other hand, in the SCC subtype, median OS in patients who died was 17 while 36 months in those who did not. With a median OS of 30.5 in ADC and 32 months in SCC, no differences were found in the OS between the two histological subtypes (p=0.715).

As reported for the relapse-free survival, we analyzed the influence of the presence of CTCs in the OS of both cohorts with the Kaplan-Meier analysis. In this case, the presence of CTC1 and CTC2 were not related to the relapse of the patients, however, the presence of CTC3 was almost statistically associated with worse OS in ADC patients, with a HR of 3.62 (p=0.057) (**Figure 22. A**). In the SCC cohort, the presence CTC3 presented a HR of 0.05 (p=0.815) (**Figure 22. B**). We also analyzed the association between high/low levels of genes and miRNAs and their association with the survival. As previously observed, ADC patients with high expression of *AXL* experienced shorter OS (HR=8.51, p=0.004) (**Figure 22. C**). No association was found in the SCC cohort (p=0.396) (**Figure 22. D**).

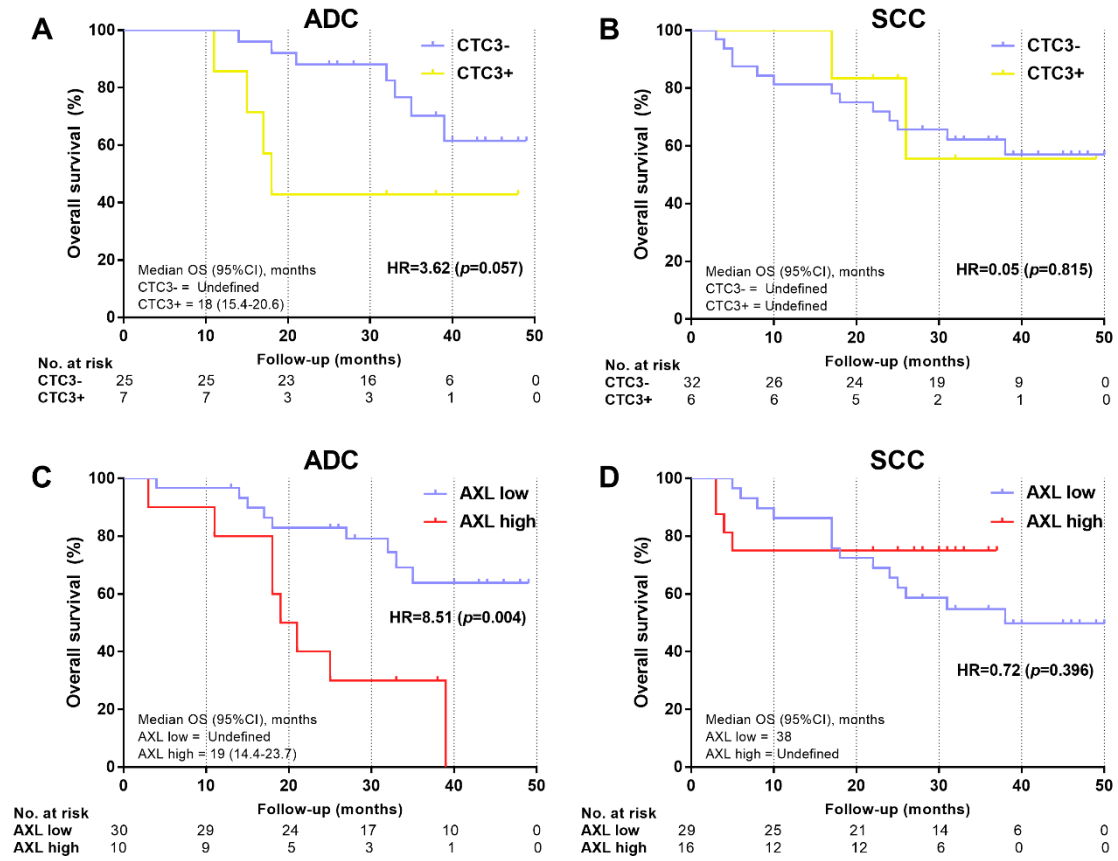

Figure 22: CTCs and tissue *AXL* expression as prognostic biomarkers for overall survival (OS). Kaplan-Meier plots of the OS according to the presence/absence of CTC3 and *AXL* expression in ADC and SCC patients. (A) In ADC patients, the positivity at CTC3 was associated with shorter OS, however not reaching statistical significance (p=0.057). (B) In SCC patients, the presence of CTC3 was not related to the death prognosis. (C) ADC patients with high levels of *AXL* presented shorter OS vs. those with lower levels. (D) The expression of *AXL* was not statistically associated with OS in SCC patients. *p:* p-value of log-rank (Mantel-Cox) test[156].

Additionally, we observed that tissue *MET* levels correlated with OS survival in ADC patients. As observed in **figure 23**, shorter OS was related to high expression of this gene (p=0.016).

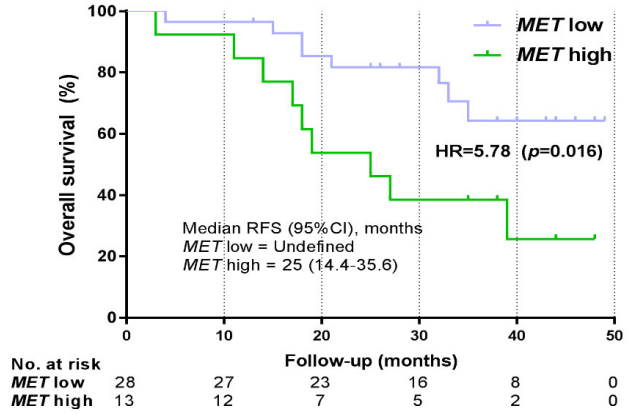

Figure 23: Tissue *AXL* expression as prognostic biomarkers for overall survival (OS). Kaplan-meier plot of the OS showing shorter OS in patients with overexpressed levels of tissue *MET. p:* p-value of log-rank (Mantel-Cox) test.

5.1.8.1 Univariate Cox's proportional hazard regression analysis for OS

In the same way, the univariate Cox's proportional hazard regression included every clinical-pathological variable, as well as the studied biomarkers in CTCs and tissue in order to find the potential risk factors involved in the death of these patients (**Table 11**). Similarly, the univariate analyses showed that the relapse, clinical stage, tumor size, node status, and the resection type were associated with worse survival.

No CTCs variables were significantly associated with the OS in ADC nor in SCC subtypes. However, despite not reaching statistical significance, the presence of CTCs 6 months after surgery (CTC3) had a HR of 3.12 (95% CI=0.91-10.76, *p*=0.072) in ADC (**Table 11**).

Moreover, the univariate regression showed that high expression of *AXL* and *MET* were associated with shorter OS in ADC patients. Patients with high levels of *AXL* had 3.8 higher risk of death (95% CI=1.44-9.99, *p*=0.007) while high levels of *MET* were associated to 3.03 higher risk of death (95% CI=1.17-7.87, *p*=0.023). CTCs immunophenotyping of CTCs, miRNA, and other gene expression were not statistically associated to OS in ADC or SCC (*p*>0.05) (**Table 11**).

Table 11: Univariate Cox's proportional hazard regression analysis for OS in ADC and SCC cohorts[156].

		Overall survival (OS)					
		ADC			SCC		
		Univariate			Univariate		
		HR	**95% CI**	***p***	**HR**	**95% CI**	***p***
Age		1.03	0.97-1.09	0.385	1.01	0.95-1.06	0.872
Gender	Men	1.36	0.39-4.74	0.630	21.81	0.0-1.9x10^5	0.506
	Women	1.00			1.00		
Relapse	Yes	5.07	1.62-19.44	**0.007***	6.91	2.43-19.66	**<0.001***
	No	1.00			1.00		
Stage	I	1.00		**0.036***	1.00		**0.028***
	II	1.81	0.58-5.63	0.303	1.77	0.56-5.58	0.331
	III	4.46	1.42-13.97	**0.010***	4.60	1.45-15.58	**0.010***
Size (cm)	>4cm	3.54	1.34-9.02	**0.008***	3.19	1.14-8.90	**0.027***
	≤4cm	1.00			1.00		
PET (SUVmax)	>9.4	2.56	0.96-6.84	0.061	1.05	0.4-2.75	0.928
	≤9.4	1.00			1.00		
N status	N0	1.00		**0.007***	1.00		**0.019***
	N1	5.83	1.93-17.55	**0.002***	2.83	0.88-9.09	0.081
	N2	1.63	0.34-7.49	0.528	4.28	1.46-12.58	**0.008***
Surgical approach	Thoracotomy	1.94	0.75-5.00	0.172	1.25	0.45-3.46	0.674
	VATS	1.00			1.00		
Resection type	Pneumonectomy	5.67	1.51-21.33	**0.010***	2.20	0.88-5.46	0.091
	Lobectomy	1.00			1.00		
Chemotherapy	Yes	1.58	0.63-3.98	0.334	1.87	1.75-4.53	0.186
	No	1.00			1.00		
Radiotherapy	Yes	2.07	0.46-9.2	0.341	1.93	0.44-8.41	0.383

	No	1.00			1.00		
CTC1	Presence	1.45	0.56-3.74	0.448	0.65	0.26-1.61	0.347
	Absence	1.00			1.00		
EGFR+ CTC1	Presence	1.56	0.59-4.18	0.372	0.67	0.22-2.02	0.476
	Absence	1.00			1.00		
CTC2	Presence	1.72	0.66-4.45	0.264	1.22	0.46-3.22	0.685
	Absence	1.00			1.00		
EGFR+ CTC2	Presence	0.77	0.10-5.83	0.804	0.28	0.04-2.11	0.217
	Absence	1.00			1.00		
CTC3	Presence	3.12	0.91-10.76	0.072	0.84	0.19-3.73	0.816
	Absence	1.00			1.00		
EGFR+ CTC3	Presence	1.41	0.20-10.19	0.731	0.71	0.04-11.79	0.809
	Absence	1.00			1.00		
EMT CTC1	Presence	1.65	0.29-9.21	0.571	0.21	0.03-1.65	0.212
	Absence	1.00			1.00		
AXL	High	3.80	1.44-9.99	**0.007***	0.47	0.17-1.32	0.150
	Low	1.00			1.00		
IL6R	High	2.02	0.76-5.32	0.157	0.42	0.00-40.56	0.366
	Low	1.00			1.00		
MET	High	3.03	1.17-7.87	**0.023***	1.86	0.74-4.72	0.189
	Low	1.00			1.00		
GAPDH	High	32.41	0.32-3311.44	0.141	2.23	0.88-5.67	0.092
	Low	1.00			1.00		
miR-21	High	0.24	0.03-1.84	0.170	1.48	0.55-3.99	0.437
	Low	1.00			1.00		
miR-222	High	2.73	0.89-8.39	0.079	0.55	0.20-1.53	0.253
	Low	1.00			1.00		
miR-24	High	2.91	0.95-8.98	0.063	0.48	0.17-1.32	0.154
	Low	1.00			1.00		
miR-30c	High	1.33	0.51-3.47	0.555	0.39	0.13-1.21	0.102
	Low	1.00			1.00		
miR155	High	0.51	0.12-2.27	0.380	0.27	0.04-2.08	0.209
	Low	1.00			1.00		

5.1.8.2 Multivariate Cox's proportional hazard regression analysis for OS

The multivariate regression analysis revealed that the presence of CTC3 (HR=10.8, 95% CI=1.54-76.4, *p*=0.017) and high *AXL* expression (HR=15.7, 95% CI=1.63-150.7, *p*=0.017) were the only independent prognostic factors for OS in adenocarcinoma patients (**Table 11**). The expression of *MET* was not associated to the OS in the multivariate analysis (*p*>0.05). On the other hand, in SCC relapse and N2 status were associated to shorter OS. None of the studied biomarkers was associated to the survival in these patients (**Table 12**).

Table 6: Multivariate Cox's proportional hazard regression model for OS in ADC and SCC[156].

	Overall Survival (OS)					
	ADC			SCC		
	HR	**95% CI**	***p***		**HR**	**95% CI**	***p***
Relapse				**Relapse**			
Yes	15.0	1.04-216.2	**0.047***	Yes	6.42	2.17-19.04	**0.001***
No	1.00			No	1.00		
PET (SUVmax)				**N status**			
>9.4	6.4	0.96-42.5	0.055	N0	1.00		0.075
≤9.4	1.00			N1	1.37	0.41-4.60	0.609
CTC3				N2	3.54	1.19-10.59	**0.024***
Presence	10.8	1.54-76.4	**0.017***				
Absence	1.00						
AXL							
High	15.7	1.63-150.7	**0.017***				
Low	1.00						

The final multivariate model for ADC patients included the presence of CTC3 and tissue *AXL* overexpression as independent prognostic biomarkers for OS. As presented in **figure 24**, the combination of these two biomarkers identified patients at higher risk of death and shorter OS. In addition, neither adjuvant chemotherapy nor post-operative radiotherapy had impact on the OS (**Table 11**) (**Figure 24**).

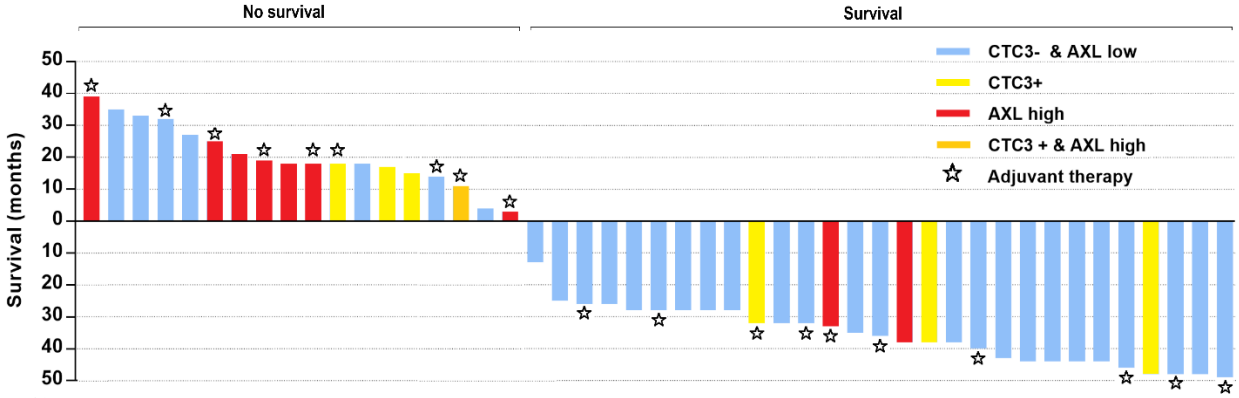

Figure 24: Waterfall plot of the OS according to the presence of CTC3 and *AXL* expression in ADC patients. The OS of ADC patients with positive CTC3 (yellow), high *AXL* tissue expression (red) or both (orange) was shorter than the survival of those with negative CTC3 and low *AXL* regardless of the adjuvant therapy administration (star)[156].

5. 2 Study 2: Advanced NSCLC population

The advanced NSCLC study enrolled a total of 41 advanced NSCLC patients with a median follow-up of 13 months (range 0-55). All patients were anatomopathologically diagnosed as non-resectable non-small lung cancer (stages IIIA, IIIB, or IV). Clinical-pathological, treatment-related and prognostic characteristics of all the 41 NSCLC patients are summarized in **Table 13**.

Table 13: Clinical-pathological, treatment-related and prognostic characteristics in advanced NSCLC patients.

Advanced NSCLC n = 41 (%)					
Histological type	ADC	12 (29.3%)	**TAC response**	Favorable	25 (61%)
	SCC	27 (65.9%)		No favorable	13 (31.7%)
	Large cell	2 (4.9%)		NA	3 (7.3%)
Gender	Men	34 (82.9%)	**PET response**	Favorable	17 (41.5%)
	Women	7 (17.1%)		No favorable	8 (19.5%)
Age (years)	Mean ± SD	66 ± 7.97		NA	16 (39%)
	<70	30 (73.2%)	**Chemotherapy treatment**	Vinorelbine-Cisplatin	30 (73.2%)
	≥70	11 (26.8%)		Taxol-Carboplatin	11 (26.8%)
Smoking habits	Never smoker	2 (4.9%)	**Second line treatment**	No	18 (45%)
	Ex-smoker	23 (56.1%)		ChT	12 (30%)
	Current smoker	16 (39%)		RT	8 (20%)
Histological subtype	ADC	12 (29.3%)		Immunotherapy	2 (5%)
	SCC	27 (65.9%)	**Progression 1**	No	11 (26.8%)
	LCC	2 (4.9%)		Yes	30 (73.2%)
Stage	IIIA	6 (14.6%)	**Progression 2**	No	7 (30.4%)
	IIIB	32 (78%)		Yes	16 (69.6%)
	IV	3 (7.3%)	**Tumor-related death**	No	24 (58.5%)
N status	N0	5 (12.2%)		Yes	17 (41.5%)
	N1	2 (4.9%)			
	N2	17 (41.5%)			
	N3	17 (41.5%)			

NA: Not available

5.2.1 Circulating tumor cell detection and characterization

As previously described in the early NSCLC cohort, the cytokeratin-positive isolation methodology was applied for advanced patients. In this population, CTCs were analyzed before (CTC1), during (CTC2) and after the ChT and RT treatment (CTC3) in 41, 39, and 33 patients respectively. In addition, CTCs were also evaluated 10 months after the initialization of the therapy (CTC4) in 17 patients. This reduction along the follow-up was caused by exitus. EMT CTCs (EMT CTC1) could be analyzed only in baseline samples from 22 patients due to exitus and technical issues regarding the preservation of the samples (**Table 14**).

Table 14: Circulating tumor cells in advanced NSCLC

		Total CTCs	Beclin-1 CTCs	EGFR CTCs	LC3B CTCs
	Mean (SD) Range	1.2 (± 2.32) 0-12			
CTC1 (N=41)	Absence	23 (56.1%)	39 (95.1%)	36 (92.3%)	29 (74.4%)
	Presence	18 (43.9%)	2 (4.9%)	3 (9.4%)	10 (25.6%)
	Mean (SD) Range	1.44 (± 6.28) 0-39			
CTC2 (N=39)	Absence	31 (79.5%)	39 (100%)	38 (97.4%)	36 (92.3%)
	Presence	8 (20.5%)	0 (0%)	1 (2.6%)	3 (7.7%)
	Mean (SD) Range	1.24 (± 2.94) 0-11			
CTC3 (N=33)	Absence	24 (72.7%)	31 (93.9%)	33 (100%)	31 (93.9%)
	Presence	9 (27.3%)	2 (6.1%)	0 (0%)	2 (6.1%)
	Mean (SD) Range	0.41 (± 1.18) 0-4			
CTC4 (N=17)	Absence	15 (88.2%)	17 (100%)	16 (94.1%)	17 (100%)
	Presence	2 (11.8%)	0 (0%)	1 (5.9%)	0 (0%)
	Mean (SD) Range	0.09 (±0.29) 0-1			
CTC1 EMT (N=22)	Absence	20 (90.9%)		20 (90.9%)	
	Presence	2 (9.1%)		2 (9.1%)	

As reported in the **table 14**, the presence of CTCs was observed in 18 (43.9%) at baseline status (CTC1). This number was reduced during the treatment, finding 8 positive patients (20.5%) at the middle of ChT and RT administration (CTC2). However, it increased at the end of it, finding 9 (27.3%) patients with CTC3 and finally decreased again at the end of the follow-up with only 2 positive (11.8%) patients at CTC4.

5.2.2 Circulating tumor cells dynamics

As presented in **table 14**, the mean number of CTCs increased from CTC1 to CTC2 but decreased at the end of the ChT-RT treatment (CTC3) and CTC4. We analyzed the dynamics of CTCs in paired samples along the follow-up (CTC1-4) and during treatment (CTC1-3).

CTC1-4 dynamics were available in only 17 patients observing no significant changes (p=0.082). However, significant dynamics during RT-ChT treatment (CTC1-3) were observed in the 33 patients (p=0.045) (**Figure 25. A**). As performed for early NSCLC patients, we analyzed advanced non-SCC and SCC cohorts separately. The non-SCC patients showed no significant variation neither in CTC1-4 nor CTC1-3 (**Figure 25. B**). To the contrary, SCC patients experienced a significant dynamic during the treatment (CTC1-3) (p=0.035) (**Figure 25. C**).

In addition, CTC fluctuations were compared with the clinical parameters, observing a significant correlation between higher RT dose and the reduction of CTCs (CTC1-3) (p=0.039).

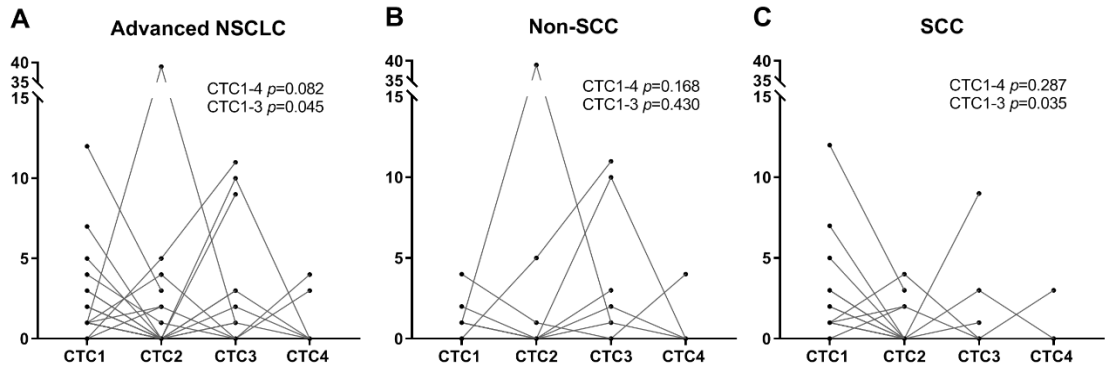

Figure 25: Circulating tumor cells dynamics in advanced NSCLC: CTCs dynamics were evaluated in paired samples along the follow-up CTC1-4. (A) In the advanced NSCLC cohort, the CTC1-4 correlation showed no significant variations in the number of CTCs (p=0.082). However, if the dynamics were evaluated during treatment (CTC1-CTC3) a significant variation (p=0.045) was observed. (B) In the non-SCC cohort, no significant dynamics could be observed, either during follow-up or during treatment (p>0.05). (C) To the contrary, in the SCC cohort, a significant variation was observed during ChT-RT treatment (CTC1-CTC3) (p=0.035). p: p-value of Friedman test.

5.2.3 Circulating tumor cell Beclin-1 characterization

We wanted to characterize the expression of Beclin-1 in CTCs. First, the lung adenocarcinoma A549 and H1975 cell lines were used for Beclin-1 antibody controls and immunofluorescence settings. After positive CTC determination by CK and AP - Fast Red, slides 1 from advanced NSCLC patients were subjected to Beclin-1 staining. Cell lines and a small CTC showed Beclin-1+ blue expression in the cytoplasm and nucleus (**Figure 26**). Beclin-1 positive CTCs were only observed in 2 (4.9%) patients at CTC1 and in 2 patients at CTC3 (6.1%) (**Table 14**).

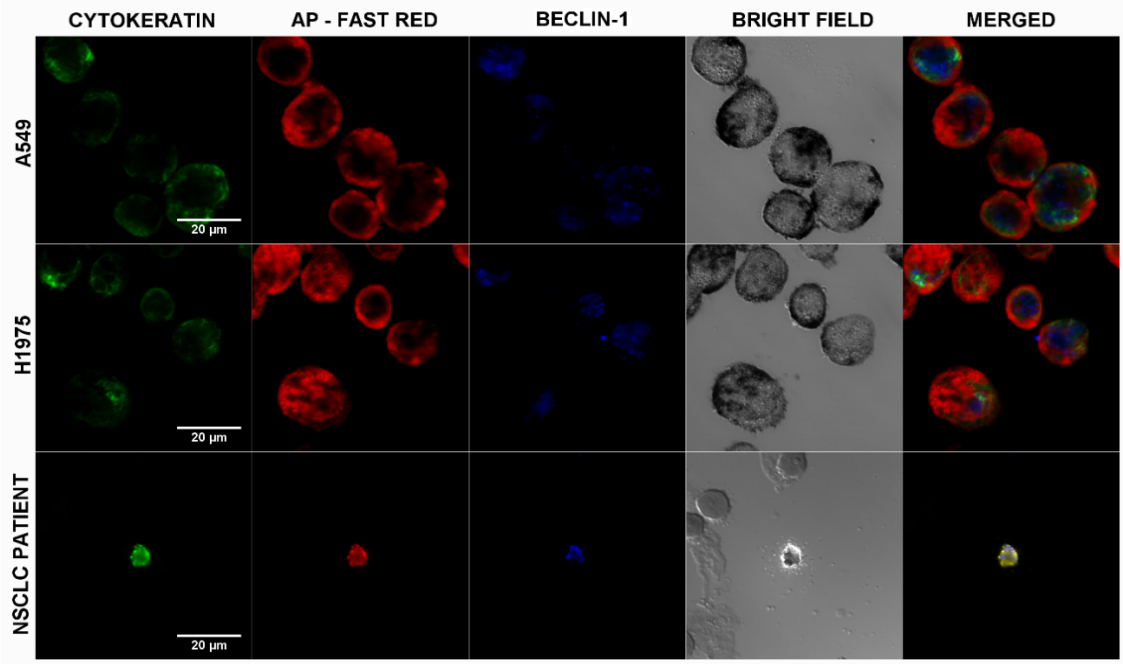

Figure 26: Epithelial and Beclin-1 CTC characterization in advanced NSCLC. The upper row depicts the A549 lung cancer cell line, with high cytokeratin (green and red) and Beclin-1 (blue) expression. Mid row shows the lung H1975 cancer cell line, with high cytokeratin and Beclin-1 (blue) expression. Lower row represents a small epithelial CTC from an advanced NSCLC patient with high cytokeratin and Beclin-1 expression. Last column represents merged green, red and blue channels. Images taken with the Zeiss LSM 710 confocal/multiphoton laser scanning microscope at 63x magnification. AP = Alkaline phosphatase

5.2.4 Circulating tumor cell EGFR and LC3B characterization

We also evaluate the expression of EGFR and LC3B in CTCs. First, the epidermal A431 (known as highly positive WT EGFR cell line) and the H820 (known as EGFR mutated cell line) cell lines were used as positive and negative controls for EGFR determination. In this case, slides 2 were subjected to both EGFR and LC3B staining, due to no previous alkaline phosphatase - Fast Red. Thus, EGFR signal was observed in red mainly in the cell membrane while LC3B signal in magenta was mainly located in cytoplasm and nucleus (**Figure 27**).

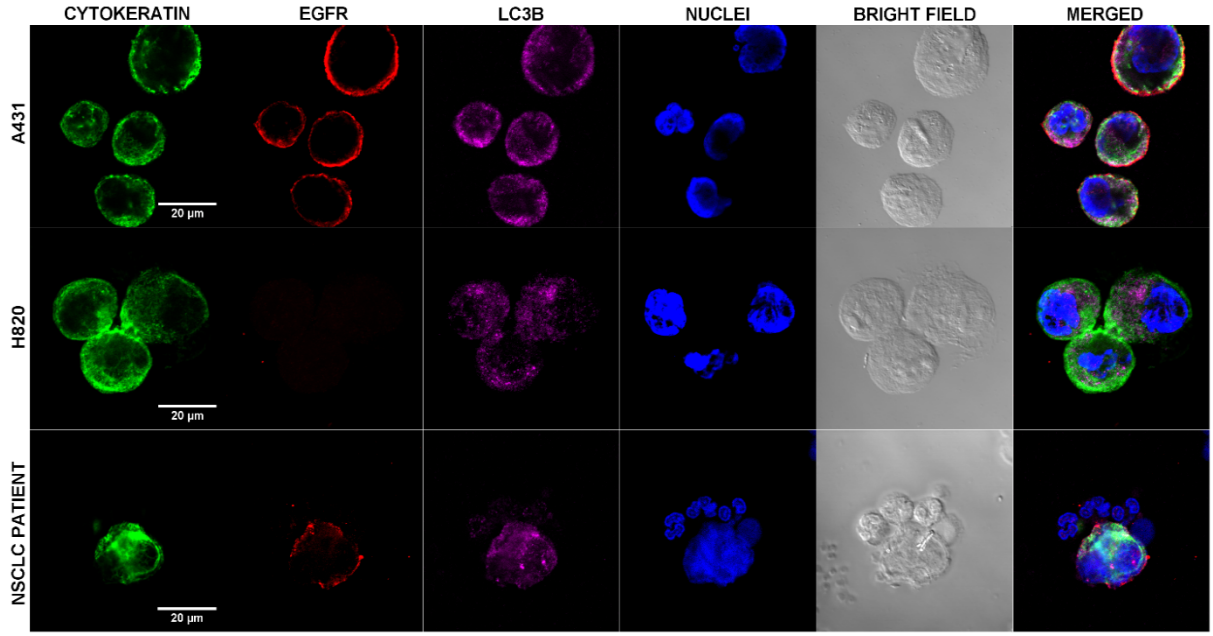

Figure 27: Epithelial CTC characterization in advanced NSCLC patients. The upper row shows the epidermal A431 cancer cell line, with high cytokeratin (green), EGFR (red) and LC3B (magenta) expression. Mid row represents the lung H820 cancer cell line, with high cytokeratin but low EGFR expression. Lower row represents an epithelial CTC from an advanced NSCLC patient with high cytokeratin, EGFR and LC3B expression, partially surrounded by PBMCs. Last column depicts merged green, red, magenta and blue channels. Images taken with the Zeiss LSM 710 confocal/multiphoton laser scanning microscope at 63x magnification.

EGFR positive CTCs could be identified in 3 (9.4%) patients at CTC1, 1 (2.6%) patient at CTC2, none at CTC3 while 1 (5.9%) at CTC4 (**Table 14**), observing a reduction during the ChT RT treatment but an increase at the end of it. In contrast, LC3B positive patients diminished during the follow-up, finding 10 (25.6%) at CTC1, 3 (7.7%) at CTC2, 2 (6.1%) CTC3 and none at CTC4 (**Table 14**).

EGFR expression was also evaluated in slides from mesenchymal CTC characterization. As previously reported in the early NSCLC controls, Vimentin expression was tested in A431, a highly epithelial cell line and H1975, a semi-mesenchymal lung cancer cell line. EMT CTCs EGFR+ CTCs showed red signal located in the plasmatic membrane and the cytoplasm (**Figure 28**).

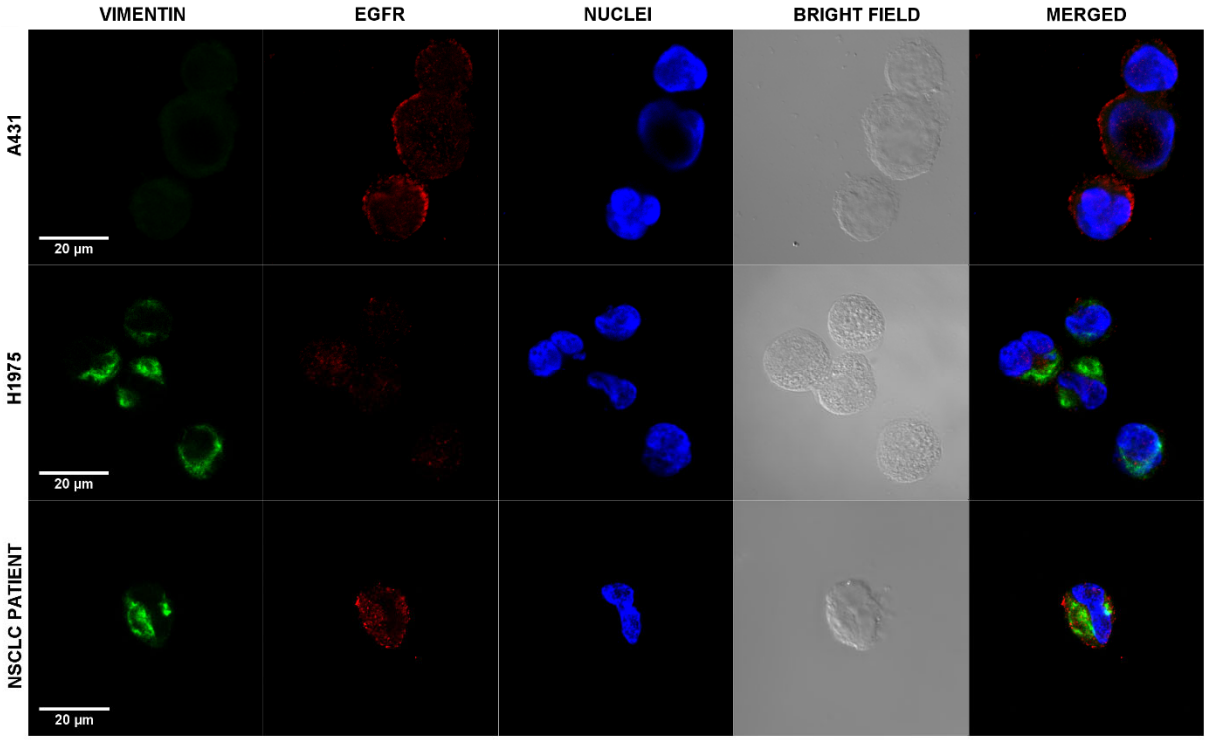

Figure 28: EMT CTC characterization in advanced NSCLC patients. The upper row depicts the epidermal A431 cancer cell line, showing low vimentin (green) expression but high levels of EGFR (red). Mid row depicts the EGFR mutated lung H1975 cancer cell line, with high vimentin expression while low expression of EGFR. Lower row represents an EMT CTC from an advanced NSCLC patient with high vimentin and EGFR expression. Last column represents merged green, red and blue channels. Images taken with the Zeiss LSM 710 confocal/multiphoton laser scanning microscope at 63x magnification.

5.2.5 Circulating tumor cells and their clinical association

The presence of epithelial and EMT CTCs was correlated to the clinical-pathological, treatment-related and the prognostic variables. No significant differences were found in the presence of CTCs at any point of the follow-up and the histological subtype *(*p>0.05). Interestingly, no relation was found between the presence of CTC1 and CTC2 and any clinical variable including progression or death (**Table 15 & 16**).

When evaluating CTCs after the concomitant ChT-RT, higher CTC3 presence was found in never smoker patients in comparison with ex-smokers and current smokers (*p*=0.049). Moreover, the presence of this cells was associated to the non-SCC histological subtype (*p*=0.036) and death (*p*=0.029). The presence of CTCs at the end of the follow-up (CTC4) correlated with patients who received Taxol-Carboplatin ChT (*p*=0.044).

Table 15: Association between CTC1 and CTC2 and clinical-pathological, treatment-related and prognosis characteristics in advanced NSCLC.

		Advanced NSCLC					
		CTC1			CTC2		
		N (%) -	N (%) +	*p*	N (%) -	N (%) +	*p*
Gender	Men	20 (58.8%)	14 (41.2%)	0.358	24 (75%)	8 (25%)	0.171
	Women	3 (42.9%)	4 (57.1%)		7 (100%)	0 (0%)	
Age (years)	<70	15 (50%)	15 (50%)	0.173	21 (72.4%)	8 (27.6%)	0.070
	≥70	8 (72.7%)	3 (27.3%)		10 (100%)	0 (0%)	
Smoking habits	Never smoker	2 (100%)	0 (0%)		2 (100%)	0 (0%)	
	Ex-smoker	12 (52.2%)	11 (47.8%)	0.425	17 (77.3%)	5 (22.7%)	0.747
	Current smoker	9 (56.3%)	7 (43.7%)		12 (80%)	3 (20%)	
Histological subtype	Non-SCC	8 (57.1%)	6 (44.4%)	0.594	10 (76,9%)	3 (23,1%)	0.544
	SCC	15 (55.6%)	12 (44.4%)		21 (80.8%)	5 (19.2%)	
Stage	IIIA	3 (50%)	3 (50%)		5 (83.3%)	1 (16.7%)	
	IIIB	20 (62.5%)	12 (37.5%)	0.108	23 (80%)	7 (20%)	0.614
	IV	0 (0%)	3 (100%)		3 (100%)	0 (0%)	
N status	N0	3 (60%)	2 (40%)		5 (100%)	0 (0%)	
	N1	0 (0%)	2 (100%)	0.367	1 (50%)	1 (50%)	0.460
	N2	11 (64.7%)	6 (35.3%)		13 (81.3%)	3 (18.8%)	
	N3	9 (52.9%)	8 (47.1%)		12 (75%)	4 (25%)	
ChT treatment	Vinorelbine based	17 (56.7%)	13 (43.3%)	0.589	25 (86.2%)	4 (13.8%)	0.097
	Taxol based	6 (54.5%)	5 (45.5%)		6 (60%)	4 (40%)	
CT response	Favorable	14 (56%)	11 (44%)	0.584	22 (88%)	3 (12%)	0.136
	Non-favorable	7 (53.8%)	6 (46.2%)		8 (66.7%)	4 (33.3%)	
PET response	Favorable	8 (47.1%)	9 (52.9%)	0.190	15 (88.2%)	2 (11.8%)	0.664
	Non-favorable	6 (75%)	2 (25%)		6 (85.7%)	1 (14.3%)	
Relapse 1	No	6 (54.5%)	5 (45.5%)	0.589	7 (70%)	3 (30%)	0.329
	Yes	17 (56.7%)	13 (43.3%)		24 (82.8%)	5 (17.2%)	
Second-line treatment	No	11 (61.1%)	7 (38.9%)	0.351	11 (64.7%)	6 (35.3%)	0.054
	Yes	11 (50%)	11 (50%)		20 (90.9%)	2 (9.1%)	
Relapse 2	No	4 (57.1%)	3 (42.9%)	0.556	6 (85.7%)	1 (14.3%)	0.526
	Yes	8 (50%)	8 (50%)		15 (93.8%)	1 (6.3%)	
Tumoral death	No	13 (54.2%)	11 (45.8%)	0.510	17 (77.3%)	5 (22.7%)	0.508
	Yes	10 (58.8%)	7 (41.2%)		14 (82.4%)	3 (17.6%)	

Table 16: Association between CTC3 and CTC4 and clinical-pathological, treatment-related and prognosis characteristics in advanced NSCLC.

		Advanced NSCLC					
		CTC3			CTC4		
		N (%) -	N (%) +	*p*	N (%) -	N (%) +	*p*
Gender	Men	19 (73.1%)	7 (26.9%)	0.635	11 (84.6%)	2 (15.4%)	0.574
	Women	5 (71.4%)	2 (28.6%)		4 (100%)	0 (0%)	
Age (years)	<70	19 (76%)	6 (24%)	0.374	11 (84.6%)	2 (15.4%)	0.574
	≥70	5 (62.5%)	3 (37.5%)		4 (100%)	0 (0%)	
Smoking habits	Never smoker	0 (0%)	2 (100%)	**0.049***	1 (100%)	0 (0%)	0.914
	Ex-smoker	14 (73.7%)	5 (26.3%)		8 (88.9%)	1 (11.1%)	
	Current smoker	10 (83.3%)	2 (16.7%)		6 (85.7%)	1 (14.3%)	
Histological subtype	Non-SCC	6 (50%)	6 (50%)	**0.036***	7 (87.5%)	1 (12.5%)	0.735
	SCC	18 (85.7%)	3 (14.3%)		8 (88.9%)	1 (11.1%)	
Stage	IIIA	5 (100%)	0 (0%)	0.331	1 (50%)	1 (50%)	0.193
	IIIB	17 (68%)	8 (32%)		12 (92.3%)	1 (7.7%)	
	IV	2 (66.7%)	1 (33.3%)		2 (100%)	0 (0%)	
N status	N0	3 (75%)	1 (25%)	0.711	1 (100%)	0 (0%)	0.270
	N1	2 (100%)	0 (0%)		1 (50%)	1 (50%)	
	N2	10 (76.9%)	3 (23.1%)		7 (100%)	0 (0%)	
	N3	9 (64.5%)	5 (35.7%)		6 (85.7%)	1 (14.3%)	
ChT treatment	Vinorelbine based	18 (69.2%)	8 (30.8%)	0.365	13 (100%)	0 (0%)	**0.044***
	Taxol based	6 (85.7%)	1 (14.3%)		2 (50%)	2 (50%)	
CT response	Favorable	19 (79.2%)	5 (20.8%)	0.178	12 (92.3%)	1 (7.7%)	0.426
	Non-favorable	5 (55.6%)	4 (44.4%)		3 (75%)	1 (25%)	
PET response	Favorable	13 (76.5%)	4 (23.5%)	0.696	11 (91.7%)	1 (8.3%)	1.000
	Non-favorable	3 (75%)	1 (25%)		0 (0%)	0 (0%)	
Relapse or progression 1	No	6 (100%)	0 (0%)	0.122	3 (75%)	1 (25%)	0.426
	Yes	18 (66.7%)	9 (33.3%)		12 (92.3%)	1 (7.7%)	
Second-line treatment	No	8 (72.7%)	3 (27.3%)	0.653	4 (80%)	1 (20%)	0.515
	Yes	16 (72.7%)	6 (27.3%)		11 (91.7%)	1 (8.3%)	
Relapse or progression 2	No	6 (85.7%)	1 (14.3%)	0.382	3 (75%)	1 (25%)	0.333
	Yes	11 (68.8%)	5 (31.2%)		8 (100%)	0 (0%)	
Tumoral death	No	16 (88.9%)	2 (11.1%)	**0.029***	7 (77.8%)	2 (22.2%)	0.265
	Yes	8 (53.3%)	7 (46.7%)		8 (100%)	0 (0%)	

5.2.6 EVs isolation and characterization

According to the ISEV recommendations, we identified the nature of our EVs and the origin of the derived miRNAs.

5.2.6.1 Transmission-electron microscopy characterization

The nanometer resolution of the TEM allowed us to distinguish single extracellular vesicles. Images taken depict double-membrane vesicles with around 150 nm of diameter with electron-dense cargo (**Figure 29. A**).

5.2.6.2 Nanoparticle tracking analysis

NTA revealed a concentration of $2.30x10^9 \pm 3.25x10^8$ particles/ml with a diameter of mode 126.4 ± 8.5 nm (**Figure 29. B**).

5.2.6.3 Western blot characterization

The Western blot revealed high protein expression of: Cytosolic proteins recovered in EVs such as Hsp70 in A549 and H1975 cell lines and derived EVs. Transmembrane, lipid-bound and soluble proteins associated to other intracellular compartments than plasmatic membrane or endosome such as GM-130 in cell lysates. Transmembrane or glycosylphosphatidylinositol (GPI)-anchored proteins associated to plasmatic membrane and/or endosomes, such as the tetraspanin CD9, in derived EVs while lower in cell lysates (**Figure 29. C**).

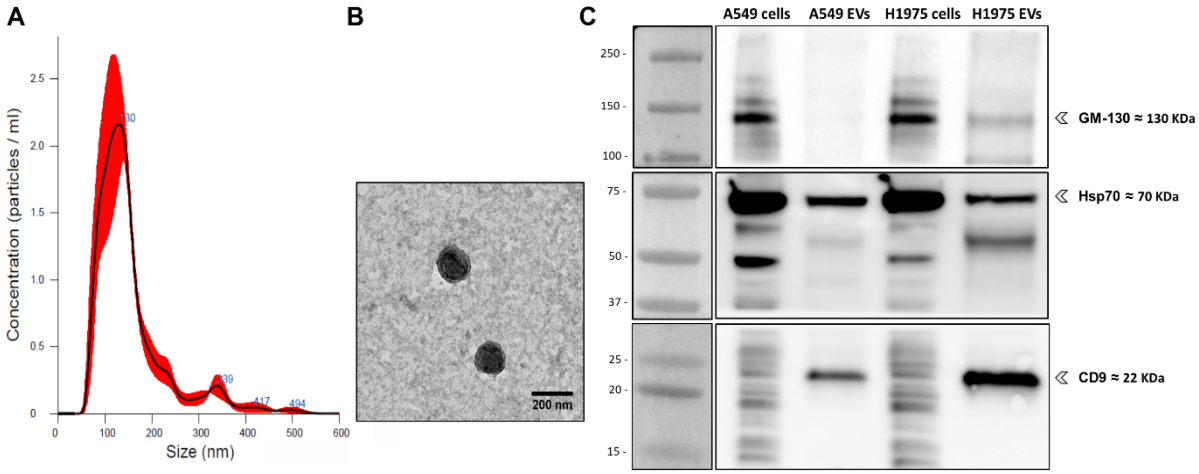

Figure 29: EVs characterization by NTA, TEM and WB: (A) Nanoparticle Tracking Analysis (NTA) of EVs from advanced NSCLC plasma samples: The NTA revealed a concentration of $2.30x10^9 \pm 3.25x10^8$ particles/ml with a diameter of mode 126.4 ± 8.5 nm. (B) The Transmission-Electron Microscopy (TEM) showed double-membrane EVs of ≈150 nm diameter. (C) The Western Blot (WB) images from lung cancer cell lines revealed EVs positive expression of the CD9 and Hsp70 proteins typically present in EVs while low expression of GM-130 present in other intracellular compartments.

5.2.7 EVs miRNAs in advanced NSCLC and healthy donors

Data from EV miRNA expression was available in 29 (70.7%) of our 41 patients and in our 15 (100%) healthy donors. When we compared both groups, high miR-21 (p<0.001) and miR-186 (p=0.002) expression was observed in advanced NSCLC patients vs. healthy donors. The other miRNAs were not differentially expressed between the two groups (*p*>0.05) (**Figure 30**).

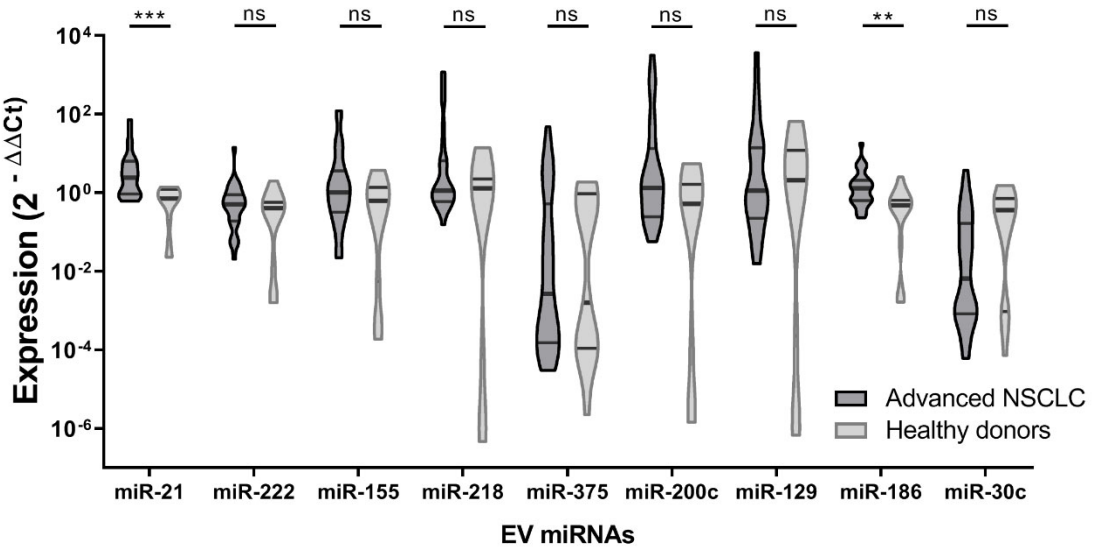

Figure 30: EV miRNA expression in advanced NSCLC patients and healthy donors. Extracellular vesicles from advanced NSCLC patients (black) showed higher expression of miR-21 and miR-186 at baseline than those from healthy donors (gray). Data are presented as violin plots (min to max) (median value is represented by a thick black line). Mann-Whitney U test: ** $p < 0.01$, *** $p < 0.001$, ns: no significant differences.

5.2.8 EV miRNA and clinic-pathological characteristics

The levels of EV miRNAs at different extractions were correlated to the clinical-pathological variables. At baseline status, higher expression of miR-21, miR-222, miR-155, miR-218, and miR-129 were found in older patients (**Table 17**). More interesting was the correlation between high levels of miR-375, 200c, and 30c and better response by CT and PET.

Table 17: Clinical-pathological characteristics and baseline miRNAs in advanced NSCLC.

	Baseline miRNAs (1) in advanced NSCLC (N=29)								
	miR-21	**miR-222**	**miR-155**	**miR-218**	**miR-375**	**miR-200c**	**miR-129**	**miR-186**	**miR-30c**
Gender	0.341	0.927	1.000	0.310	0.124	0.160	0.203	0.647	0.562
Age	**0.018***	0.218	**0.036***	**0.032***	0.083	0.075	**0.013***	0.139	0.549
Smoking habits	0.435	0.830	0.523	0.569	0.619	0.574	0.851	0.681	0.488
Histological subtype	0.456	0.636	0.456	0.735	0.769	0.701	0.946	0.573	1.000
Stage	0.616	0.383	0.166	0.566	0.339	0.386	0.475	0.315	0.120
N status	0.088	0.360	0.225	0.246	0.132	0.176	0.084	0.206	0.282
ChT treatment	0.550	0.387	0.238	0.061	0.438	0.429	0.159	0.276	0.412
CT response	0.323	0.217	0.277	0.373	**0.002***	**0.016***	0.103	0.323	**0.025***
PET response	0.536	0.650	0.773	0.299	**0.036***	**0.017***	0.227	1.000	**0.022***

Values represent the p-value from Mann-Whitney U or Kruskal-wallis test.

During ChT-RT, the expression of miR-200c and miR-30c correlated with the N status, observing higher levels of this miRNAs in N1 patients. In addition, high levels of miR-155 were found in taxol-carboplatin treated patients in comparison to vinorelbine-cisplatin group. EV miR-21 expression correlated with worse PET responses (**Table 18**).

Table 18: Clinical-pathological characteristics and during ChT-RT miRNAs in advanced NSCLC.

	During ChT-RT treatment miRNAs (2) in advanced NSCLC (N=28)								
	miR-21	**miR-222**	**miR-155**	**miR-218**	**miR-375**	**miR-200c**	**miR-129**	**miR-186**	**miR-30c**
Gender	0.186	0.825	0.042	0.681	0.186	0.874	0.681	0.322	0.110
Age (years)	0.354	0.709	0.043	0.381	0.823	0.980	0.980	0.237	0.940
Smoking habits	0.454	0.244	0.102	0.553	0.235	0.638	0.094	0.907	0.059
Histological subtype	0.340	0.919	0.551	0.256	0.419	0.353	0.409	0.323	0.436
Stage	0.881	0.881	0.794	0.512	0.760	0.721	0.241	0.351	0.760
N status	0.247	0.300	0.321	0.215	0.772	**0.011***	0.183	0.097	**0.049***
ChT treatment	0.109	0.356	**0.021***	0.494	0.796	0.245	0.759	0.080	0.944
CT response	0.109	0.646	0.121	0.054	0.610	0.134	0.041	0.109	0.760
PET response	**0.041***	0.102	0.335	0.151	0.820	0.820	0.385	0.151	0.553

Values represent the *p*-value from Mann-Whitney U or Kruskal-wallis test.

After ChT-RT, differential expression of miR-129 was found between SCC and non-SCC patients, with higher levels of this miRNA in the squamous group. Furthermore, higher miR-21 and miR-186 were found in patients with non-favorable PET responses (**Table 19**).

Table 19: Clinical-pathological characteristics and after ChT-RT miRNAs in advanced NSCLC.

	After ChT-RT treatment miRNAs (3) in advanced NSCLC (N=20)								
	miR-21	**miR-222**	**miR-155**	**miR-218**	**miR-375**	**miR-200c**	**miR-129**	**miR-186**	**miR-30c**
Gender	0.479	0.616	0.216	0.689	0.921	0.842	0.842	1.000	0.179
Age (years)	0.933	0.612	0.866	1.000	0.230	0.395	0.866	0.735	0.553
Smoking habits	0.348	0.408	0.444	0.417	0.962	0.962	0.212	0.545	0.609
Histological subtype	0.634	0.174	0.323	0.392	0.531	0.291	**0.011***	0.253	0.162
Stage	0.195	0.238	0.198	0.724	0.180	0.409	0.179	0.099	0.114
N status	0.690	0.945	0.998	0.746	0.204	0.915	0.992	0.966	0.289
ChT treatment	0.588	0.877	0.588	0.275	0.817	0.588	0.536	0.588	0.699
CT response	0.056	0.393	0.877	0.275	0.157	0.643	0.757	0.643	0.877
PET response	**0.014***	0.469	0.469	0.217	0.811	0.811	0.371	**0.028***	0.937

Values represent the p-value from Mann-Whitney U or Kruskal-wallis test.

Finally, EV miRNAs samples at the fourth time point (4) were available in only 10 patients and no significant results were observed (data not shown).

5.2.9 EV miRNAs and CTCs

In addition to clinic-pathological variables, the EV derived miRNAs were compared to the presence of different CTC subpopulations to identify specific miRNAs involved in the release and survival of CTCs in the blood circulation in advanced NSCLC.

As a result, we observed that lower expression of miR-222 (p=0.029) and miR-155 (p=0.016) at baseline (1) were associated to the presence of CTC1. In the same way, low expression of miR-218 was observed patients with LC3B + CTC1 (p=0.035) (**Figure 31**). During the treatment, CTC2 correlated with lower levels of baseline (1) miR-222 (p=0.023), miR-155 (p=0.010), and miR-375 (p=0.036). Finally, presence of CTC3 was associated to high levels of miR-218 2 (p=0.039) (**Figure 31**).

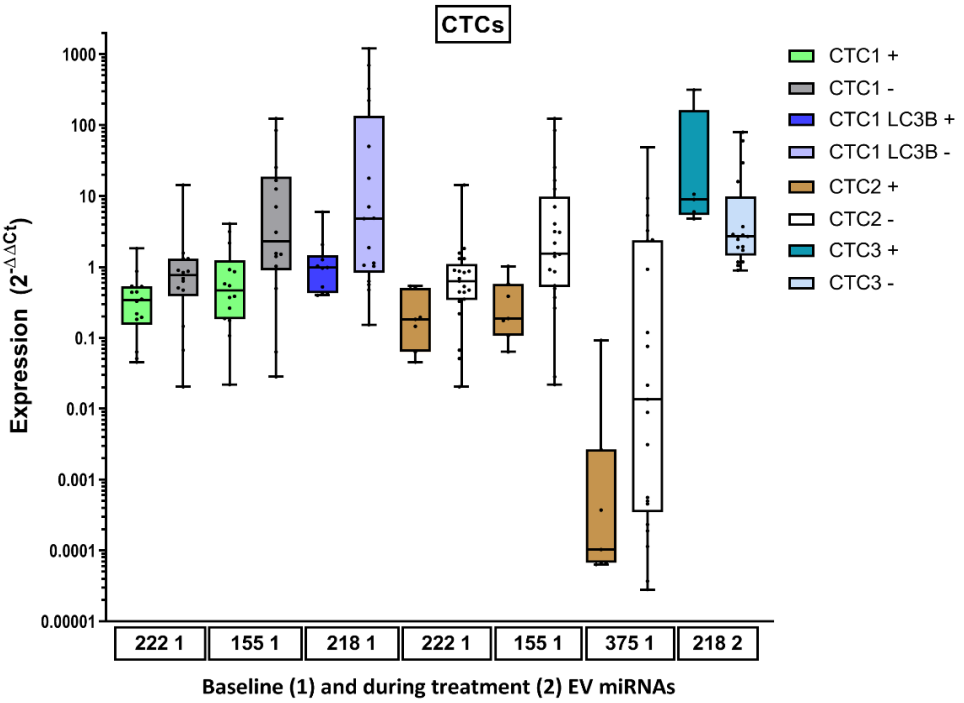

Figure 31: miRNA expression in advanced NSCLC patients according to CTC presence. Presence of CTC1 (green) vs. absence (gray); presence of LC3B+ CTC1 (dark blue) vs. absence (light blue); presence of CTC2 (red) vs. absence (white); and presence of CTC3 (blue-green) vs. absence (light blue-green) in advanced NSCLC patients correlated with EV miRNA expression during the follow-up. Data are presented as box and whiskers plots (min to max). Mann-Whitney U test.

5.13.1 EV miRNAs and CTCs dynamics

For deeper understanding of EV-miRNAs role, we evaluated their dynamics along the treatment. Between the 9 miRNAs analyzed, miR-222 (p=0.007), miR-218 (p=0.015), and miR30c (p=0.0001), were increased during ChT-RT treatment (1-3). Interestingly, the dynamic of miR-155 dynamic during- after treatment (2-3) showed a strong correlation with CTC fluctuations during the same period (p=0.008). Thus, the previously reported reduction of CTC2-3 was consistent to an increase in EV miR-155 levels.

5.2.10 Prognostic markers of relapse-free survival

During the follow-up 30 (73.2%) advanced NSCLC patients progressed (**Table 13**). Patients who progressed experienced a median RFS of 5 vs. 6 months of those who did not. The influence of the studied biomarkers on the RFS was analyzed by the Kaplan-Meier method. Thus, we found that the presence CTC2 LC3B positive cells was linked to shorter PFS (HR=8.9; *p*=0.003) (**Figure 32**). Moreover, the presence of CTC3 showed a non-statistically significant association to worse survival (HR=3.53; *p*=0.060).

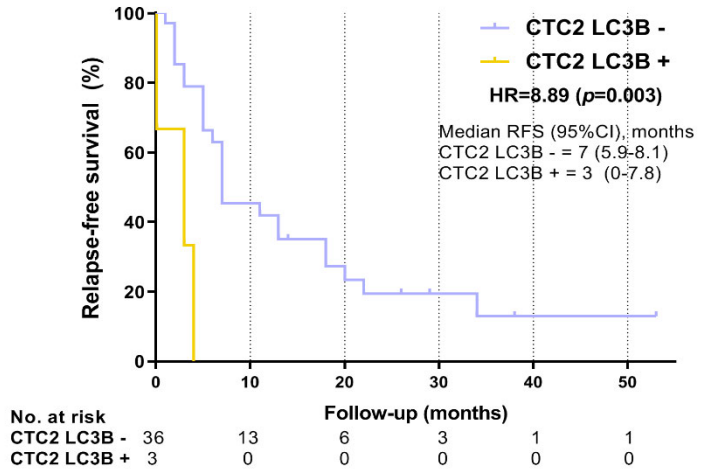

Figure 32: CTC2 LC3B expression as prognostic biomarker for PFS. The presence of CTCs with high expression of LC3B during ChT-RT was associated to shorter RFS in advanced NSCLC. *p: p*-value of log-rank (Mantel-Cox) test.

To evaluate the prognostic role of EV miRNAs in these patients, a cut-off categorization was performed on every miRNA based on the best value for RFS identification. The miRNAs which categorization had a potential impact on RFS are displayed in **table 20**.

Table 20: Cut-off categorization and Kaplan-Meier analysis for RFS

	Relapse-free survival (RFS)							
	Evaluate cutpoints application		Kaplan-Meier analysis			Evaluate cutpoints application		Kaplan-Meier analysis	
miRNA (High vs low)	**Cut-off value**	***p***	**HR**	***p***	**miRNA (High vs low)**	**Cut-off value**	***p***	**HR**	***p***
miR-21 1	0.750	0.068	3.59	0.058	**miR-21 3**	8.301	0.0003	10.66	0.001
miR-155 1	0.187	0.026	5.23	0.022	**miR-186 3**	6.167	0.013	4.79	0.029
miR-375 1	0.929	0.051	0.26	0.051	**miR-21 4**	2.295	0.078	2.34	0.126
miR-30c 1	0.003	0.027	0.11	0.002	**miR-222 4**	2.507	0.078	2.34	0.126
miR-375 2	0.002	0.028	0.29	0.061	**miR-155 4**	10.05	0.012	5.63	0.018
miR-200c 2	0.343	0.043	4.34	0.037	**miR-375 4**	2.553	0.027	4.80	0.028
miR-186 2	0.749	0.034	4.53	0.033	**miR-129 4**	2.039	0.027	4.80	0.028
miR-30c 2	0.003	0.024	0.30	0.067	**miR-186 4**	2.614	0.005	6.90	0.009
					miR-30c 4	1.920	0.032	0.21	0.028

Among all EV miRNAs, miR-30c 1 and miR-21 3 were the most associated with RFS. Higher levels of miR-30c 1 were associated to a longer RFS in these patients (HR=0.11; *p*=0.002) (**Figure 33. A**). Inversely, higher levels of miR-21 3 were associated to shorter RFS (HR=10.7; *p*=0.001) (**Figure 33. B**).

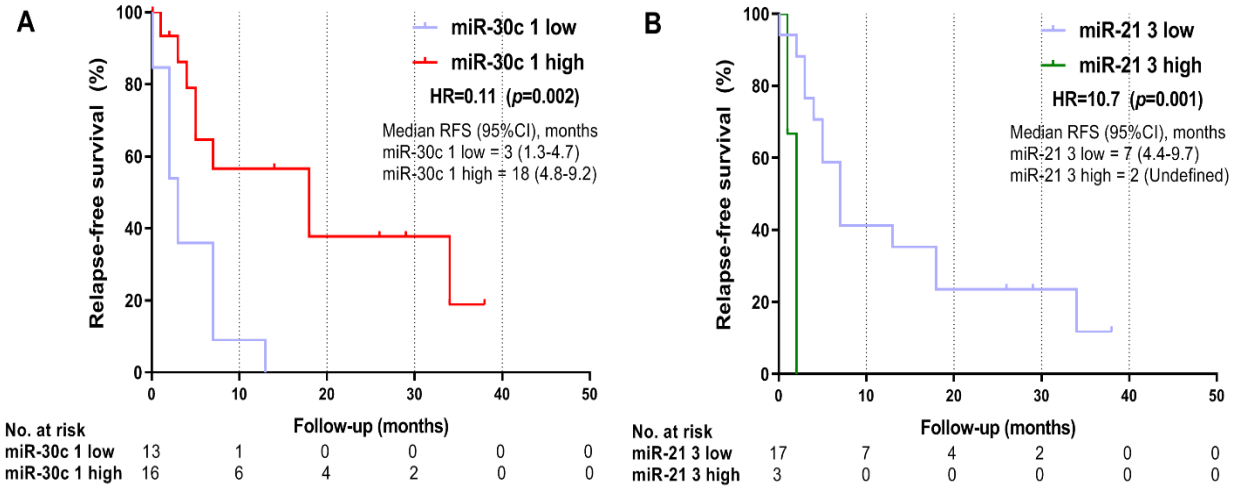

Figure 33: EV miR-30c 1 and miR-21 3 as prognostic biomarkers for RFS. Kaplan-meier plots of the RFS according to high/low levels of EV miR-30c at baseline (A) and miR-21 after treatment (B). Low expression of miR-30c and high expression of miR-21 identified patients with shorter RFS. *p: p*-value of log-rank (Mantel-Cox) test.

5.2.10.1 Univariate and multivariate Cox's proportional hazard regression analysis for RFS

The univariate Cox's proportional hazard regression was performed on every clinical-pathological variable, the studied biomarkers in CTCs as well as the categorized miRNAs. This analysis revealed that two clinical variables, RT total dose (HR=0.96, *p*=0.036) and PET response (HR=0.26, *p*=0.020), were associated to RFS (**Table 21.1**).

More interestingly, as reported in the Kaplan-Meier analysis three biomarkers including CTC2 LC3B+ (HR=5.70, *p*=0.010) (**Table 21.1**), miR-30c 1 (HR=0.25, *p*=0.007), and miR-21 3 (HR=10.37, *p*=0.011) were associated to the prognosis of this patients (**Table 21.2**).

Table 21.1: Univariate and multivariate Cox's proportional hazard regression analysis RFS

		RFS Advanced NSCLC					
		Univariate			Multivariate		
		HR	95% CI	*p*	HR	95% CI	*p*
Gender	Men	1.56	0.54-4.50	0.408			
	Women	1.00					
Age (years)	<70	1.56	0.68-3.61	0.296			
	≥70	1.00					
Smoking habits	Never smoker	1.00		0.509			
	Ex-smoker	0.46	0.10-2.01	0.300			
	Current smoker	0.40	0.09-1.87	0.245			
Histological subtype	Non-SCC	1.07	0.51-2.25	0.857			
	SCC	1.00					

Stage	IIIA	1.00		0.970			
	IIIB	0.93	0.32-2.71	0.891			
	IV	1.06	0.24-4.81	0.937			
N status	N0	1.00		0.467			
	N1	0.69	0.12-3.90	0.672			
	N2	0.39	0.12-1.30	0.126			
	N3	0.57	0.18-1.78	0.331			
M status	M0	0.88	0.27-2.93	0.837			
	M1	1.00					
ChT treatment	Vinorelbine based	0.82	0.36-1.85	0.629			
	Taxol based	1.00					
RT total dose	(continuous)	0.96	0.92-1.00	**0.036***	0.89	0.82-0.98	**0.016***
ECOC diagnosis	(continuous)	1.33	0.62-2.86	0.461			
CT response	Favorable	0.66	0.30-1.44	0.300			
	Non-favorable	1.00					
PET response	Favorable	0.26	0.09-0.81	**0.020***			
	Non-favorable	1.00					
CTC1	Presence	0.72	0.35-1.50	0.384			
	Absence	1.00					
EGFR+ CTC1	Presence	1.33	0.38-4.59	0.657			
	Absence	1.00					
LC3B+ CTC1	Presence	1.27	0.54-3.02	0.581			
	Absence	1.00					
Beclin-1+ CTC1	Presence	2.99	0.68-13.19	0.149			
	Absence	1.00					
CTC2	Presence	0.68	0.26-1.80	0.437			
	Absence	1.00					
EGFR+ CTC2	Presence	3.64	0.46-28.73	0.221			
	Absence	1.00					
LC3B+ CTC2	Presence	5.70	1.51-21.60	**0.010***	30.18	2.39-381.88	**0.009***
	Absence	1.00			1.00		
Beclin-1+ CTC2	Presence	0.87	0.20-3.70	0.850			
	Absence	1.00					
CTC3	Presence	2.09	0.91-4.80	0.083			
	Absence	1.00					
LC3B+ CTC3	Presence	2.20	0.51-9.55	0.291			
	Absence	1.00					
BEclin-1+ CTC4	Presence	0.26	0.03-2.16	0.213			
	Absence	1.00					
CTC4	Presence	0.47	0.06-3.64	0.467			
	Absence	1.00					

EGFR+ CTC4	Presence	1.25	0.16-9.92	0.834
	Absence	1.00		
EMT CTC1	Presence	0.17	0.02-1.41	0.101
	Absence	1.00		

EGFR+ CTC3, LC3B+ CTC4, and Beclin-1+ CTC4 showed undefined results and are not represented in the table.

Table 21.2: Univariate and multivariate Cox's proportional hazard regression analysis RFS

		RFS Advanced NSCLC					
		Univariate			Multivariate		
		HR	**95% CI**	***p***	**HR**	**95% CI**	***p***
miR-21 1	High	3.46	0.80-15.04	0.097			
	Low	1.00					
miR-155 1	High	4.39	1.00-19.27	0.050			
	Low	1.00					
miR-375-1	High	0.33	0.10-1.14	0.081			
	Low	1.00					
miR-30c 1	High	0.25	0.09-0.69	**0.007***			
	Low	1.00					
miR-375 2	High	0.45	0.18-1.13	0.088			
	Low	1.00					
miR-186 2	High	4.01	0.92-17.51	0.065			
	Low	1.00					
miR-30c 2	High	0.42	0.15-1.16	0.094			
	Low	1.00					
miR-21 3	High	10.37	1.72-62.48	**0.011***	84.52	4.33-1650.5	**0.003***
	Low	1.00			1.00		
miR-186 3	High	5.53	0.92-33.09	0.061			
	Low	1.00					
miR-21 4	High	3.62	0.51-25.71	0.199			
	Low	1.00					
miR-222 4	High	3.62	0.51-25.71	0.199			
	Low	1.00					
miR-375 4	High	5.13	0.91-29.06	0.065			
	Low	1.00					
miR-129 4	High	5.13	0.91-29.06	0.065			
	Low	1.00					

miR-200c 2, miR-155 4, miR-186 4, and miR-30c 4 presented undefined results and are not represented in the table.

The multivariate analysis showed that the RT total dose (HR=0.89, *p*=0.016), presence of CTC2 LC3B+ (HR=30.2, *p*=0.009) and EV miR-21 expression after therapy (HR=84.52, *p*=0.003) were independent prognostic factors for RFS, identifying patients at high risk of progression. The expression of miR-30c 1 was not an independent biomarker in the multivariate analysis (*p*>0.05) (**Table 21. 1 & 21. 2**). As presented in **figure 34**, the combination of CTC2 LC3B+ and EV-miR-21 3 as prognostic biomarkers identified patients with shorter RFS.

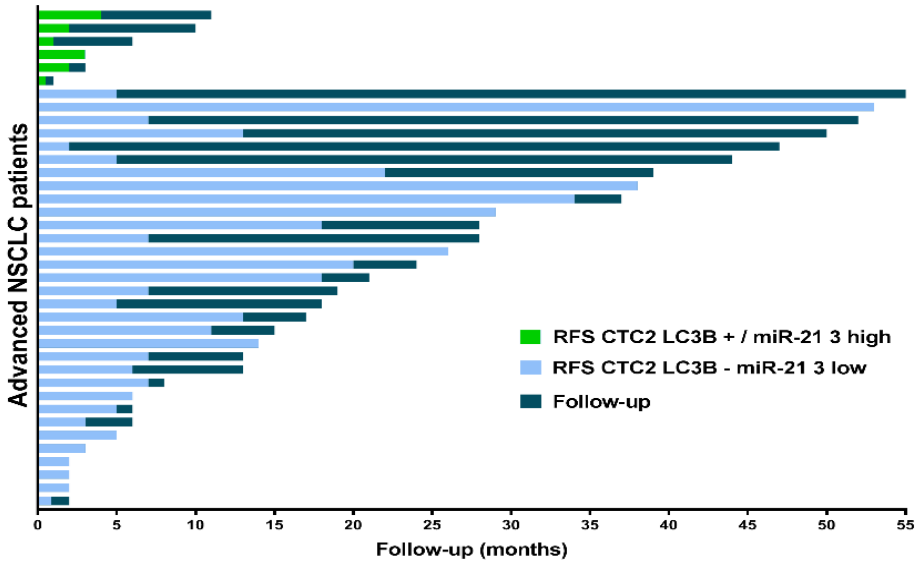

Figure 34: Swimmer plot of the RFS during follow-up according to the presence of CTC2-LC3B and EV miR-21 3 in advanced NSCLC. Patients with presence of CTC2-LC3B (green) and/or high levels of EV miR-21 after ChT-RT (3) presented lower RFS than those with negative CTC2-LC3B (light-blue) and low expression of this miRNA. The graph shows the 39 patients were CTC2-LC3B could be evaluated but 1 patient is missing due to progression before the conclusion of the treatment. EV miR-21 3 was only evaluated in 20 of them.

5.2.11 Prognostic makers of overall survival

During the follow-up 17 (41.5%) advanced NSCLC patients experienced a tumor-related death (**Table 13**). Patients who died experienced a median RFS of 11 vs. 15.5 months of those who did not. We evaluated the role of CTCs and EV miRNAs in the survival by the Kaplan-Meier analysis. The presence of CTC2 EGFR+ (HR=7.32; *p*=0.007), CTC2 LC3B+ (HR=14.6; *p<0.001*), CTC3 (HR=6.23; *p*=0.013), and CTC3 LC3B+ phenotype (HR=6.88; *p*=0.009) were associated with shorter overall survival (**Figure 35**).

To evaluate the role of EV miRNAs in the OS, same scheme was followed as previously explained for RFS. miRNAs which categorization showed a potential impact on OS are displayed in **table 22**.

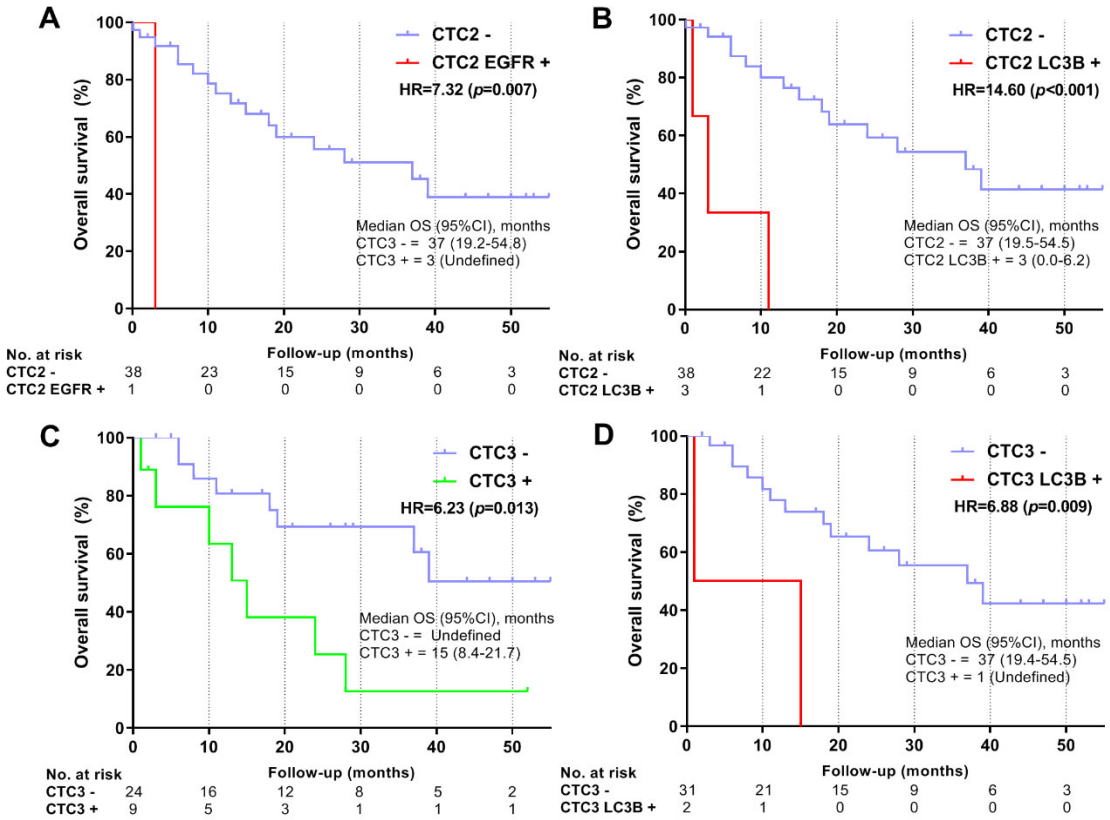

Figure 35: CTC2 and CTC3 phenotypes as prognostic biomarker for OS. The presence of CTCs with high expression of EGFR (A) or LC3B (B) during ChT-RT was associated to shorter OS, as well as the presence of CTC3 and its LC3B+ phenotype. *p: p*-value of log-rank (Mantel-Cox) test.

Table 22: Cut-off categorization and Kaplan-Meier analysis for OS

	Overall survival (OS)							
	Evaluate cutpoints application		Kaplan-Meier analysis			Evaluate cutpoints application		Kaplan-Meier analysis	
miRNA (High vs low)	**Cut-off value**	***p***	**HR**	***p***	**miRNA (High vs low)**	**Cut-off value**	***p***	**HR**	***p***
miR-21 1	2.420	0.060	3.53	0.060	**miR-21 3**	8.301	0.082	10.66	0.001
miR-222 1	0.471	0.079	3.13	0.077	**miR-155 3**	2.066	0.016	0.17	0.015
miR-375 1	0.929	0.080	0.29	0.065	**miR-129 3**	0.920	0.062	0.29	0.065
miR-186 1	1.397	0.063	3.53	0.060	**miR-30c 3**	2.122	0.058	0.27	0.056
miR-155 2	6.430	0.057	3.67	0.055	**miR-21 4**	7.390	0.003	10.41	0.001
miR-30c 2	0.029	0.029	3.73	0.053	**miR-222 4**	1.551	0.009	6.91	0.009
					miR-218 4	4.573	0.028	4.83	0.028

Several miRNAs were strongly associated with OS but only those that are finally included in the following multivariate analysis are depicted in the **figure 36**. We found that higher levels of miR-21 at baseline status (1) presented a no significant association to shorter OS in these patients (HR=3.53; *p*=0.060). Inversely, lower levels of miR-155 after the treatment (3) were associated to a shorter OS (HR=0.17; *p*=0.015) (**Figure 36**).

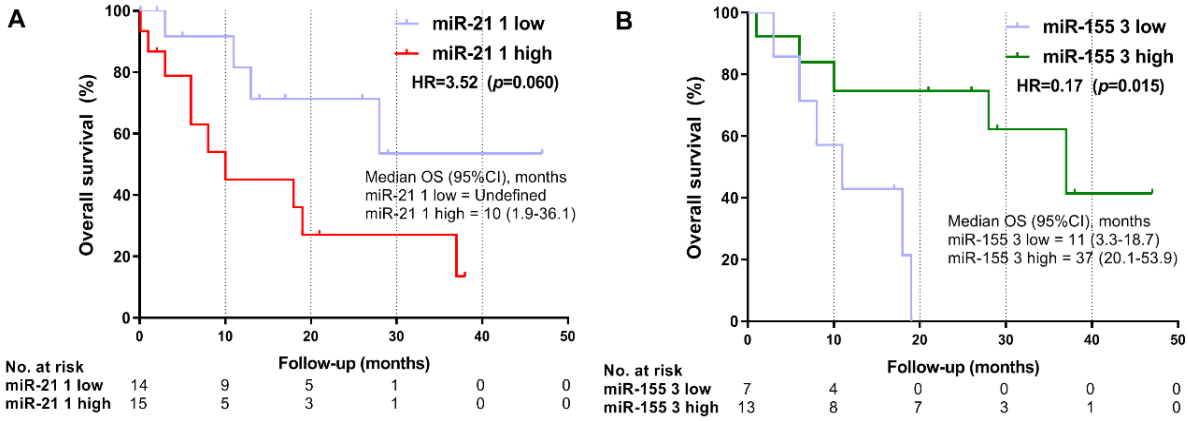

Figure 36: EV miR-21 1 and miR-155 3 as prognostic biomarkers for OS. Low expression of miR-21 1 showed non-statistical association with shorter OS (p=0.060) while high expression of miR-155 3 identified patients with shorter OS (p=0.015). p: p-value of log-rank (Mantel-Cox) test.

5.2.11.1 Univariate and multivariate Cox's proportional hazard regression analysis for OS

The univariate Cox's proportional hazard regression was performed on every clinical-pathological variable, the studied biomarkers in CTCs as well as the categorized miRNAs. In this case, CT response, CTC2 EGFR+, CTC2 LC3B+, CTC3, CTC3 LC3B+ phenotypes, and miR-155 3 were statistically associated with the prognosis of OS (**Table 23.1 & 23.2**).

Table 23.1: Univariate and multivariate Cox proportional hazards regression analysis OS

		OS Advanced NSCLC					
		Univariate analysis			Multivariate analysis		
		HR	95% CI	*p*	HR	95% CI	*p*
Gender	Men	2.10	0.48-9.26	0.328			
	Women	1.00					
Age (years)	<70	1.96	0.71-5.44	0.194			
	≥70	1.00					
Smoking habits	Never smoker	1.00		0.887			
	Ex-smoker	0.65	0.08-5.31	0.691			
	Current smoker	0.79	0.10-6.39	0.824			
Histological subtype	Non-SCC	2.26	0.86-5.94	0.099			
	SCC	1.00					
Stage	IIIA	1.00		0.638			
	IIIB	2.32	0.30-17.68	0.418			
	IV	3.18	0.29-35.27	0.346			

N status	N0	1.00		0.825			
	N1	0.00	0.00-UN	0.987			
	N2	0.73	0.14-3.76	0.704			
	N3	1.23	0.27-5.64	0.793			
M status	M0	0.67	0.15-2.94	0.595			
	M1	1.00					
ChT treatment	Vinorelbine based	1.15	0.36-3.62	0.816			
	Taxol based	1.00					
RT total dose		0.95	0.90-1.00	0.060			
ECOC diagnosis		1.07	0.34-3.34	0.909			
CT response	Favorable	0.26	0.10-0.71	**0.009***			
	Non-favorable	1.00					
PET response	Favorable	0.43	0.11-1.70	0.228			
	Non-favorable	1.00					
Progression 1	No	0.22	0.03-1.64	0.138			
	Yes	1.00					
CTC1	Presence	0.72	0.27-1.90	0.504			
	Absence	1.00					
EGFR+ CTC1	Presence	0.04	0.00-48.49	0.377			
	Absence	1.00					
LC3B+ CTC1	Presence	1.43	0.45-4.48	0.545			
	Absence	1.00					
Beclin-1+ CTC1	Presence	0.44	0.00-381.33	0.500			
	Absence	1.00					
CTC2	Presence	0.93	0.27-3.26	0.915			
	Absence	1.00					
EGFR+ CTC2	Presence	11.53	1.20-110.98	**0.034***			
	Absence	1.00					
LC3B+ CTC2	Presence	9.33	2.30-37.94	**0.002***			
	Absence	1.00					
CTC3	Presence	3.41	1.22-9.48	**0.019***	17.00	2.65-105.09	**0.003***
	Absence	1.00			1.00		
LC3B+ CTC3	Presence	6.27	1.30-30.33	**0.023***			
	Absence	1.00					
Beclin-1+ CTC3	Presence	0.66	0.09-5.08	0.694			
	Absence	1.00					
EMT CTC1	Presence	0.82	0.10-6.95	0.859			
	Absence	1.00					

Beclin-1 CTC2, EGFR+ CTC3, CTC4, LC3B+ CTC4, and Beclin-1+ CTC4 showed undefined results and are not represented in the table.

Table 23.2: Univariate and multivariate Cox proportional hazards regression analysis OS

		OS Advanced NSCLC					
		Univariate			Multivariate		
		HR	95% CI	*p*	HR	95% CI	*p*
miR-21 1	High	2.91	0.90-9.39	0.074	5.23	0.86-31.95	0.073
	Low	1.00			1.00		
miR-222 1	High	2.99	0.83-10.77	0.094			
	Low	1.00					
miR-375 1	High	0.20	0.03-1.55	0.124			
	Low	1.00					
miR-186 1	High	2.75	0.91-8.30	0.073			
	Low	1.00					
miR-155 2	High	3.22	0.90-11.57	0.073			
	Low	1.00					
miR-30c 2	High	0.28	0.07-1.10	0.068			
	Low	1.00					
miR-21 3	High	3.93	0.71-21.90	0.119			
	Low	1.00					
miR-155 3	High	0.20	0.05-0.84	**0.028***	0.11	0.02-0.65	**0.015***
	Low	1.00			1.00		
miR-129 3	High	0.33	0.10-1.14	0.080			
	Low	1.00					
miR-30 3	High	0.16	0.02-1.34	0.091			
	Low	1.00					

miR-21 4, miR-218 3, mir-375 4, and miR-186 4 presented undefined results and are not represented in the table.

As we can observed in the final multivariate model, CTC3 (HR=17.00, *p*=0.003) and miR-155 3 (HR=0.11, *p*=0.015) were the independent prognostic biomarkers for OS. However, despite not reaching statistical significance miR-21 1 expression (HR=5.23, *p*=0.073) was included in the final model as a cofactor that modulates the OS in advanced NSCLC patients (**Table 23.1 & 2**). As shown in the waterfall plot (**Figure 37**), the combination of these two biomarkers identified patients at higher risk of death and shorter OS.

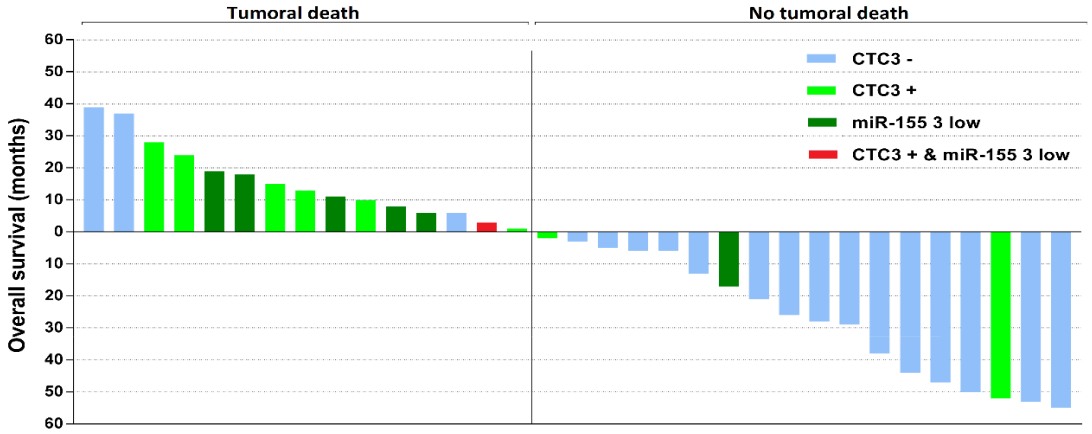

Figure 37: Waterfall plot of the OS according to the presence of CTC3 and miR-155 3 expression in advanced NSCLC patients. Patients with positive CTC3 (light-green), low EV miR-155 3 expression (dark-green) and both (red) presented higher risk of death and shorter OS. The graph shows the 33 patients were CTC3 could be evaluated while EV miR-155 3 was only evaluated in 20 of them.

6. Discussion

6.1 Discussion in early NSCLC

Lung cancer is the leading cause of cancer-related death in the world. Despite major breakthroughs in the diagnosis and treatment of this neoplasia, including the development of minimally invasive surgical approaches or molecular targeted therapies, the survival rate remains still low, with a 5-year rate of ~18%[1].

In early stages, the surgical resection the most effective treatment. Even after complete resection more than 20% of the patients will relapse. The implementation of adjuvant treatments such as platinum-based chemotherapy has presented controversial results, showing only some benefits in stage II NSCLC patients[19]. Probably due to the heterogeneous and dynamic of tumors, in which tissue biopsies might not reflex the complexity and the evolution of cellular subpopulations and not being able to stratify patients for an accurate treatment selection. Thus, new prognostic and predictive biomarkers are needed. The detection of CTCs in peripheral blood has been postulated as a potential prognostic factor in these patients. However, only few reports have revealed conclusive results about the role of CTCs in early NSCLC[82–89], some of them in pulmonary vein. Moreover, little is known about how heterogeneous subpopulations of CTCs can be found in a single patient. Therefore, we investigated the prognostic role of epithelial and EMT cells and their relation with the molecular profile of the tumors.

Presence of CTCs

Our study revealed a reduction not only in the number of epithelial CTCs, but also in the percentage of positive patients after the surgical resection in the ADC and SCC cohorts. From the initial 31.9% and 50% positive patients in ADC and SCC cohorts respectively, to the 25.5% and 30% after the surgery. This reduction could be caused by the effect of the complete resection of the tumors, as previously reported in surgical resected NSCLC patients[169]. The absence of CTCs could indicate the success of the operation while the presence of CTCs could denote possible micrometastasis undetected with the imaging techniques.

Moreover, these rates were also diminished at the third extraction, with a 21.9% and a 15.8% respectively. Neither the number of CTCs or the percentage of patients were different between ADC and SCC. However, the SCC cohort might have experienced a higher reduction along the follow-up. In fact, the analysis of CTC in paired samples showed a statistically significant reduction in the number of CTCs in the SCC cohort (p=0.001), while in ADC, the numbers remained similar (p=0.378).

Moreover, we observed no influence of the adjuvant therapy in the number of CTCs in ADC, as both the receiving and the non-receiving groups experienced no statistical reduction. In the SCC cohort, both groups manifested a reduction in the number of CTCs although no statistical significance was reached (p=0.067) in the no ChT group. Hence, these results suggest that the cisplatin-based adjuvant chemotherapy had no impact in the number of CTCs in ADC and probably neither in SCC patients.

CTC subpopulations and tissue expression

We observed specific tissue gene-miRNA correlations in the two histological subtypes. Interestingly, miR-155 expression was negatively correlated with *AXL* and *IL6R*, and these, in turn, were associated with the presence of EMT CTCs in ADC. This concur with previous evidence that reported potential repression by miR-155[170] and the association of *AXL* and *IL6R* with the promotion of the EMT[171,172]. Moreover, EMT CTCs were related to high expression of *GAPDH*,

which is known to upregulate the EMT via Snail[123] and is associated to poor prognosis in resected NSCLC patients[122]. In this way, the low miR-155/high *AXL-IL6R-GAPDH* tissue profile may result in the presence of CTCs with an EMT phenotype. CTCs could act as non-invasive tissue surrogates, revealing their molecular profile and if analyzed during the treatment, serve as predictive biomarkers of the tumor clonal evolution.

We did not observe any correlation between the tissue profile and the presence of EGFR positive or epithelial CTCs. This might be explained by the few numbers of miRNAs and genes analyzed. The analysis of RNA and miRNA-sequencing of the tissue, or even of single-CTCs, would broaden the spectrum of molecules analyzed and potentially reveal more complex pathways involved in the release of each subtype of CTCs[173].

Prognostic role of CTCs and tissue biomarkers

In our study, ADC and SCC patients showed similar survival with no statistical differences regarding RFS or OS. We analyzed the prognostic role of CTCs subpopulations and of every gene and miRNA in both cohorts.

According to the Kaplan-Meier analysis of the RFS, the presence of CTCs after surgery (HR=4.34, *p*=0.037) and high levels of tissue *AXL* (HR=4.54, *p*=0.033) and *GAPDH* (HR=6.27, *p*=0.012) correlated with shorter RFS only in the ADC cohort. To the contrary, high levels of tissue miR-222 (HR=4.72, *p*=0.030) and low of miR-30c (HR=0.16, *p*=0.011) identified SCC patients at higher risk of relapse. Similar results were reported in the univariate Cox's regression analysis. However, in the multivariate analysis of the RFS, only the presence of CTCs after surgery increased the risk of a shorter RFS in ADC patients (HR=2.51, 95% CI=1.07–5.87, *p*=0.034) with no effect of the adjuvant treatment. In the SCC cohort, the studied biomarkers presented non-statistical significance and the tumoral size was most informative variable.

miR-222 and miR-30c, both previously described to have a dual role in cancer[136,139], acted as an oncomiRNA and a tumor-suppressor miRNA, respectively, in our cohort of SCC patients. However, in the final multivariate model, they were not prognostic factors for RFS in ADC nor SCC. Consistent with a very recent study, the presence of CTCs after surgery was associated with higher stages (*p*=0.006)[174]. In fact, according to the few previous studies reported in early NSCLC[82–84,89], our results suggest that the detection of CTCs after surgery could contribute to the risk-evaluation of early stage NSCLC.

On the other hand, the Kaplan-Meier analysis of the OS revealed that the presence of CTC at six months after surgery (HR=3.62, *p*=0.057), again high levels of tissue *AXL* (HR=8.51, *p*=0.004), and high levels of *MET* (HR=5.78, *p*=0.016) were associated with worse survival only in ADC. In the multivariate analysis, the presence of CTCs after surgery (HR=10.8, 95% CI=1.54–76.4, *p*=0.017) and the expression of *AXL* in the tissue (HR=15.7, 95% CI=1.63–150.7, *p*=0.017) significantly decreased OS, again, with no impact of the adjuvant treatment. Consistent with previous findings, the expression of *AXL* was a biomarker of poor prognosis in resected ADC patients[175]. To the best of our knowledge, this is the first time that the presence of CTCs six months after surgery is identified as prognostic biomarkers for OS in ADC patients.

Unlike previous studies in early NSCLC[82–84,89], which were not divided by histological subtype, no CTC subpopulation gave any prognostic value in our SCC cohort. Here, CTCs were isolated by pan-cytokeratin antibodies that in comparison to EpCAM recovery, could enhance the isolation of semi-mesenchymal CTCs due to the preservation of cytokeratin-7 during EMT but it could also hamper the isolation of high EpCAM/ low cytokeratin CTCs[176]. The reduction of CTCs during the follow-up, only observed the SCC cohort, could mean a shift to a non-isolated phenotype such

as high EpCAM/low CK. As a result, we hypothesize that the lack of prognostic value of CTC after surgery and after 6 months in SCC patients might be caused by the proteins used in the isolation and a different molecular process involved in the dissemination. This emphasizes the need to identify and validate new markers for the isolation of CTCs with metastatic potential in SCC.

On the other hand, the presence of EMT CTCs at correlated with higher N stage (p=0.007) in ADC patients, consistent with the previously reported metastatic role of this subpopulation[177]. This phenotype was also associated to poor prognosis in ADC, as presented in the univariate analysis of RFS (HR=2.29) and OS (HR=1.65). However, non-statistically significant association was found, probably due to the fact that EMT CTCs were analyzed only 22 ADC patients. Further studies will be needed to confirm the prognostic value of this phenotype.

Potential clinical applications

This study characterized different subtypes of CTCs and the relation with the molecular profile of the tissue. In particular, we focused on *AXL* expression and its role as promotor of the EMT. Our results corroborate the importance of *AXL* as a predictor of poor prognosis and its role in the activation of the EMT.

Studies have proven that *AXL* is directly involved in the mechanism of resistance to cisplatin chemotherapy as well as EGFR targeted therapies by the acquisition of the EMT. Further evidence suggests that *AXL* inhibition decreases PD-L1 expression and CXCR6 in lung adenocarcinoma, especially in EGFR mutated patients[178]. In fact, PD-L1 positive CTCs showed a semi-mesenchymal phenotype, what might be the reason why these cells have enhanced immune escape and metastatic potential[179]. *AXL* overexpression was associated to immunotherapy resistance by suppressing MHCI and preventing antigen presentation[116]. However, tissue biopsy might not reflect real *AXL* levels before and during the treatment and multiple and longitudinal samples are hard to be obtained. A recent report tried to use of plasma *AXL* levels as a tissue surrogate with negative results[180]. In fact, according to our results, the analysis of EMT CTCs could serve as a viable alternative to determinate *AXL* levels in these cases. *AXL* inhibition has proven benefits by hampering the EMT as well as activating the antitumor immune response. Taken together, these data suggest that anti-*AXL* drugs could increase the benefit of immune drugs such as nivolumab or pembrolizumab, as well as the cisplatin adjuvant regimen. The combination of immunotherapy with chemotherapy, radiotherapy and other treatments, despite only showing preliminary results so far, has emerged as an effective strategy with a bright future use in NSCLC[32].

To conclude, the detection and characterization of CTCs after surgery might serve as prognostic tool identifying patients with poor prognosis. Moreover, our study could justify the inclusion of tissue *AXL* expression and the characterization of EMT CTCs as potential biomarkers for treatment selection and activity for those agents in early stage adenocarcinoma. Furthermore, these ideas could serve as the basis for the use of AXL inhibitors to improve the survival of resected NSCLC.

6.2 Discussion in advanced NSCLC

Most NSCLC patients are diagnosed at advanced stages where survival rates are even lower, with a reported 5-year survival rate of 5%. In these unresectable cases, concomitant chemo-radiotherapy is the standard of care but progression is also early developed and patients die due to the evolution of the disease[28].

Autophagy is activated under stress conditions to maintain homeostasis. In cancer, it has a dual role, leading to the apoptosis of altered cells during tumorigenesis but also promoting cell survival to cell damage. Despite controversial reports, recent evidence has suggested that autophagy might be a modulator of the resistance to chemotherapy and radiation regimens [37]. Little is known about the specific molecular mechanism that might trigger each way but miRNAs, as post-transcriptional rapid regulators of a broad range of genes could aid in the explanation[30].

Autophagy and EV formation are closely related processes through shared molecular machinery or organelles. For example, the ATG5-16 complex that mediates LC3B lipidation is located in the MVBs. Moreover, it also plays an important role in exosome biogenesis by preventing lysosome degradation[181]. This could suggest that under stress conditions, a common molecular pathway is activated, regulating autophagy to maintain cellular homeostasis as well as the formation of EVs. Moreover, EV miRNA cargo is selectively incorporated[104]. Therefore, cancer cells can transfer specific miRNAs into EVs to that would act as cellular communicators, modulating the tumor microenvironment. The diagnostic role of EV contained miRNAs has been extensively studied in NSCLC, but only few studies have reported their role in treatment resistance, immune evasion, or metastasis[182].

As described before, CTCs are important modulators of NSCLC metastasis, acting as prognostic biomarkers of the disease. In comparison to early stages, several studies have investigated the role of CTCs in advanced stages[90–94]. Nevertheless, most of those studies have enrolled patients under adjuvant chemotherapy and radiotherapy. Only one study, enrolling 13 patients, analyzed the prognostic role of PD-L1 expression in CTCs during concomitant ChT-RT in advanced stages[183]. Due to the lack of clinical evidence and the uncertain role of autophagy in the resistance to this treatment, we investigated the role of the level of autophagy in CTCs combined with EV miRNAs in the prognosis of these patients.

Presence of CTCs

Our study manifested a reduction in the number of positive CTC patients to during ChT-RT treatment while an increase at the end of it. From initially 43.9% positive patients at baseline, 20.5% at the middle of the treatment, to 27.3% at the end. However, when analyzing the total number of CTCs in paired samples, they first rose and finally fell during the same period (CTC1-3), resulting a significant fluctuation (p=0.045). In fact, this reduction correlated with the total radiotherapy dose (p=0.039), as patients who did not received the full 60 Gy, presented minor reduction in the number of CTCs. This concur with a previous study were increased number of CTCs were observed after the initiation of the RT treatment. In this study an elevated γ-H2AX (a DNA damage biomarker or radiation induced DNA double-strand breaks) signal was observed in post-RT blood samples, what suggested the presence of CTCs derived from irradiated tumors[184]. In addition, the final reduction of CTCs at the end of the treatment would be caused by the sequential exposition to the radiation and it could mean a good performance of the treatment[185].

As observed in the early NSCLC cohorts, non-SCC and SCC subtypes experienced different CTC dynamic. CTCs did not significantly change during treatment (p=0.430) in non-SCC patients but

they did fluctuate in SCC (p=0.035). In fact, non-SCC patients had significant higher levels of CTCs at the end of the treatment (p=0.036). However, this study only included 27 SCC and 14 non-SCC patients. Larger populations would be needed to confirm the histological differences.

EV miRNA expression:

According to the MISEV guidelines at that time[113], we analyzed the expression of miRNAs contained in EVs. As previous studies described[153], we observed higher expression of EV miR-21 (p<0.001) and miR-186 (p=0.002) in samples from NSCLC compared to healthy donors, moreover, this miRNAs were also elevated in patients with poor responses according to PET evaluation. [30,153]

Interestingly, patients who manifested favorable responses in the imaging test had significant high levels of miR-375, 200c, and 30c at baseline. miR-30c has a dual role in cancer, however, our results, in concordance to most studies in NSCLC, give these genes a tumor suppressor role[149,150]. Moreover, lymph node affected patients (N1) showed low expression of miR-30c and 200c during the treatment, two miRNAs that blocks the EMT[135,149]. This agree with previous studies in NSCLC tissues that associated the inhibition of these miRNAs to more invasive properties and lymph node metastasis[139,186]. Hence, we propose that encapsulated miR-30c and miR200c could identify lymph node metastasis associated with an unfavorable PET response.

CTC subpopulations and EV miRNA expression:

To date, the correlation between CTCs and EVs has been analyzed at the same time in only few studies, however not resulting in specific common patterns between the two biomarkers. Our results revealed specific miRNA signatures regarding some subpopulations of CTCs. In particular, the expression of miR-218 was associated with a high LC3B+ CTCs at baseline. LC3B is a common biomarker of autophagic status, as it is expressed in the autophagosomes. Increased levels of this protein has been observed in radiation-resistant cells, indicating high autophagic levels[38]. On the other hand, miR-218 targets *HMGB1*, inhibiting autophagy[146]. In our patients, miR-218 levels were increased during the treatment (p=0.015) and accordingly, the presence of autophagic CTCs diminished. As a result, we observed that the presence of epithelial CTCs correlated with high levels miR-218 at the end of the treatment. Therefore, this suggest that LC3B in CTCs and EV miR-218 might reflect the evolution of autophagic process in the tumor tissue during the ChT-RT concomitant therapy.

Prognostic role of CTCs and EV miRNAs:

During the follow-up of these patients, a high number of them relapse (73.2%). With the objective to identify prognostic biomarkers, we analyzed the role of different CTCs subpopulations and EVs miRNAs in the RFS. According to the Kaplan-Meier analysis, the presence of high LC3B+ CTCs during the treatment was linked to a dramatic shorter RFS (HR=8.89, p=0.003). In the same way, low levels of EV miR30c at baseline (HR=0.11, p=0.002). and high of miR-21 after the surgery (HR=10.7, p=0.001) identified patients at higher risk of relapse. Similar results were observed in the univariate Cox's analysis, where also favorable PET responses and higher radiation dose correlated with better prognosis. This matches the described association between low levels of miR-30c, PET response, and lymph node status, what could imply shorter RFS.

The multivariate analysis manifested that only the presence of LC3B+ CTCs during the treatment (HR=30.18, 95% CI=2.39-381.8, p=0.009), levels of EV miR-21 after ChT-RT (HR=84.52, 95% CI=4.33–1650.5, p=0.003), and the radiation dose (HR=0.89, 95% CI=0.82-0.98, p=0.016) were independent prognostic factors for RFS. Patients who received higher radiation dose,

which was also associated with higher reduction of CTCs, presented better prognosis with longer RFS. As suggested in a previous publication[185], the sequential radiation was effective at eliminating most of these CTCs and their dynamics would reflect the response to treatment. Moreover, the presence of LC3B+ CTC was an independent prognostic factor for RFS. This matches previous reports that associate radiotherapy resistance to the increase of autophagy markers such as LC3B[38]. This suggests that autophagy activation conferred these cells an enhanced resistance to the treatment, finally being responsible for the poor survival of these patients. Moreover, as observed before, miR-218 could be directly implicated in the acquisition of this autophagic phenotype. The EV miR-21 was also associated with worse survival. This concur with previous evidence that associated this high levels of this miRNA to the resistance to radiotherapy and chemotherapy in NSCLC by targeting the tumor suppressor genes *PTEN* and *PDCD4*[30,133]. Moreover, EV miR-21 has been reported to bind to macrophage TLR-8, induce the secretion of IL-6 and TNF-α, finally promoting prometastatic inflammation[134].

Regarding prognostic factors for overall survival, the Kaplan-Meier analysis associated the presence of several CTC phenotypes and EV miRNAs to a shorter survival. Patients that presented EGFR+ (HR=7.32 p=0.007) and LC3B+ (HR=14.60 p<0.001) CTCs during treatment experienced shorter overall survival as well as those with CTCs (HR=6.23 p=0.013) and LCB+ CTCs (HR=6.88 p=0.009) at the end of it. As reported in the PFS, the presence of LC3B CTCs, could be associated to enhanced chemoradioresistance by autophagy activation. The association of EGFR+ CTCs with worse survival concur could be explained by the enhanced radioresistance in wild-type EGFR vs. mutated EGFR advanced patients[187]. On the other hand, higher levels of EV miR-21 (HR=3.52 p=0.060) at baseline and lower of EV miR-155 (HR=0.17 p=0.015) at the conclusion of the treatment were associated with shorter OS.

In the subsequent multivariate analysis, only the presence of CTCs (HR=17.00, 95% CI=2.65-105.09, p=0.003) and lower levels of EV miR-155 (HR=0.11, 95% CI=0.02-0.65, p=0.015) after the treatment were independent prognostic biomarkers for OS. The specific phenotypes of CTCs lost prognostic value, probably due to the low number of patients detected in each case.

Interestingly both, CTCs and EV miR-155, detected after the treatment. The analysis of the dynamics revealed that the reduction of CTCs from the middle to the end of the treatment (CTC2-3) was consistent to an increase in EV miR-155 levels. EV miR-155 expression may exert a dual role in NSCLC, however, in our patients, high miR-155 levels in EV were associated with good prognosis, consistent with previous findings[142,143]. EV miR-155 also plays an important role during immune responses promoting the expression of inflammatory genes[188].

Furthermore, presence of CTCs after the concomitant treatment were associated with worse prognosis. According to a similar study in locally advanced NSCLC patients, CTCs before the RT treatment were not associated to the relapse, to the contrary, but those detected after RT were[189]. Unlike that study, which only suggested a possible prognostic impact on RFS due to the lack of statistical significance, our study provided for the first time, enough evidence to support that LC3B CTCs during and CTCs post-concomitant ChT-RT treatment are independent prognostic factors of PFS and OS, respectively.

On the other hand, we did not observe any prognostic value of EMT or Beclin-1 CTCs, probably due to the low number of patients. In the case of Beclin-1, its detection with a blue fluorescent dye in samples that were previously chromogenically stained this could imply a reduced signal. On the other hand, despite differences in the dynamics of CTCs in the histological subtypes, the multivariate analysis showed no differences between SCC and non-SCC patients.

Further studies should be performed including larger cohorts of advanced patients to investigate the prognostic role of CTCs separately.

As we know, miRNAs are selectively incorporate into EVs, being potential tissue surrogates with the benefits of the liquid biopsy approach[190]. However, EVs studies presented some disadvantages as high heterogeneity and impurity of EVs described so far. However, the application of the new MISEV guidelines[113] is expected to solve these issues by the standardization of EVs assays. Added to their important role as intercellular communicators, EVs have a promising future as prognostic biomarkers in NSCLC and EV miR-21 and miR-155 levels in the blood could identify patients with more aggressive and resistant tumors with poor survival.

Clinical implications

EVs and autophagy play crucial roles in response to cellular stress for the consequent maintenance of cellular homeostasis and their crosstalk might represent therapeutic opportunities in NSCLC. Moreover, the detection and characterization of CTCs can contribute to the understanding of tumor heterogeneity during tumor evolution in response to therapies. In a novel study, sequential CTC xenograft revealed how CTCs can provide organ-specific signatures as well as biomarkers with therapeutic potential. Thus, the combination of new therapies and CTC targeted drugs could improve the outcome of NSCLC patients[60]. Stereotactic body radiation therapy (SBRT) is an effective non-invasive modality that shows promising results in early stage NSCLC. Owing to the impact of new lung cancer screening programs, early cases of this disease are expected to increase and accordingly, the use of SBRT[191]. Moreover, a preliminary study in unresectable NSCLC patients showed that SBRT treatment enhanced the immunoactive and decreased the immunosuppressive components of the immune system over six months[192]. This idea supports the potential of future combinations of SBRT and immunotherapy, where our radiotherapy biomarkers LC3B CTCs and EV miRNAs might represent a viable option in the management of these patients.

Recent strategies in cancer have included autophagy targeting in combination to chemotherapy or immunotherapy. Autophagy inhibition with chloroquine downregulated mesenchymal characteristics in NSCLC cells and enhanced cisplatin sensitivity in a novel *in vivo* model[193]. Another lung *in vivo* study showed that cancer cell autophagy was promoted by natural killer cells but the administration of the autophagy inhibitor rocaglamide restored natural killer-mediated elimination of tumor cells[194]. Nevertheless, autophagy plays a dual role in immune responses, activating antigen presentation by dendritic cells and B cells, or mediating immune tolerance via M2 polarization of tumor associated macrophages[195]. As a consequence, the clinical development of autophagy promotors or inhibitors remains complex. However, our study could shed some light into this dark scenario. Taken together, all these data suggest that the study of specific EV miRNAs and CTCs, due to their repeatable and non-invasive nature, could provide the real-time information of the autophagic status of the tumor, acting as potential predictors of combinatory treatments based on autophagy inhibition and immune antibodies.

7. Conclusions

7.1 Conclusions of sub-study 1: Early stages

- ADC and SCC patients showed contrary dynamics in the number of CTCs, with a reduction of the CTC count along the follow-up only in SCC patients.
- ADC and SCC tissues differed in their molecular and biological behavior as differential gene and miRNA signatures were observed.
- The presence of EMT CTCs was associated with a low miR-155/high *AXL-IL6R-GAPDH* tissue profile and a higher nodal status in ADC patients, what suggested the potential of CTCs as tissue surrogates, revealing the complexity of temporal and spatial intratumor heterogeneity.
- The presence of CTCs one month after surgery was an independent prognostic biomarker for RFS in adenocarcinoma, possibly denoting the presence of micrometastasis.
- The presence of CTCs 6 months after surgery and tissue *AXL* expression were independent prognostic biomarkers for OS in adenocarcinoma.
- Tissue *AXL* and CTCs could potentially represent biomarkers of stratification of adenocarcinoma patients that might benefit from new adjuvant therapies.

7.12 Conclusions of sub-study 2: Advanced stages

- NSCLC patients showed an increase of CTC counts during concomitant ChT-RT treatment and a decrease at its conclusion.
- The decrease in CTC counts was correlated with higher total dose of RT implying a potential good performance of the treatment.
- EV miRNAs from plasma can be correctly analyzed and might act as tissue surrogates.
- Levels of EV miR-218 were increased during ChT-RT treatment and inversely correlated with the activation of autophagy in CTCs.
- A higher total dose of RT was an independent prognostic factor for better RFS.
- The presence of autophagy activated CTCs during the treatment was an independent prognostic biomarker for RFS, suggesting the activation of autophagy as a mechanism of resistance.
- High expression of EV miR-21 after the treatment was an independent prognostic biomarker for RFS.
- The reduction of CTCs correlated inversely with levels of EV miR-155.
- The presence of CTCs and low levels of EV miR-155 after the treatment were independent prognostic biomarkers for OS.
- EV miRNAs and CTCs might be used as biomarkers for the stratification and management of NSCLC that might benefit from ChT-RT treatments but also from combinatory strategies based on autophagy activation, immune therapy or SBRT.

8. References

1. Ferlay J, Colombet M, Soerjomataram I, et al. Estimating the global cancer incidence and mortality in 2018: GLOBOCAN sources and methods. *Int J Cancer*. 2019;144(8):1941-1953. doi:10.1002/ijc.31937

2. de Groot PM, Wu CC, Carter BW, Munden RF. The epidemiology of lung cancer. *Transl Lung Cancer Res*. 2018;7(3):220-233. doi:10.21037/tlcr.2018.05.06

3. Nanavaty P, Alvarez MS, Alberts WM. Lung Cancer Screening: Advantages, Controversies, and Applications. *Cancer Control*. 2014;21(1):9-14. doi:10.1177/107327481402100102

4. Hecht SS. Tobacco Smoke Carcinogens and Lung Cancer. *JNCI J Natl Cancer Inst*. 1999;91(14):1194-1210. doi:10.1093/jnci/91.14.1194

5. Yang IA, Holloway JW, Fong KM. Genetic susceptibility to lung cancer and co-morbidities. *J Thorac Dis*. 2013;5(SUPPL.5). doi:10.3978/j.issn.2072-1439.2013.08.06

6. Brennan P, Hainaut P, Boffetta P. Genetics of lung-cancer susceptibility. *Lancet Oncol*. 2011;12(4):399-408. doi:10.1016/S1470-2045(10)70126-1

7. Kanwal M, Ding XJ, Cao Y. Familial risk for lung cancer. *Oncol Lett*. 2017;13(2):535-542. doi:10.3892/ol.2016.5518

8. Osmani L, Askin F, Gabrielson E, Li QK. Current WHO guidelines and the critical role of immunohistochemical markers in the subclassification of non-small cell lung carcinoma (NSCLC): Moving from targeted therapy to immunotherapy. *Semin Cancer Biol*. 2018;52:103-109. doi:10.1016/j.semcancer.2017.11.019

9. Qiu ZW, Bi JH, Gazdar AF, Song K. Genome-wide copy number variation pattern analysis and a classification signature for non-small cell lung cancer. *Genes Chromosom Cancer*. 2017;56(7):559-569. doi:10.1002/gcc.22460

10. Barta JA, Powell CA, Wisnivesky JP. Global epidemiology of lung cancer. *Ann Glob Heal*. 2019;85(1). doi:10.5334/aogh.2419

11. Lortet-Tieulent J, Soerjomataram I, Ferlay J, Rutherford M, Weiderpass E, Bray F. International trends in lung cancer incidence by histological subtype: Adenocarcinoma stabilizing in men but still increasing in women. *Lung Cancer*. 2014;84(1):13-22. doi:10.1016/j.lungcan.2014.01.009

12. Yano T, Haro A, Shikada Y, Maruyama R, Maehara Y. Non-small cell lung cancer in never smokers as a representative “non-smoking-associated lung cancer”: Epidemiology and clinical features. *Int J Clin Oncol*. 2011;16(4):287-293. doi:10.1007/s10147-010-0160-8

13. Lee H, Alberts WM, Nanavaty P, Alvarez MS. *Lung Cancer Screening: Advantages, Controversies, and Applications*. Vol 21.; 2014. https://journals.sagepub.com/doi/pdf/10.1177/107327481402100102. Accessed November 15, 2018.

14. Sahiner I, Vural GU. Positron emission tomography/computerized tomography in lung cancer. *Quant Imaging Med Surg*. 2014;4(3):195-206. doi:10.3978/j.issn.2223-4292.2014.03.05

15. Lim W, Ridge CA, Nicholson AG, Mirsadraee S. The 8th lung cancer TNM classification and clinical staging system: Review of the changes and clinical implications. *Quant Imaging Med Surg*. 2018;8(7):709-718. doi:10.21037/qims.2018.08.02

16. Guo F, Ma D, Li S, Adamek M. Compare the prognosis of da Vinci robot-Assisted thoracic surgery (RATS) with video-Assisted thoracic surgery (VATS) for non-small cell lung cancer: A Meta-Analysis. *Med (United States)*. 2019;98(39). doi:10.1097/MD.0000000000017089

17. Shin JY, Yoon JK, Marwaha G. Progress in the Treatment and Outcomes for Early-Stage Non-Small Cell Lung Cancer. *Lung*. 2018;196(3):351-358. doi:10.1007/s00408-018-0110-1

18. Arriagada R, Bergman B, Dunant A, Le Chevalier T, Pignon JP, Vansteenkiste J. Cisplatin-Based Adjuvant Chemotherapy in Patients with Completely Resected Non-Small-Cell Lung Cancer. *N Engl J Med*. 2004;350(4):351-360. doi:10.1056/NEJMoa031644

19. Howington JA, Blum MG, Chang AC, Balekian AA, Murthy SC. Treatment of stage I and II non-small cell lung cancer: Diagnosis and management of lung cancer, 3rd ed: American college of chest physicians evidence-based clinical practice guidelines. *Chest*. 2013;143(5 SUPPL). doi:10.1378/chest.12-2359

20. Burdett S, Pignon JP, Tierney J, et al. Adjuvant chemotherapy for resected early-stage non-small cell lung cancer. *Cochrane Database Syst Rev*. 2015;(3):CD011430. doi:10.1002/14651858.CD011430

21. Drake JA, Portnoy DC, Tauer K, Weksler B. Adding Radiotherapy to Adjuvant Chemotherapy Does Not Improve Survival of Patients With N2 Lung Cancer. *Ann Thorac Surg*. 2018;106(4):959-965. doi:10.1016/j.athoracsur.2018.04.074

22. Sebastian NT, Xu-Welliver M, Williams TM. Stereotactic body radiation therapy (SBRT) for early stage nonsmall cell lung cancer (NSCLC): Contemporary insights and advances. *J Thorac Dis*. 2018;10:S2451-S2464. doi:10.21037/jtd.2018.04.52

23. Singh AK, Hennon M, Ma SJ, et al. A pilot study of stereotactic body radiation therapy (SBRT) after surgery for stage III non-small cell lung cancer. *BMC Cancer*. 2018;18(1). doi:10.1186/s12885-018-5039-5

24. Griesinger F, Korol EE, Kayaniyil S, Varol N, Ebner T, Goring SM. Efficacy and safety of first-line carboplatin-versus cisplatin-based chemotherapy for non-small cell lung cancer: A meta-analysis. *Lung Cancer*. 2019;135:196-204. doi:10.1016/j.lungcan.2019.07.010

25. Chang WJ, Sun JM, Lee JY, Ahn JS, Ahn MJ, Park K. A retrospective comparison of adjuvant chemotherapeutic regimens for non-small cell lung cancer (NSCLC): Paclitaxel plus carboplatin versus vinorelbine plus cisplatin. *Lung Cancer*. 2014;84(1):51-55. doi:10.1016/j.lungcan.2014.01.017

26. Ohe Y, Ohashi Y, Kubota K, et al. Randomized phase III study of cisplatin plus irinotecan versus carboplatin plus paclitaxel, cisplatin plus gemcitabine, and cisplatin plus vinorelbine for advanced non-small-cell lung cancer: Four-Arm Cooperative Study in Japan. *Ann Oncol*. 2006;18(2):317-323. doi:10.1093/annonc/mdl377

27. Lerouge D, Rivière A, Dansin E, et al. A phase II study of cisplatin with intravenous and oral vinorelbine as induction chemotherapy followed by concomitant chemoradiotherapy with oral vinorelbine and cisplatin for locally advanced non-small cell lung cancer. *BMC Cancer*. 2014;14(1). doi:10.1186/1471-2407-14-231

28. Flentje M, Huber RM, Engel-Riedel W, et al. GILT – Eine randomisierte Phase-III-Studie mit oralem Vinorelbin und Cisplatin plus konkomitanter Strahlentherapie gefolgt von konsolidierender Therapie mit oralem Vinorelbin und Cisplatin oder bestmöglicher supportiver Therapie bei nicht-kleinzelligem Lungenkarzinom Stadium III. *Strahlentherapie und Onkol*. 2016;192(4):216-222. doi:10.1007/s00066-016-0941-8

29. Yin E, Nelson DO, Coleman MA, Peterson LE, Wyrobek AJ. Gene expression changes in mouse brain after exposure to low-dose ionizing radiation. *Int J Radiat Biol*. 2003;79(10):759-775. doi:10.1080/09553000310001610961

30. Macdonagh L, Gray SG, Finn SP, Cuffe S, O'byrne KJ, Barr MP. The emerging role of microRNAs in resistance to lung cancer treatments. *Cancer Treat Rev*. 2015;41:160-169. doi:10.1016/j.ctrv.2014.12.009

31. Rolfo C, Caglevic C, Santarpia M, et al. Immunotherapy in NSCLC: A promising and revolutionary

weapon. In: *Advances in Experimental Medicine and Biology*. Vol 995. Springer New York LLC; 2017:97-125. doi:10.1007/978-3-319-53156-4_5

32. Camidge DR, Doebele RC, Kerr KM. Comparing and contrasting predictive biomarkers for immunotherapy and targeted therapy of NSCLC. *Nat Rev Clin Oncol*. 2019;16(6):341-355. doi:10.1038/s41571-019-0173-9

33. Hanahan D, Weinberg RA. Hallmarks of cancer: The next generation. *Cell*. 2011;144(5):646-674. doi:10.1016/j.cell.2011.02.013

34. Marquez RT, Xu L. Bcl-2:Beclin 1 complex: multiple, mechanisms regulating autophagy/apoptosis toggle switch. *Am J Cancer Res*. 2012;2(2):214-221. http://www.ncbi.nlm.nih.gov/pubmed/22485198. Accessed January 4, 2020.

35. Kondo Y, Kanzawa T, Sawaya R, Kondo S. The role of autophagy in cancer development and response to therapy. *Nat Rev Cancer*. 2005;5(9):726-734. doi:10.1038/nrc1692

36. Chen J, Zhang L, Zhou H, et al. Inhibition of autophagy promotes cisplatin-induced apoptotic cell death through Atg5 and Beclin 1 in A549 human lung cancer cells. *Mol Med Rep*. 2018;17(5):6859-6865. doi:10.3892/mmr.2018.8686

37. Wu YW, Lin CF, Lin YS, Su WC, Chiu WH. Autophagy regulates vinorelbine sensitivity due to continued Keap1-mediated ROS generation in lung adenocarcinoma cells. *Cell Death Discov*. 2018;4(1). doi:10.1038/s41420-018-0098-6

38. Liu Z, Huang S. Inhibition of miR-191 contributes to radiation-resistance of two lung cancer cell lines by altering autophagy activity. 2011. doi:10.1186/s12935-015-0165-5

39. Kang R, Zeh HJ, Lotze MT, Tang D. The Beclin 1 network regulates autophagy and apoptosis. *Cell Death Differ*. 2011;18. doi:10.1038/cdd.2010.191

40. Levy JMM, Towers CG, Thorburn A. Targeting autophagy in cancer. *Nat Rev Cancer*. 2017;17(9):528-542. doi:10.1038/nrc.2017.53

41. Saleh T, Cuttino L, Gewirtz DA. Autophagy is not uniformly cytoprotective: a personalized medicine approach for autophagy inhibition as a therapeutic strategy in non-small cell lung cancer. *Biochim Biophys Acta - Gen Subj*. 2016;1860(10):2130-2136. doi:10.1016/j.bbagen.2016.06.012

42. Zheng T, Li D, He Z, Feng S, Zhao S. Prognostic and clinicopathological significance of beclin-1 in non-small-cell lung cancer: A meta-analysis. *Onco Targets Ther*. 2018;11:4167-4175. doi:10.2147/OTT.S164987

43. Kwon Y, Kim M, Jung HS, Kim Y, Jeoung D. Targeting autophagy for overcoming resistance to anti-EGFR treatments. *Cancers (Basel)*. 2019;11(9). doi:10.3390/cancers11091374

44. Tang D, Kang R, Livesey KM, et al. Endogenous HMGB1 regulates autophagy. *J Cell Biol*. 2010;190(5):881-892. doi:10.1083/jcb.200911078

45. Mowers EE, Sharifi MN, Macleod KF. Autophagy in cancer metastasis. *Oncogene*. 2017;36(12):1619-1630. doi:10.1038/onc.2016.333

46. Chambers AF, Groom AC, MacDonald IC. Dissemination and growth of cancer cells in metastatic sites. *Nat Rev Cancer*. 2002;2(8):563-572. doi:10.1038/nrc865

47. De Groot AE, Roy S, Brown JS, Pienta KJ, Amend SR. Revisiting seed and soil: Examining the primary tumor and cancer cell foraging in metastasis. *Mol Cancer Res*. 2017;15(4):361-370. doi:10.1158/1541-7786.MCR-16-0436

48. Nguyen DX, Bos PD, Massagué J. Metastasis: From dissemination to organ-specific colonization. *Nat Rev Cancer*. 2009;9(4):274-284. doi:10.1038/nrc2622

49. Liu Q, Zhang H, Jiang X, Qian C, Liu Z, Luo D. Factors involved in cancer metastasis: A better

understanding to “seed and soil” hypothesis. *Mol Cancer*. 2017;16(1). doi:10.1186/s12943-017-0742-4

50. Heppner GH. Tumor Heterogeneity. *Cancer Res*. 1984;44(6).

51. Dagogo-Jack I, Shaw AT. Tumour heterogeneity and resistance to cancer therapies. *Nat Rev Clin Oncol*. 2018;15(2):81-94. doi:10.1038/nrclinonc.2017.166

52. Vessoni AT, Filippi-Chiela EC, Lenz G, Batista LFZ. Tumor propagating cells: drivers of tumor plasticity, heterogeneity, and recurrence. *Oncogene*. 2019. doi:10.1038/s41388-019-1128-4

53. Findlay JM, Castro-Giner F, Makino S, et al. Differential clonal evolution in oesophageal cancers in response to neo-adjuvant chemotherapy. *Nat Commun*. 2016;7. doi:10.1038/ncomms11111

54. Nowell PC. The clonal evolution of tumor cell populations. *Science (80-)*. 1976;194(4260):23-28. doi:10.1126/science.959840

55. Li W, Wang H, Zhao Z, et al. Emerging Nanotechnologies for Liquid Biopsy: The Detection of Circulating Tumor Cells and Extracellular Vesicles. *Adv Mater*. 2019;31(45):1805344. doi:10.1002/adma.201805344

56. Al-Mehdi AB, Tozawa K, Fisher AB, Shientag L, Lee A, Muschel RJ. Intravascular origin of metastasis from the proliferation of endothelium-attached tumor cells: A new model for metastasis. *Nat Med*. 2000;6(1):100-102. doi:10.1038/71429

57. Ashworth TR. A Case of Cancer in Which Cells Similar to Those in the Tumours Were Seen in the Blood after Death. *Aust Med J*. 1869;14:146-147.

58. Keller L, Pantel K. Unravelling tumour heterogeneity by single-cell profiling of circulating tumour cells. *Nat Rev Cancer*. 2019;19(10):553-567. doi:10.1038/s41568-019-0180-2

59. Bednarz-Knoll N, Alix-Panabières C, Pantel K. Clinical relevance and biology of circulating tumor cells. *Breast Cancer Res*. 2011;13(6). doi:10.1186/bcr2940

60. Vishnoi M, Liu NH, Yin W, et al. The identification of a TNBC liver metastasis gene signature by sequential CTC-xenograft modeling. *Mol Oncol*. 2019;13(9):1913-1926. doi:10.1002/1878-0261.12533

61. Kalluri R. EMT: When epithelial cells decide to become mesenchymal-like cells. *J Clin Invest*. 2009;119(6):1417-1419. doi:10.1172/JCI39675

62. Jie XX, Zhang XY, Xu CJ. Epithelial-to-mesenchymal transition, circulating tumor cells and cancer metastasis: Mechanisms and clinical applications. *Oncotarget*. 2017;8(46):81558-81571. doi:10.18632/oncotarget.18277

63. Koren A, Rijavec M, Kern I, Sodja E, Korosec P, Cufer T. BMI1, ALDH1A1, and CD133 transcripts connect epithelial-mesenchymal transition to cancer stem cells in lung carcinoma. *Stem Cells Int*. 2016;2016. doi:10.1155/2016/9714315

64. Suda K, Murakami I, Yu H, et al. CD44 facilitates epithelial-to-mesenchymal transition phenotypic change at acquisition of resistance to EGFR kinase inhibitors in lung cancer. *Mol Cancer Ther*. 2018;17(10):2257-2265. doi:10.1158/1535-7163.MCT-17-1279

65. Dongre A, Weinberg RA. New insights into the mechanisms of epithelial–mesenchymal transition and implications for cancer. *Nat Rev Mol Cell Biol*. 2019;20(2):69-84. doi:10.1038/s41580-018-0080-4

66. Roche J. The Epithelial-to-Mesenchymal Transition in Cancer. *Cancers (Basel)*. 2018;10:52. doi:10.3390/cancers10020052

67. Xu J, Lamouille S, Derynck R. TGF-B-induced epithelial to mesenchymal transition. *Cell Res*. 2009;19(2):156-172. doi:10.1038/cr.2009.5

68. Brabletz T, Kalluri R, Nieto MA, Weinberg RA. EMT in cancer. *Nat Rev Cancer*. 2018;18(2):128-134. doi:10.1038/nrc.2017.118

69. Potdar P, Lotey N. Role of circulating tumor cells in future diagnosis and therapy of cancer. *J Cancer Metastasis Treat*. 2015;1(2):44. doi:10.4103/2394-4722.158803

70. Lecharpentier A, Vielh P, Perez-Moreno P, Planchard D, Soria JC, Farace F. Detection of circulating tumour cells with a hybrid (epithelial/ mesenchymal) phenotype in patients with metastatic non-small cell lung cancer. *Br J Cancer*. 2011;105(9):1338-1341. doi:10.1038/bjc.2011.405

71. Fischer KR, Durrans A, Lee S, et al. Epithelial-to-mesenchymal transition is not required for lung metastasis but contributes to chemoresistance. *Nature*. 2015;527(7579):472-476. doi:10.1038/nature15748

72. Pastushenko I, Blanpain C. EMT Transition States during Tumor Progression and Metastasis. *Trends Cell Biol*. 2018;xx. doi:10.1016/j.tcb.2018.12.001

73. Wu S, Liu S, Liu Z, et al. Classification of Circulating Tumor Cells by Epithelial-Mesenchymal Transition Markers. Samant R, ed. *PLoS One*. 2015;10(4):e0123976. doi:10.1371/journal.pone.0123976

74. Krebs MG, Hou JM, Sloane R, et al. Analysis of circulating tumor cells in patients with non-small cell lung cancer using epithelial marker-dependent and -independent approaches. *J Thorac Oncol*. 2012;7(2):306-315. doi:10.1097/JTO.0b013e31823c5c16

75. Coppolino A, Gao DC, Wagner PL, et al. Standard markers for detection of circulating tumor cells are variably expressed in pulmonary adenocarcinomas and are downregulated in cells undergoing mesenchymal transition. *J Am Coll Surg*. 2012;215(3):S40. doi:10.1016/j.jamcollsurg.2012.06.122

76. Thiele J-A, Bethel K, Králíčková M, Kuhn P. Circulating Tumor Cells: Fluid Surrogates of Solid Tumors. *Annu Rev Pathol Mech Dis*. 2017;12(1):419-447. doi:10.1146/annurev-pathol-052016-100256

77. Zacharias M, Brcic L, Eidenhammer S, Popper H. Bulk tumour cell migration in lung carcinomas might be more common than epithelial-mesenchymal transition and be differently regulated. *BMC Cancer*. 2018;18(1):717. doi:10.1186/s12885-018-4640-y

78. Aceto N, Bardia A, Miyamoto DT, et al. Circulating tumor cell clusters are oligoclonal precursors of breast cancer metastasis. *Cell*. 2014;158(5):1110-1122. doi:10.1016/j.cell.2014.07.013

79. Szczerba BM, Castro-Giner F, Vetter M, et al. Neutrophils escort circulating tumour cells to enable cell cycle progression. *Nature*. 2019;566(7745):553-557. doi:10.1038/s41586-019-0915-y

80. Padua D, Zhang XHF, Wang Q, et al. TGFβ Primes Breast Tumors for Lung Metastasis Seeding through Angiopoietin-like 4. *Cell*. 2008;133(1):66-77. doi:10.1016/j.cell.2008.01.046

81. Garrido-Navas, de Miguel-Perez, Exposito-Hernandez, et al. Cooperative and Escaping Mechanisms between Circulating Tumor Cells and Blood Constituents. *Cells*. 2019;8(11):1382. doi:10.3390/cells8111382

82. Hofman V, Ilie MI, Long E, et al. Detection of circulating tumor cells as a prognostic factor in patients undergoing radical surgery for non-small-cell lung carcinoma: Comparison of the efficacy of the CellSearch Assay™ and the isolation by size of epithelial tumor cell method. *Int J Cancer*. 2011;129(7):1651-1660. doi:10.1002/ijc.25819

83. Bayarri-Lara C, Ortega FG, Cueto Ladrón De Guevara A, et al. Circulating tumor cells identify early recurrence in patients with non-small cell lung cancer undergoing radical resection. *PLoS One*. 2016;11(2). doi:10.1371/journal.pone.0148659

84. Bayarri-Lara CI, de Miguel Pérez D, Cueto Ladrón de Guevara A, et al. Association of circulating tumour cells with early relapse and 18F-fluorodeoxyglucose positron emission tomography uptake in resected non-small-cell lung cancers†. *Eur J Cardio-Thoracic Surg*. 2017;52(1):55-62.

doi:10.1093/ejcts/ezx049

85. Sienel W, Seen-Hibler R, Mutschler W, Pantel K, Passlick B. Tumour cells in the tumour draining vein of patients with non-small cell lung cancer: detection rate and clinical significance. *Eur J Cardiothorac Surg*. 2003;23(4):451-456. doi:10.1016/s1010-7940(02)00865-5

86. Crosbie PAJ, Shah R, Krysiak P, et al. Circulating tumor cells detected in the tumor-draining pulmonary vein are associated with disease recurrence after surgical resection of NSCLC. *J Thorac Oncol*. 2016;11(10):1793-1797. doi:10.1016/j.jtho.2016.06.017

87. Dong J, Zhu D, Tang X, et al. Detection of circulating tumor cell molecular subtype in pulmonary vein predicting prognosis of stage i–iii non-small cell lung cancer patients. *Front Oncol*. 2019;9(OCT). doi:10.3389/fonc.2019.01139

88. Chemi F, Rothwell DG, McGranahan N, et al. Pulmonary venous circulating tumor cell dissemination before tumor resection and disease relapse. *Nat Med*. 2019;25(10):1534-1539. doi:10.1038/s41591-019-0593-1

89. Murlidhar V, Reddy RM, Fouladdel S, et al. Poor prognosis indicated by venous circulating tumor cell clusters in early-stage lung cancers. *Cancer Res*. 2017;77(18):5194-5206. doi:10.1158/0008-5472.CAN-16-2072

90. Huang J, Wang K, Xu J, Huang J, Zhang T. Prognostic significance of circulating tumor cells in non-small-cell lung cancer patients: A meta-analysis. *PLoS One*. 2013;8(11). doi:10.1371/journal.pone.0078070

91. Krebs MG, Sloane R, Priest L, et al. Evaluation and prognostic significance of circulating tumor cells in patients with non-small-cell lung cancer. *J Clin Oncol*. 2011;29(12):1556-1563. doi:10.1200/JCO.2010.28.7045

92. Qi Y, Wang W. Clinical significance of circulating tumor cells in squamous cell lung cancer patients. *Cancer Biomarkers*. 2017;18(2):161-167. doi:10.3233/CBM-160090

93. Shishido SN, Carlsson A, Nieva J, et al. Circulating tumor cells as a response monitor in stage IV non-small cell lung cancer. *J Transl Med*. 2019;17(1):294. doi:10.1186/s12967-019-2035-8

94. Muinelo-Romay L, Vieito M, Abalo A, et al. Evaluation of Circulating Tumor Cells and Related Events as Prognostic Factors and Surrogate Biomarkers in Advanced NSCLC Patients Receiving First-Line Systemic Treatment. *Cancers (Basel)*. 2014;6(1):153-165. doi:10.3390/cancers6010153

95. Mamdouhi T, Twomey JD, McSweeney KM, Zhang B. Fugitives on the run: circulating tumor cells (CTCs) in metastatic diseases. *Cancer Metastasis Rev*. 2019;38(1-2):297-305. doi:10.1007/s10555-019-09795-4

96. Allard WJ, Matera J, Miller MC, et al. Tumor cells circulate in the peripheral blood of all major carcinomas but not in healthy subjects or patients with nonmalignant diseases. *Clin Cancer Res*. 2004;10(20):6897-6904. doi:10.1158/1078-0432.CCR-04-0378

97. Farace F, Massard C, Vimond N, et al. A direct comparison of CellSearch and ISET for circulating tumour-cell detection in patients with metastatic carcinomas. *Br J Cancer*. 2011;105(6):847-853. doi:10.1038/bjc.2011.294

98. Hosokawa M, Kenmotsu H, Koh Y, et al. Size-Based Isolation of Circulating Tumor Cells in Lung Cancer Patients Using a Microcavity Array System. *PLoS One*. 2013;8(6). doi:10.1371/journal.pone.0067466

99. Su Y, Tian Q, Pan D, et al. Antibody-Functional Microsphere-Integrated Filter Chip with Inertial Microflow for Size–Immune-Capturing and Digital Detection of Circulating Tumor Cells. *ACS Appl Mater Interfaces*. 2019;11(33):29569-29578. doi:10.1021/acsami.9b09655

100. Van Niel G, D'Angelo G, Raposo G. Shedding light on the cell biology of extracellular vesicles. *Nat Rev Mol Cell Biol*. 2018;19(4):213-228. doi:10.1038/nrm.2017.125

101. Raposo G, Stoorvogel W. Extracellular vesicles: Exosomes, microvesicles, and friends. *J Cell Biol*. 2013;200(4):373-383. doi:10.1083/jcb.201211138

102. Latifkar A, Hur YH, Sanchez JC, Cerione RA, Antonyak MA. New insights into extracellular vesicle biogenesis and function. 2019. doi:10.1242/jcs.222406

103. Abels ER, Breakefield XO. Introduction to Extracellular Vesicles: Biogenesis, RNA Cargo Selection, Content, Release, and Uptake. *Cell Mol Neurobiol*. 2016;36(3):301-312. doi:10.1007/s10571-016-0366-z

104. Ostrowski M, Carmo NB, Krumeich S, et al. Rab27a and Rab27b control different steps of the exosome secretion pathway. *Nat Cell Biol*. 2010;12(1):19-30. doi:10.1038/ncb2000

105. O'Brien J, Hayder H, Zayed Y, Peng C. Overview of microRNA biogenesis, mechanisms of actions, and circulation. *Front Endocrinol (Lausanne)*. 2018;9(AUG). doi:10.3389/fendo.2018.00402

106. Hoshino A, Costa-Silva B, Shen TL, et al. Tumour exosome integrins determine organotropic metastasis. *Nature*. 2015;527(7578):329-335. doi:10.1038/nature15756

107. Huang C, Liu S, Tong X, Fan H. Extracellular vesicles and ctDNA in lung cancer: biomarker sources and therapeutic applications. *Cancer Chemother Pharmacol*. 2018;82(2):171-183. doi:10.1007/s00280-018-3586-8

108. Zheng H, Zhan Y, Liu S, et al. The roles of tumor-derived exosomes in non-small cell lung cancer and their clinical implications 11 Medical and Health Sciences 1112 Oncology and Carcinogenesis. *J Exp Clin Cancer Res*. 2018;37(1). doi:10.1186/s13046-018-0901-5

109. Reclusa P, Taverna S, Pucci M, et al. Exosomes as diagnostic and predictive biomarkers in lung cancer. *J Thorac Dis*. 2017;9:S1373-S1382. doi:10.21037/jtd.2017.10.67

110. Masaoutis C, Mihailidou C, Tsourouflis G, Theocharis S. Exosomes in lung cancer diagnosis and treatment. From the translating research into future clinical practice. *Biochimie*. 2018;151:27-36. doi:10.1016/j.biochi.2018.05.014

111. Rabinowits G, Gerçel-Taylor C, Day JM, Taylor DD, Kloecker GH. Exosomal microRNA: A diagnostic marker for lung cancer. *Clin Lung Cancer*. 2009;10(1):42-46. doi:10.3816/CLC.2009.n.006

112. Silva J, García V, Zaballos A´, et al. Vesicle-related microRNAs in plasma of nonsmall cell lung cancer patients and correlation with survival. doi:10.1183/09031936.00029610

113. Théry C, Witwer KW, Aikawa E, et al. Minimal information for studies of extracellular vesicles 2018 (MISEV2018): a position statement of the International Society for Extracellular Vesicles and update of the MISEV2014 guidelines. *J Extracell Vesicles*. 2018;7(1). doi:10.1080/20013078.2018.1535750

114. Zhang S, Xu XS, Yang JX, Guo JH, Chao TF, Tong YX. The prognostic role of Gas6/Axl axis in solid malignancies: A meta-analysis and literature review. *Onco Targets Ther*. 2018;11:509-519. doi:10.2147/OTT.S150952

115. Shieh YS, Lai CY, Kao YR, et al. Expression of Axl in lung adenocarcinoma and correlation with tumor progression. *Neoplasia*. 2005;7(12):1058-1064. doi:10.1593/neo.05640

116. Aguilera TA, Rafat M, Castellini L, et al. Reprogramming the immunological microenvironment through radiation and targeting Axl. *Nat Commun*. 2016;7. doi:10.1038/ncomms13898

117. Qu Z, Sun F, Zhou J, Li L, Shapiro SD, Xiao G. Interleukin-6 prevents the initiation but enhances the progression of lung cancer. *Cancer Res*. 2015;75(16):3209-3215. doi:10.1158/0008-5472.CAN-14-3042

118. Shang GS, Liu L, Qin YW. IL-6 and TNF-α promote metastasis of lung cancer by inducing epithelial-mesenchymal transition. *Oncol Lett*. 2017;13(6):4657-4660. doi:10.3892/ol.2017.6048

119. Kita H, Shiraishi Y, Watanabe K, et al. Does postoperative serum interleukin-6 influence early

recurrence after curative pulmonary resection of lung cancer? *Ann Thorac Cardiovasc Surg*. 2011;17(5):454-460. doi:10.5761/atcs.oa.10.01627

120. Drilon A, Cappuzzo F, Ou SHI, Camidge DR. Targeting MET in Lung Cancer: Will Expectations Finally Be MET? *J Thorac Oncol*. 2017;12(1):15-26. doi:10.1016/j.jtho.2016.10.014

121. Masuya D, Huang C, Liu D, et al. The tumour-stromal interaction between intratumoral c-Met and stromal hepatocyte growth factor associated with tumour growth and prognosis in non-small-cell lung cancer patients. *Br J Cancer*. 2004;90(8):1555-1562. doi:10.1038/sj.bjc.6601718

122. Puzone R, Savarino G, Salvi S, et al. *Glyceraldehyde-3-Phosphate Dehydrogenase Gene over Expression Correlates with Poor Prognosis in Non Small Cell Lung Cancer Patients*. Vol 12.; 2013. doi:10.1186/1476-4598-12-97

123. Liu K, Tang Z, Huang A, et al. Glyceraldehyde-3-phosphate dehydrogenase promotes cancer growth and metastasis through upregulation of SNAIL expression. *Int J Oncol*. 2017;50(1):252-262. doi:10.3892/ijo.2016.3774

124. Falleni M, Pellegrini C, Marchetti A, et al. Survivin gene expression in early-stage non-small cell lung cancer. *J Pathol*. 2003;200(5):620-626. doi:10.1002/path.1388

125. Endo C, Sun Z, Molina JR, Attewell JR, Yang P. Evaluation of reference genes for normalization of quantitative real time PCR in non-small cell lung cancer. *Int J Cancer Res*. 2007;3(1):1-12. doi:10.3923/ijcr.2007.1.12

126. Gebert LFR, MacRae IJ. Regulation of microRNA function in animals. *Nat Rev Mol Cell Biol*. 2019;20(1):21-37. doi:10.1038/s41580-018-0045-7

127. Greene SB, Herschkowitz JI, Rosen JM. Small players with big roles: microRNAs as targets to inhibit breast cancer progression. *Curr Drug Targets*. 2010;11(9):1059-1073. doi:10.2174/138945010792006762

128. Treiber T, Treiber N, Meister G. Regulation of microRNA biogenesis and its crosstalk with other cellular pathways. *Nat Rev Mol Cell Biol*. 2019;20(1):5-20. doi:10.1038/s41580-018-0059-1

129. Leva G Di, Garofalo M, Croce CM. MicroRNAs in Cancer. *Annu Rev Pathol Mech Dis*. 2014;9:287-314. doi:10.1146/annurev-pathol-012513-104715

130. Anfossi S, Fu X, Nagvekar R, Calin GA. MicroRNAs, regulatory messengers inside and outside cancer cells. In: *Advances in Experimental Medicine and Biology*. Vol 1056. Springer New York LLC; 2018:87-108. doi:10.1007/978-3-319-74470-4_6

131. Kai K, Dittmar RL, Sen S. Secretory microRNAs as biomarkers of cancer. *Semin Cell Dev Biol*. 2018;78:22-36. doi:10.1016/j.semcdb.2017.12.011

132. Wang Y, Li J, Tong L, et al. The Prognostic Value of miR-21 and miR-155 in Non-small-cell Lung Cancer: A Meta-analysis. *Jpn J Clin Oncol*. 2013;43(8):813-820. doi:10.1093/jjco/hyt084

133. Yang Y, Meng H, Peng Q, et al. Downregulation of microRNA-21 expression restrains non-small cell lung cancer cell proliferation and migration through upregulation of programmed cell death 4. *Cancer Gene Ther*. 2015;22(1):23-29. doi:10.1038/cgt.2014.66

134. Fabbri M, Paone A, Calore F, et al. MicroRNAs bind to Toll-like receptors to induce prometastatic inflammatory response. *Proc Natl Acad Sci U S A*. 2012;109(31). doi:10.1073/pnas.1209414109

135. Garofalo M, Romano G, Di Leva G, et al. EGFR and MET receptor tyrosine kinase-altered microRNA expression induces tumorigenesis and gefitinib resistance in lung cancers. *Nat Med*. 2012;18(1):74-82. doi:10.1038/nm.2577

136. Yamashita R, Sato M, Kakumu T, et al. Growth inhibitory effects of miR-221 and miR-222 in non-small cell lung cancer cells. *Cancer Med*. 2015;4(4):551-564. doi:10.1002/cam4.412

137. Wang X hai, Gan C zhi, Xie J yong. Inhibition of miR-24 suppresses malignancy of human non-small

cell lung cancer cells by targeting WWOX in vitro and in vivo. *Thorac Cancer*. 2018;9(12):1583-1593. doi:10.1111/1759-7714.12824

138. Pan B, Chen Y, Song H, Xu Y, Wang R, Chen L. Mir-24-3p downregulation contributes to VP16-DDP resistance in small-cell lung cancer by targeting ATG4A. *Oncotarget*. 2015;6(1):317-331. doi:10.18632/oncotarget.2787

139. Xia Y, Chen Q, Zhong Z, et al. Down-Regulation of MiR-30c Promotes the Invasion of Non-Small Cell Lung Cancer by Targeting MTA1. *Cell Physiol Biochem*. 2013;32(2):476-485. doi:10.1159/000354452

140. Liu F, Song D, Wu Y, Liu X, Zhu J, Tang Y. MiR-155 inhibits proliferation and invasion by directly targeting PDCD4 in non-small cell lung cancer. *Thorac Cancer*. 2017;8(6):613-619. doi:10.1111/1759-7714.12492

141. Lv X, Yao L, Zhang J, Han P, Li C. Inhibition of microRNA-155 sensitizes lung cancer cells to irradiation via suppression of HK2-modulated glucose metabolism. *Mol Med Rep*. 2016;14(2):1332-1338. doi:10.3892/mmr.2016.5394

142. Svoronos AA, Engelman DM, Slack FJ. OncomiR or tumor suppressor? The duplicity of MicroRNAs in cancer. *Cancer Res*. 2016;76(13):3666-3670. doi:10.1158/0008-5472.CAN-16-0359

143. Donnem T, Eklo K, Berg T, et al. Prognostic Impact of MiR-155 in Non-Small Cell Lung Cancer Evaluated by in Situ Hybridization. *J Transl Med*. 2011;9. doi:10.1186/1479-5876-9-6

144. Tili E, Michaille JJ, Calin GA. Expression and function of micro RNAs in immune cells during normal or disease state. *Int J Med Sci*. 2008;5(2):73-79. doi:10.7150/ijms.5.73

145. Yang Y, Ding L, Hu Q, et al. MicroRNA-218 functions as a tumor suppressor in lung cancer by targeting IL-6/STAT3 and negatively correlates with poor prognosis. *Mol Cancer*. 2017;16(1). doi:10.1186/s12943-017-0710-z

146. Wu L, Yang L. The function and mechanism of HMGB1 in lung cancer and its potential therapeutic implications. *Oncol Lett*. 2018;15(5):6799-6805. doi:10.3892/ol.2018.8215

147. Zhu K, Ding H, Wang W, et al. Tumor-suppressive miR-218-5p inhibits cancer cell proliferation and migration via EGFR in non-small cell lung cancer. *Oncotarget*. 2016;7(19):28075-28085. doi:10.18632/oncotarget.8576

148. Zarogoulidis P, Petanidis S, Kioseoglou E, Domvri K, Anestakis D, Zarogoulidis K. MiR-205 and miR-218 expression is associated with carboplatin chemoresistance and regulation of apoptosis via Mcl-1 and Survivin in lung cancer cells. *Cell Signal*. 2015;27(8):1576-1588. doi:10.1016/j.cellsig.2015.04.009

149. Gibbons DL, Lin W, Creighton CJ, et al. Contextual extracellular cues promote tumor cell EMT and metastasis by regulating miR-200 family expression. *Genes Dev*. 2009;23(18):2140-2151. doi:10.1101/gad.1820209

150. Zhan B, Lu D, Luo P, Wang B. Prognostic Value of Expression of MicroRNAs in Non-Small Cell Lung Cancer: A Systematic Review and Meta-Analysis. *Clin Lab*. 2016;62(11/2016). doi:10.7754/Clin.Lab.2016.160426

151. Li G, Xie J, Wang J. Tumor suppressor function of mir-129-5p in lung cancer. *Oncol Lett*. 2019;17(6):5777-5783. doi:10.3892/ol.2019.10241

152. Wang Z, Sha HH, Li HJ. Functions and mechanisms of miR-186 in human cancer. *Biomed Pharmacother*. 2019;119. doi:10.1016/j.biopha.2019.109428

153. Feng H, Zhang Z, Qing X, French SW, Liu D. miR-186-5p promotes cell growth, migration and invasion of lung adenocarcinoma by targeting PTEN. *Exp Mol Pathol*. 2019;108:105-113. doi:10.1016/j.yexmp.2019.04.007

154. Szpechcinski A, Florczuk M, Duk K, et al. The expression of circulating miR-504 in plasma is

associated with EGFR mutation status in non-small-cell lung carcinoma patients. *Cell Mol Life Sci*. 2019;76(18):3641-3656. doi:10.1007/s00018-019-03089-2

155. Xiang M, Zeng Y, Yang R, et al. U6 is not a suitable endogenous control for the quantification of circulating microRNAs. *Biochem Biophys Res Commun*. 2014;454(1):210-214. doi:10.1016/j.bbrc.2014.10.064

156. De Miguel-Pérez D, Bayarri-Lara CI, Ortega FG, et al. Post-surgery circulating tumor cells and AXL overexpression as new poor prognostic biomarkers in resected lung adenocarcinoma. *Cancers (Basel)*. 2019;11(11). doi:10.3390/cancers11111750

157. Goldstraw P, Chansky K, Crowley J, et al. The IASLC lung cancer staging project: Proposals for revision of the TNM stage groupings in the forthcoming (eighth) edition of the TNM Classification for lung cancer. *J Thorac Oncol*. 2016;11(1):39-51. doi:10.1016/j.jtho.2015.09.009

158. Kris MG, Gaspar LE, Chaft JE, et al. Adjuvant Systemic Therapy and Adjuvant Radiation Therapy for Stage I to IIIA Completely Resected Non–Small-Cell Lung Cancers: American Society of Clinical Oncology/Cancer Care Ontario Clinical Practice Guideline Update. *J Clin Oncol*. 2017;35(25):2960-2974. doi:10.1200/JCO.2017.72.4401

159. Rodríguez-Martínez A, de Miguel-Pérez D, Ortega FG, et al. Exosomal miRNA profile as complementary tool in the diagnostic and prediction of treatment response in localized breast cancer under neoadjuvant chemotherapy. *Breast Cancer Res*. 2019;21(1):21. doi:10.1186/s13058-019-1109-0

160. De Miguel-Pérez D, Rodriguez-Martínez A, Ortigosa Palomo A, et al. Extracellular vesicle-miRNAs as liquid biopsy biomarkers for disease identification and prognosis in metastatic colorectal cancer patients. *Sci Rep*. 2020;Forthcoming.

161. Lötvall J, Hill AF, Hochberg F, et al. Minimal experimental requirements for definition of extracellular vesicles and their functions: a position statement from the International Society for Extracellular Vesicles. *J Extracell Vesicles*. 2014;3(1):26913. doi:10.3402/jev.v3.26913

162. Li J-H, Liu S, Zhou H, Qu L-H, Yang J-H. starBase v2.0: decoding miRNA-ceRNA, miRNA-ncRNA and protein–RNA interaction networks from large-scale CLIP-Seq data. *Nucleic Acids Res*. 2014;42(D1):D92-D97. doi:10.1093/nar/gkt1248

163. Andersen CL, Jensen JL, Ørntoft TF. Normalization of real-time quantitative reverse transcription-PCR data: A model-based variance estimation approach to identify genes suited for normalization, applied to bladder and colon cancer data sets. *Cancer Res*. 2004;64(15):5245-5250. doi:10.1158/0008-5472.CAN-04-0496

164. Schmittgen TD, Livak KJ. Analyzing real-time PCR data by the comparative CT method. *Nat Protoc*. 2008;3(6):1101-1108. doi:10.1038/nprot.2008.73

165. Ogłuszka M, Orzechowska M, Jędroszka D, Witas P, Bednarek AK. Evaluate Cutpoints: Adaptable continuous data distribution system for determining survival in Kaplan-Meier estimator. *Comput Methods Programs Biomed*. 2019;177:133-139. doi:10.1016/j.cmpb.2019.05.023

166. Maldonado G, Greenland S. Simulation study of confounder-selection strategies. *Am J Epidemiol*. 1993;138(11):923-936. http://www.ncbi.nlm.nih.gov/pubmed/8256780. Accessed May 2, 2019.

167. Meng S, Tripathy D, Frenkel EP, et al. Circulating tumor cells in patients with breast cancer dormancy. *Clin Cancer Res*. 2004;10(24):8152-8162. doi:10.1158/1078-0432.CCR-04-1110

168. Nadal R, Ortega FG, Salido M, et al. CD133 expression in circulating tumor cells from breast cancer patients: Potential role in resistance to chemotherapy. *Int J Cancer*. 2013;133(10):2398-2407. doi:10.1002/ijc.28263

169. Yoon SO, Kim YT, Jung KC, Jeon YK, Kim BH, Kim CW. TTF-1 mRNA-positive circulating tumor cells in the peripheral blood predict poor prognosis in surgically resected non-small cell lung cancer patients. *Lung Cancer*. 2011;71(2):209-216. doi:10.1016/j.lungcan.2010.04.017

170. Kang S, Tanaka T, Kishimoto T. Therapeutic uses of anti-interleukin-6 receptor antibody. *Int Immunol*. 2015;27(1):21-29. doi:10.1093/intimm/dxu081

171. Zhang G, Wang M, Zhao H, Cui W. Function of axl receptor tyrosine kinase in non-small cell lung cancer (Review). *Oncol Lett*. 2018;15(3):2726-2734. doi:10.3892/ol.2017.7694

172. LIU R-Y, ZENG Y, LEI Z, et al. JAK/STAT3 signaling is required for TGF-β-induced epithelial-mesenchymal transition in lung cancer cells. *Int J Oncol*. 2014;44(5):1643-1651. doi:10.3892/ijo.2014.2310

173. Park SM, Wong DJ, Ooi CC, et al. Molecular profiling of single circulating tumor cells from lung cancer patients. *Proc Natl Acad Sci U S A*. 2016;113(52):E8379-E8386. doi:10.1073/pnas.1608461113

174. Manjunath Y, Upparahalli S V., Avella DM, et al. PD-L1 expression with epithelial mesenchymal transition of circulating tumor cells is associated with poor survival in curatively resected non-small cell lung cancer. *Cancers (Basel)*. 2019;11(6). doi:10.3390/cancers11060806

175. Ishikawa M, Sonobe M, Nakayama E, et al. Higher Expression of Receptor Tyrosine Kinase Axl, and Differential Expression of its Ligand, Gas6, Predict Poor Survival in Lung Adenocarcinoma Patients. *Ann Surg Oncol*. 2013;20(S3):467-476. doi:10.1245/s10434-012-2795-3

176. Deng G, Herrler M, Burgess D, Manna E, Krag D, Burke JF. Enrichment with anti-cytokeratin alone or combined with anti-EpCAM antibodies significantly increases the sensitivity for circulating tumor cell detection in metastatic breast cancer patients. *Breast Cancer Res*. 2008;10(4):R69. doi:10.1186/bcr2131

177. Xie Z, Gao X, Cheng K, Yu L. Correlation between the presence of circulating tumor cells and the pathologic type and staging of non-small cell lung cancer during the early postoperative period. *Oncol Lett*. 2017;14(5):5825-5830. doi:10.3892/ol.2017.6910

178. Tsukita Y, Fujino N, Miyauchi E, et al. Axl kinase drives immune checkpoint and chemokine signalling pathways in lung adenocarcinomas. *Mol Cancer*. 2019;18(1):24. doi:10.1186/s12943-019-0953-y

179. Raimondi C, Carpino G, Nicolazzo C, et al. PD-L1 and epithelial-mesenchymal transition in circulating tumor cells from non-small cell lung cancer patients: A molecular shield to evade immune system **?** *Oncoimmunology*. 2017;6(12):e1315488. doi:10.1080/2162402X.2017.1315488

180. Nonagase Y, Takeda M, Azuma K, et al. Tumor tissue and plasma levels of AXL and GAS6 before and after tyrosine kinase inhibitor treatment in EGFR-mutated non–small cell lung cancer. *Thorac Cancer*. 2019;10(10):1928-1935. doi:10.1111/1759-7714.13166

181. Xu J, Camfield R, Gorski SM. The interplay between exosomes and autophagy-partners in crime. 2018. doi:10.1242/jcs.215210

182. Fortunato O, Gasparini P, Boeri M, Sozzi G. Exo-miRNAs as a new tool for liquid biopsy in lung cancer. *Cancers (Basel)*. 2019;11(6). doi:10.3390/cancers11060888

183. Wang Y, Kim TH, Fouladdel S, et al. PD-L1 Expression in Circulating Tumor Cells Increases during Radio(chemo)therapy and Indicates Poor Prognosis in Non-small Cell Lung Cancer. *Sci Rep*. 2019;9(1). doi:10.1038/s41598-018-36096-7

184. Martin OA, Anderson RL, Russell PA, et al. Mobilization of viable tumor cells into the circulation during radiation therapy. *Int J Radiat Oncol Biol Phys*. 2014;88(2):395-403. doi:10.1016/j.ijrobp.2013.10.033

185. Dorsey JF, Kao GD, MacArthur KM, et al. Tracking viable circulating tumor cells (CTCs) in the peripheral blood of non-small cell lung cancer (NSCLC) patients undergoing definitive radiation therapy: Pilot study results. *Cancer*. 2015;121(1):139-149. doi:10.1002/cncr.28975

186. Si L, Tian H, Yue W, et al. Potential use of microRNA-200c as a prognostic marker in non-small cell lung cancer. *Oncol Lett*. 2017;14(4):4325-4330. doi:10.3892/ol.2017.6667

187. Mak RH, Doran E, Muzikansky A, et al. Outcomes After Combined Modality Therapy for EGFR-Mutant and Wild-Type Locally Advanced NSCLC. *Oncologist*. 2011;16(6):886-895. doi:10.1634/theoncologist.2011-0040

188. Alexander M, Hu R, Runtsch MC, et al. Exosome-delivered microRNAs modulate the inflammatory response to endotoxin. *Nat Commun*. 2015;6. doi:10.1038/ncomms8321

189. Chinniah C, Aguarin L, Cheng P, et al. Early Detection of Recurrence in Patients With Locally Advanced Non–Small-Cell Lung Cancer via Circulating Tumor Cell Analysis. *Clin Lung Cancer*. 2019;20(5):384-390.e2. doi:10.1016/j.cllc.2019.04.011

190. Li C, Qin F, Hu F, et al. Characterization and selective incorporation of small non-coding RNAs in non-small cell lung cancer extracellular vesicles. *Cell Biosci*. 2018;8(1):2. doi:10.1186/s13578-018-0202-x

191. Shinde A, Li R, Kim J, Salgia R, Hurria A, Amini A. Stereotactic body radiation therapy (SBRT) for early-stage lung cancer in the elderly. *Semin Oncol*. 2018;45(4):210-219. doi:10.1053/j.seminoncol.2018.06.002

192. Navarro-Martín A, Galiana IL, Frances MAB, et al. Preliminary study of the effect of stereotactic body radiotherapy (SBRT) on the immune system in lung cancer patients unfit for surgery: Immunophenotyping analysis. *Int J Mol Sci*. 2018;19(12). doi:10.3390/ijms19123963

193. Hao C, Liu G, Tian G. Autophagy inhibition of cancer stem cells promotes the efficacy of cisplatin against non-small cell lung carcinoma. *Ther Adv Respir Dis*. 2019;13. doi:10.1177/1753466619866097

194. Yao C, Ni Z, Gong C, et al. Rocaglamide enhances NK cell-mediated killing of non-small cell lung cancer cells by inhibiting autophagy. *Autophagy*. 2018;14(10):1831-1844. doi:10.1080/15548627.2018.1489946

195. Jiang GM, Tan Y, Wang H, et al. The relationship between autophagy and the immune system and its applications for tumor immunotherapy. *Mol Cancer*. 2019;18(1). doi:10.1186/s12943-019-0944-z

9. Rights and permissions:

Figure 1 and 2:

License Number	4742210652586
License date	Jan 04, 2020

Licensed Content

Licensed Content Publisher	John Wiley and Sons
Licensed Content Publication	International Journal of Cancer
Licensed Content Title	Estimating the global cancer incidence and mortality in 2018: GLOBOCAN sources and methods
Licensed Content Author	J. Ferlay, M. Colombet, I. Soerjomataram, et al
Licensed Content Date	Dec 6, 2018
Licensed Content Volume	144
Licensed Content Issue	8
Licensed Content Pages	13

Order Details

Type of use	Dissertation/Thesis
Requestor type	University/Academic
Format	Print and electronic
Portion	Figure/table
Number of figures/tables	2
Will you be translating?	No

Figure 3:

Licensed Content

Licensed Content Publisher	Springer Nature
Licensed Content Publication	Nature Reviews Cancer
Licensed Content Title	Targeting autophagy in cancer
Licensed Content Author	Jean M. Mulcahy Levy et al
Licensed Content Date	Jul 28, 2017

Order Details

Type of Use	Thesis/Dissertation
Requestor type	academic/university or research institute
Format	print and electronic
Portion	figures/tables/illustrations
Number of figures/tables/illustrations	1
High-res required	no
Will you be translating?	no
Circulation/distribution	1 - 29
Author of this Springer Nature content	no

Figure 4:

Liu *et al. Molecular Cancer* (2017) 16:176
DOI 10.1186/s12943-017-0742-4

Molecular Cancer

REVIEW Open Access

Figure 5:

Licensed Content

Licensed Content Publisher	Springer Nature
Licensed Content Publication	Nature Reviews Clinical Oncology
Licensed Content Title	Tumour heterogeneity and resistance to cancer therapies
Licensed Content Author	Ibiayi Dagogo-Jack et al
Licensed Content Date	Nov 8, 2017

Order Details

Type of Use	Thesis/Dissertation
Requestor type	academic/university or research institute
Format	print and electronic
Portion	figures/tables/illustrations
Number of figures/tables/illustrations	1
High-res required	no
Will you be translating?	no
Circulation/distribution	1 - 29
Author of this Springer Nature content	no

Figure 6:

Licensed Content

Licensed Content Publisher	Springer Nature
Licensed Content Publication	Nature Reviews Cancer
Licensed Content Title	Unravelling tumour heterogeneity by single-cell profiling of circulating tumour cells
Licensed Content Author	Laura Keller et al
Licensed Content Date	Aug 27, 2019

Order Details

Type of Use	Thesis/Dissertation
Requestor type	academic/university or research institute
Format	print and electronic
Portion	figures/tables/illustrations
Number of figures/tables/illustrations	1
High-res required	no
Will you be translating?	no
Circulation/distribution	1 - 29
Author of this Springer Nature content	no

Figure 7:

Licensed Content

Licensed Content Publisher	Springer Nature
Licensed Content Publication	Nature Reviews Molecular Cell Biology
Licensed Content Title	New insights into the mechanisms of epithelial–mesenchymal transition and implications for cancer
Licensed Content Author	Anushka Dongre et al
Licensed Content Date	Nov 20, 2018

Order Details

Type of Use	Thesis/Dissertation
Requestor type	academic/university or research institute
Format	print and electronic
Portion	figures/tables/illustrations
Number of figures/tables/illustrations	1
High-res required	no
Will you be translating?	no
Circulation/distribution	1 - 29
Author of this Springer Nature content	no

Figure 8:

Licensed Content

Licensed Content Publisher	Springer Nature
Licensed Content Publication	Nature Reviews Molecular Cell Biology
Licensed Content Title	Shedding light on the cell biology of extracellular vesicles
Licensed Content Author	Guillaume van Niel et al
Licensed Content Date	Jan 17, 2018

Order Details

Type of Use	Thesis/Dissertation
Requestor type	academic/university or research institute
Format	print and electronic
Portion	figures/tables/illustrations
Number of figures/tables/illustrations	1
High-res required	no
Will you be translating?	no
Circulation/distribution	1 - 29
Author of this Springer Nature content	no

Figure 9:

Licensed Content

Licensed Content Publisher	Springer Nature
Licensed Content Publication	Nature Reviews Molecular Cell Biology
Licensed Content Title	Regulation of microRNA biogenesis and its crosstalk with other cellular pathways
Licensed Content Author	Thomas Treiber et al
Licensed Content Date	Sep 18, 2018

Order Details

Type of Use	Thesis/Dissertation
Requestor type	academic/university or research institute
Format	print and electronic
Portion	figures/tables/illustrations
Number of figures/tables/illustrations	1
High-res required	no
Will you be translating?	no
Circulation/distribution	1 - 29
Author of this Springer Nature content	no

Figures and whole article premission:

De Miguel-Pérez D, Bayarri-Lara CI, Ortega FG, et al. Post-surgery circulating tumor cells and AXL overexpression as new poor prognostic biomarkers in resected lung adenocarcinoma. *Cancers (Basel)*. 2019;11(11). doi:10.3390/cancers11111750